

CharitéCentrum 3 für Zahn-, Mund- und Kieferheilkunde
Abteilung für zahnärztliche Prothetik, Alterszahnmedizin und Funktionslehre
Direktor: Prof. Dr. med. dent. Florian Beuer, MME

HABILITATIONSSCHRIFT

Implant prosthodontic rehabilitation in a digital workflow

zur Erlangung der Lehrbefähigung
für das Fach Zahn-, Mund- und Kieferheilkunde

vorgelegt dem Fakultätsrat der Medizinischen Fakultät

Charité-Universitätsmedizin Berlin

von

Dr. med. dent. Stefano Pieralli

Eingereicht: Juni 2023
Dekan: Prof. Dr. Joachim Spranger
1. Gutachter: Prof. Dr. Jan-Frederik Güth, Frankfurt am Main
2. Gutachter: Prof. Dr. Petra Gierthmühlen, Düsseldorf

Für meine Großmutter, Paula und meine Nichte, Livia.

TABLE OF CONTENTS

ABBREVIATIONS	5
1 INTRODUCTION.....	8
1.1 Implant prosthodontics	8
1.1.1 Principles of dental implants	8
1.1.2 Restorative materials and retention mode.....	10
1.2 From data acquisition to implant scanning in a digital workflow.....	13
1.2.1 Clinical data acquisition	13
1.2.2 Computer-aided implant planning.....	15
1.2.3 Implant selection	16
1.2.4 Computer-aided design and -manufacturing of the surgical guide.....	18
1.2.5 Intraoral implant digitization	20
1.3 Scientific question(s).....	22
2 PERSONAL RESEARCH PROJECTS.....	24
2.1 Manuscript 1 – Influence of reducing the radiographic field of view on the accuracy of registration with intraoral surface scans.....	24
2.2 Manuscript 2 – Clinical outcomes and Patient-Reported Outcome Measures of CAD/CAM root-analogue implants	36
2.3 Manuscript 3 – Trueness of implant installation using sterilizable surgical guides fabricated in office by material extrusion.....	57
2.4 Manuscript 4 – Impact of planning software and template design on the accuracy of implant installation using surgical guides created by material extrusion.....	72

2.5	Manuscript 5 – Cytotoxicity of polymers intended for the additive manufacturing of surgical guides by material extrusion	83
2.6	Manuscript 6 – Accuracy of one-piece zirconia implant scan body–free digitization	97
3	DISCUSSION	110
3.1	Study outcomes	110
3.2	Outlook and future perspectives	114
3.2.1	Virtual implant imaging with reduced field of view	114
3.2.2	CAD/CAM custom-made root-analogue implants for immediate placement.....	115
3.2.3	Surgical guides fabricated with material extrusion technology.....	117
3.2.4	Scan body–free implant digitization	119
4	CONCLUSION	120
5	SUMMARY	122
6	REFERENCES	124
7	ACKNOWLEDGMENT.....	135
	EIDESSTATTLICHE ERKLÄRUNG.....	137

ABBREVIATIONS

ALADA	As Low As Diagnostically Acceptable
ALARA	As Low As Reasonably Achievable
AM	Additive manufacturing
CAD/CAM	Computer-aided design/Computer-aided manufacturing
CBCT	Cone beam computed tomography
CT	Computed tomography
dCAIS	Dynamic computer-assisted implant surgery
DGI	German Association of Oral Implantology (<i>Deutsche Gesellschaft für Implantologie e.V.</i>)
DICOM	Digital imaging and communication in medicine
DLP	Digital light processing
EAO	European Association for Osseointegration
FDM	Fused deposition modeling
FDP	Fixed dental prosthesis
FFF	Fused filament fabrication
FOV	Field of view
HGKs	Human gingival keratinocytes
IOS	Intraoral scanner
ME	Material extrusion

MRI	Magnetic resonance imaging
OHIP	Oral Health Impact Profile
PEEK	Polyether-ether-ketone
PLA	Polylactic acid
PROMs	Patient reported outcome measures
PROSEC	Progress in Science and Education with Ceramics
RAI	Root-analogue implant
SC	Single crown
sCAIS	Static computer-assisted implant surgery
SD	Standard deviation
SLA	Stereolithography
SM	Subtractive manufacturing
STL	Standard tessellation language
ZrO ₂	Zirconium dioxide, zirconia
2D	Two-dimensional
3D	Three-dimensional

The presented clinical case illustrations have been reproduced with permission of the Department of Prosthodontics, Geriatric Dentistry and Craniomandibular Disorders, Charité-Universitätsmedizin Berlin, Berlin, Germany (Credits: Dr. Mats Böse and Dr. Stefano Pieralli). Informed written consent for publishing their pictures was obtained from all patients.

1 INTRODUCTION

1.1 Implant prosthodontics

Implant-supported restorations are successfully used to replace single and multiple missing teeth (1, 2). Moreover, reports from Oral Health Impact Profile (OHIP) scales and patient reported outcome measures (PROMs) confirm that partially and fully edentulous patients significantly increase life quality after an implant prosthodontics treatment (3). The current edition of the Glossary of Prosthodontic Terms defines *implant prosthodontics* as "*the selection, planning, development, placement, replacement of missing teeth and/or associated structures, and maintenance of restoration(s) with dental implants*" (4).

1.1.1 Principles of dental implants

A dental implant serves as an artificial root to retain or support a fixed or removable prosthesis (4). Modern implantology is based on the research group's findings around Professor Per-Ingvar Brånemark, which named "osseointegration" the stable fixation of a titanium cylinder and the surrounding bone (5). Titanium alloys are, up to this day, the most investigated and clinically used implant bulk materials (6) (Fig. 1). A drawback of titanium is its grayish color, which can lead to increased esthetic impairment in case of < 3 mm peri-implant soft tissue thickness (7). An additional alternative for the clinician is offered by ceramic implants, which are zirconia based (8) and have a whitish color. According to the Delphi study of the European Association

for Osseointegration (EAO), evaluating the possible trends in implant dentistry, both bulk materials will coexist in the next decade (9).

While the implant functions as a substitute for the dental root, the overhead abutment (Fig. 2) serves as a prepared natural tooth to retain the prosthetic restoration. Implant and abutment can be created as a single unit (one-piece design) or separately (two-piece design), with the second type finding more clinical application. In the case of a two-piece design, the abutment can be prefabricated or personalized with different angulations and made of several materials such as titanium or zirconium dioxide, zirconia (ZrO_2) (10). To fix the abutment to the implant, a screw is usually used.



Figure 1: Close up of a dental implant for the rehabilitation of a missing maxillary central right incisor. This prefabricated screw-shaped cylindrical implant has a two-piece design and is made of titanium. For accurate implant installation, a surgical guide is used.



Figure 2: Detail of a custom-made abutment in the position of the maxillary right central incisor. The CAD/CAM abutment is made of ZrO_2 and screw retained to the implant below. Subsequently, the abutment is used for intraoral luting of the definitive single crown (SC). Manufactured by MDT Robert Nicic, Berlin.

1.1.2 Restorative materials and retention mode

To restore single implants, ceramic materials are used either to veneer a metal or high-performance ceramic framework or in a monolithic form (1, 2) (Fig. 3). Metal-ceramic single-unit restorations are the most documented in the literature, and Jung et al. reported a 95.8% 5-year survival rate (11). Moreover, when focusing on implant-supported all-ceramic single crowns (SCs), an estimated survival rate of 96.1% was calculated after 3 years by Pjetursson et al. (1). No significant differences in terms of survival rate were assessed between the evaluated materials: monolithic and veneered reinforced glass-ceramic, veneered densely sintered alumina, and veneered and monolithic ZrO₂. However, monolithic SCs showed significantly lower porcelain fracture (chipping) rates compared to veneered ones. Chipping of the restorative material has a multifactorial origin and represents the most frequent technical complication (12). When focusing on partial span fixed dental prostheses (FDPs), veneered-ZrO₂ shows a high 5-year survival estimate (98.3%) but also an increased chipping rate (22.8%) (13). Furthermore, insufficient data about monolithic restorations are available. According to a meta-analysis by Sailer et al., metal ceramic partial FDPs show an estimated 5-year survival rate of 98.7% and a chipping rate of 11.6% (2). Similar high survival rates between metal ceramic and veneered ZrO₂ FDPs have been reported. However, chipping remains the most frequent technical complication also for FDPs.

Cementation and screw retaining are the two most common retention modalities for implant-supported restorations (14). Nevertheless, removing the excess cement after intraoral luting is a priority to avoid peri-implant biological complications (15). Multiple

studies have confirmed that complete cleansing from cement residuals located ≤ 1 mm subgingivally is challenging or impossible (16, 17). Luting of the restoration onto single or multiple abutments can also occur in advance in the dental lab. In this case, the restoration-abutment complex is provided with a single passing screw for retention.



Figure 3: Exemplary samples of all-ceramic CAD/CAM implant-supported SCs. The ceramic SCs are adhesively luted onto the prefabricated titanium abutment in the lab. Thereafter, they are delivered as occlusally screw-retained restorations. Manufactured by MDT Jürgen Mehrhof, Berlin.

When planning a full-arch implant-supported rehabilitation, fixed and removable treatment options are available. Full-arch FDPs can be fabricated from all ceramic materials, based on ZrO_2 (18), or show a metal framework veneered with ceramic (19) or resin (20). After 5 years, Papaspyridakos et al. reported a survival rate of 97.7% for full-arch ZrO_2 -based FDPs and of 98.2% for metal-ceramic FDPs (19). To rehabilitate an edentulous maxilla or mandible with a full-arch FDP, ≥ 4 implants are needed (21). Furthermore, to retain a removable prosthesis, also called an overdenture, at least four implants in the maxilla and two interforaminal implants in the mandible are required (22). A single implant placed in the mandible midline to retain an overdenture should be limited to selected cases because decreased survival rates were observed after 5 years. In addition, for initial cost savings, the expense to the patient increases over the years due to the necessary maintenance of the prosthesis, particularly the

attachment system (23, 24). Various prosthetic solutions are available to retain/support overdentures. One can distinguish between a fixed retentive element to splint the implants with primary locking (e.g., a bar) and secondary locking (e.g., locator attachments) (Fig. 4). In the latter case, the removable prosthesis itself serves to splint the implants. Furthermore, retentive elements can be divided into rigid (e.g., bars) and more "flexible" ones (e.g., locator attachment). The choice for the ideal retentive element depends on multiple parameters and relies, among others, on the number and distribution of the implants and the patient's anatomical characteristics (22).

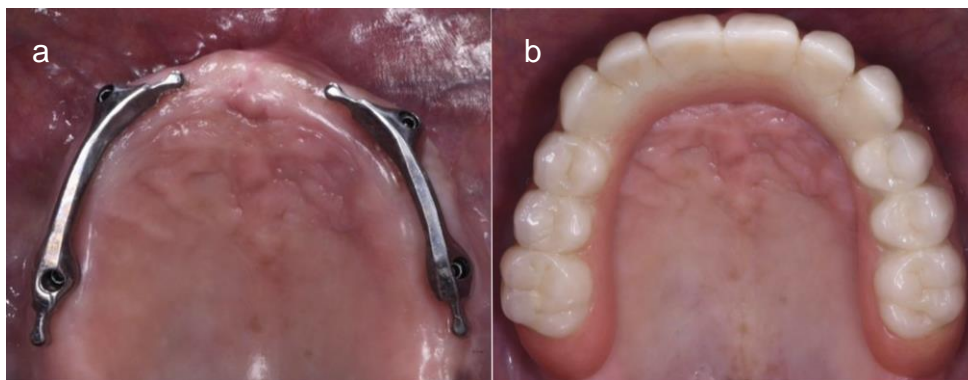


Figure 4: Exemplary samples of rigid retentive elements. Two CAD/CAM titanium bars (a) serve to splint two implants each and support a metal-resin maxillary overdenture (b). Manufactured by MDT Wolf Wörner, Freiburg.

With the advent of new digital features, including implant planning software, intraoral scanner (IOS) systems and computer-aided design/computer-aided manufacturing (CAD/CAM) technology, novel workflows become possible for implant prosthodontics.

1.2 From data acquisition to implant scanning in a digital workflow

The term *digital* refers to anything involving or relating to the use of computer technology (25). The application of digital technologies to implant dentistry and prosthodontics radically changed the clinical routine, from data collection to manufacturing of the restoration (26). Section 1.2 describes the standard digital workflow for implant rehabilitation, from clinical data acquisition and virtual implant planning to guided implant installation and intraoral implant digitization.

1.2.1 Clinical data acquisition

Computed tomography (CT) and cone beam computed tomography (CBCT) are used to deliver 3D radiographic images (27). Besides being developed after the CT, the CBCT technology rapidly took over CT for its decreased irradiation dose and costs (28). Nevertheless, the radiation dose of a CBCT full-arch scan ranges between 10 and 1000 μ Sv and reaches up to 200 times that of a two-dimensional (2D) panoramic image (29). Irrespective of two- or three-dimensional (3D) imaging, the potential risk of developing radiation-induced cancer due to repeated X-rays for dental purposes must not be underestimated (30). According to the EAO Delphi study, a consensus of > 80% was obtained in favor of 3D compared to 2D imaging in providing adequate information for virtual implant planning (9). In fact, 2D imaging (e.g., periapical, and panoramic radiographs) delivers inferior diagnostic information and is more prone to distortion (27).

For each CBCT scan, multiple images are acquired and subsequently exported from the tomography device as digital imaging and communication in medicine (DICOM) files. The DICOM format was created as a universal standard extension for medical data to facilitate information acquisition, management, and transmission (31). In a review article by Kernen et al., all evaluated virtual implant-planning systems were DICOM compliant (32). Guidelines for imaging in implant dentistry were published in 2011 by the EAO and included the call for novel techniques to reduce patients' exposure to ionizing irradiation (33). More than a decade later, attempts to reduce irradiation are scarce and include, among others, reducing the milliamperage and the voxels' size (34, 35). Specific instructions for virtual implant planning with reduced radiation dose protocols still need to be included (35).

For planning purposes, intraoral surface scans are combined with 3D radiographic data. IOS systems are used for digitization (36), whereas indirect digitization in the lab of stone casts produced from the analog impression is also possible. Both techniques deliver a virtual surface image to import into the planning software for registration. Intraoral scans replace conventional impression techniques with hydrocolloids or elastomers in the digital workflow. Both Siqueira et al. and Bishti et al. reported more favorable PROMs scores for intraoral scans than for conventional impressions (37, 38).

The accuracy of an intraoral scan depends on multiple factors. Light condition (39), room temperature and scanning path (40) are only some of the parameters that can affect the accuracy of digitization and must be kept in mind. After intraoral digitization, the surface scan is exported, usually in standard tessellation language (STL) file

extension (41). The STL file format carries the information about the shell of the object based on a mosaic of geometric shapes (in this case, triangles) (42).

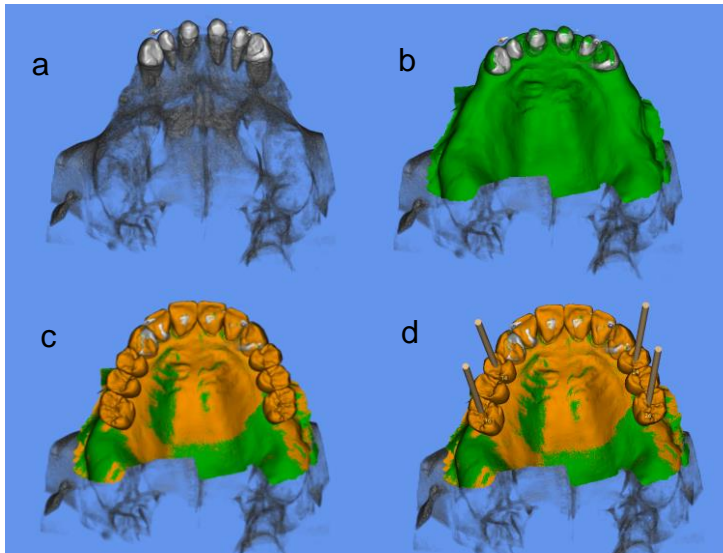


Figure 5: Computer-aided implant planning of two posterior 3-unit FDPs. 3D radiography in gray (a) and surface scans in green were superimposed for registration (b). Thereafter, a prosthetic set up/wax up (in orange) was aligned and used as a reference to position the implants (c). Four implants, two on each side, were planned for the support of all-ceramic FDPs (d).

1.2.2 Computer-aided implant planning

Considering the immobility of implants once osseointegrated, precise backward planning based on the future prosthetic restoration(s) is mandatory to achieve predictable results and avoid complications (43) (Fig. 5). Dedicated implant planning software is used to plan the implant prosthodontic treatment in advance. By virtually combining 3D radiographic (DICOM) and intraoral surface (STL) images, a 3D patient can be created (32).

Both DICOM and STL datasets are imported into the planning software and superimposed by a best-fit algorithm in a process called registration (44). Mutual

reference objects, such as natural teeth, can help to match the different datasets, and final manual fine tuning may be required for ideal registration. Accurate registration is mandatory to avoid planning errors, which lead to implant mispositioning (45). After accurate registration, the implant is virtually positioned according to the combined DICOM/STL images and then locked to the STL scan. Based on the implant position and the surface scan, a surgical guide is virtually created by CAD/CAM. To accurately transfer the virtual implant position into the patient's mouth in a digital workflow, static (s) or dynamic (d) computer-assisted implant surgery (CAIS) can be adapted (46). For sCAIS, custom-made templates based on the previous virtual planning are created to guide the drilling procedure and to install the implant (47). Furthermore, for dCAIS, implants are installed while real-time tracking of the drills on a monitor (48). In the present thesis, the focus was set on sCAIS.

1.2.3 Implant selection

A virtual portfolio containing dozens of implant brands and types is available in most planning software and provides the user with a vast choice of options for ideal planning.

Dental implants are mostly created by milling, but additive manufacturing (AM) (49) and injection molding techniques (50) are also described in the literature. As for the shape, prefabricated dental implants are similar to screws. They have either a cylindrical or conical profile or show a combination of both. Dental implants have a rough enossal part to enhance osseointegration (51). To increase and accelerate this phenomenon, mechanical and/or chemical modifications are applied to process the

surface of the implant (52). The most coronal parts of the implant, called the implant shoulder, can present a machined collar for better soft-tissue adaptation (53). Depending on the implant design, its shoulder is placed at the hard or soft tissue level (54). The implants' length varies from 4 mm of the extra short ones (55) to ≥ 13 mm (56), whereas the implant diameter ranges from < 3.0 mm of a "mini-implant" (57) to ≥ 4.5 mm (58).

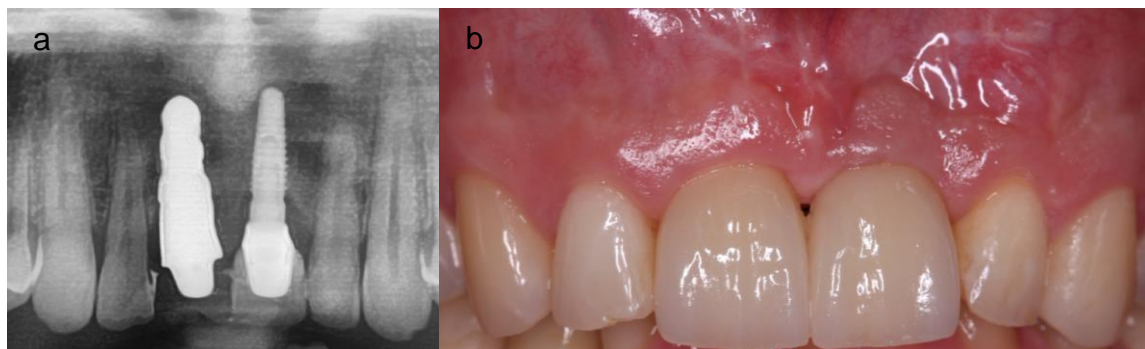


Figure 6: Exemplary radiographic (a) and intraoral (b) images of a CAD/CAM RAI made of ZrO_2 (left) and a prefabricated screw-shaped titanium implant (right). This type of RAI has a one-piece design, whereas the threaded implant shows a two-piece design. Clinical outcomes and PROMs of RAIs were collected and analyzed in Manuscript 2. X-ray and picture: Courtesies of Dr. Mats Böse.

For an ideal fit with patients' anatomy, custom-made root-analogue implant (RAI) systems represent an alternative to the standard prefabricated implants (59) (Fig. 6). First described by Hodosh et al. in the 1970s (60), various RAI types are currently being commercialized (61). The critical difference from prefabricated standard implants relates to their shape. Such a root-analogue design precludes screwing them into an implant bed prepared with a standard sequence of drills. In fact, RAIs are installed by pressing into the post-extraction site. To better adapt to the alveolar cavity anatomy and ensure it is ready to use immediately after the tooth extraction, custom-made RAIs are digitally planned before the tooth extraction and, subsequently,

typically created by subtractive manufacturing (SM) (62). For this purpose, the DICOM images of the root(s) are segmented and thereafter exported to a design software (63).

1.2.4 Computer-aided design and -manufacturing of the surgical guide

Numerous preclinical and clinical investigations have demonstrated superiority in the accuracy of implant installation using sCAIS compared to free-hand techniques (64, 65). Based on the ideal implant position, a surgical guide is created using the implant planning or an additional CAD software. Most of the market-available surgical guide types have a closed-frame design, which can limit the visibility and accessibility to the operator and the irrigation of the rotating instruments. To control the intraoral fit, windows are digitally added to the surgical guides with a closed-frame design. An alternative, open-frame tubular design is proposed by the implant planning software SMOP (Swissmeda AG, Baar, Switzerland) with selective support on the tooth surface (32), which allows the drilling procedures to be performed and the implant to be installed under direct sight.

To manufacture the surgical guides in a digital workflow, either subtractive (e.g., milling) or additive (e.g., 3D printing) manufacturing technologies are used (Fig. 7). Henprasert et al. reported comparable accuracy in implant installation using AM- or SM-based surgical guides (66). To date, AM is preferred over SM due to the inferior production costs and waste of material. VAT polymerization is the most adapted AM technique to create surgical guides (67). It relies on the selective laser-induced polymerization of the liquid resin contained in a vat. Both stereolithography (SLA) and digital light processing (DLP) rely on VAT technology. The former utilizes a point laser

beam for photopolymerization, whereas the latter uses a larger light beam. SLA and DLP allow the creation of objects with high dimensional accuracy (68). Indeed, several parameters, such as resin type, build angle, and light intensity, affect the accuracy of the printing process (69). Once the printing procedure is completed, the object is washed with alcohol and successively light cured. Extensive postprocessing and high production costs represent the two main disadvantages of VAT polymerization (70).

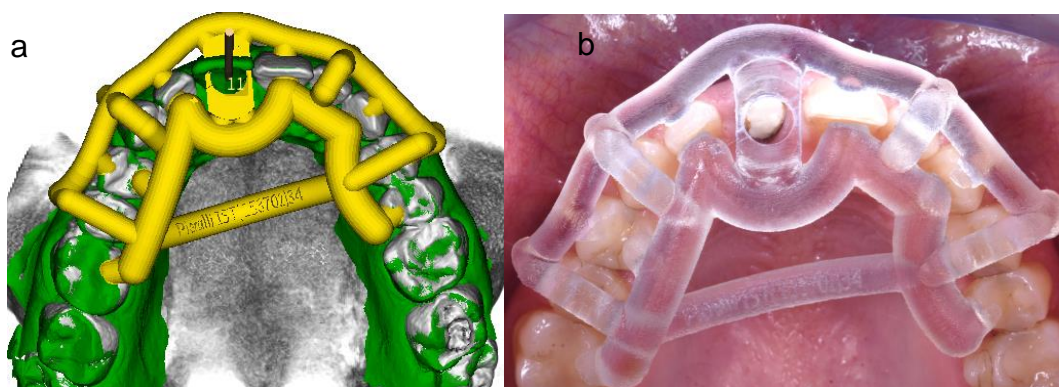


Figure 7: Exemplary sample of a surgical guide designed (a) with an open frame and subsequently created (b) by SLA for immediate implant installation in the position of the central maxillary right incisor. This surgical guide was made of resin and underwent two steps of postprocessing, namely washing with alcohol and light curing.

An alternative, easier, and more economical 3D printing method is material extrusion (ME), also called fused filament fabrication (FFF) or fused deposition modeling (FDP) (71). Dentistry has recently shown increased interest in this technology (72). ME technology is based on using thermoplastic filaments to print objects, layer by layer, onto a printing bed. A broad spectrum of feedstock materials (among others, polymers) are available for ME (73). ME relies on a straightforward printing process, minimal postprocessing time, and inferior production costs compared to SLA or DLP (74). The quality of extruded objects is strictly dependent on the printing parameters. Studies have reported a lack of dimensional accuracy or low surface characteristics as the

main potential drawbacks of ME (75). In dentistry, customized impression trays, models, and surgical guides can be created by ME (72) (Fig. 8).

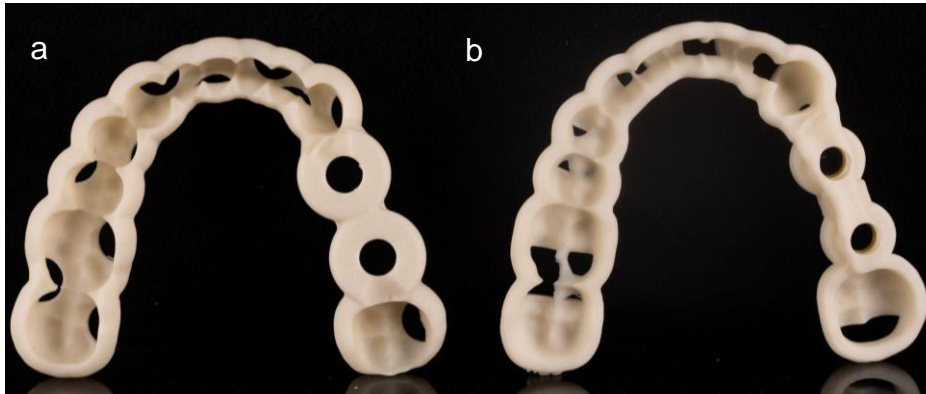


Figure 8: Surgical guides planned with a closed frame design and two implant planning software (a. coDiagnostiX, DentalWings, Montreal, Canada; b. ImplantStudio, 3Shape, Copenhagen, Denmark). Both surgical guides were made of an experimental biocopolyester, and created by ME. This type of surgical guide was tested in Manuscript 4. Picture: Courtesy of Mr. Severin Rothlauf.

1.2.5 Intraoral implant digitization

After guided implant installation, the information regarding the intraoral implant position must be communicated to the lab to create the prosthetic reconstruction. To transfer the information from the clinic to the lab, within a digital workflow, a scan body is screwed onto the implant and digitized using an IOS (Fig. 9). Scan bodies are usually made of polyether-ether-ketone (PEEK) and represent the equivalents of copings for conventional impressions. They serve as an intermediate reference for the IOS to capture the subgingival implant position by providing a point cloud dataset. Market-available IOS systems are based on various technologies, such as confocal microscopy or optical triangulation, which can influence their accuracy (76, 77). In addition, multiple other factors, such as scan body design (78), material (79), and scanning strategy (80), can affect the digitization process.

The accuracy of a system can be defined as the combination of trueness and precision, according to ISO standard 5725 (81). On the one hand, trueness describes the nearest representation of the arithmetic mean from multiple measurements to a “true or accepted reference number.” On the other hand, the consistency and repeatability across the test results are referred to as precision. A system’s precision is related to the standard deviation intervals. To date, equal or even higher accuracy can be achieved when directly digitizing a single (82) or two adjacent implants (83) compared to conventional impressions with elastomers. Differently, significant discrepancies in terms of accuracy have been measured in the case of full-arch implant scans (84). Major deviations are caused by multiple image stitching, reflective surfaces, mobile mucosa, and further factors (85). For full-arch scans, using scanning aids to splint the implants seems to improve the trueness of the procedure significantly. However, future clinical studies must confirm the in vitro results (86).

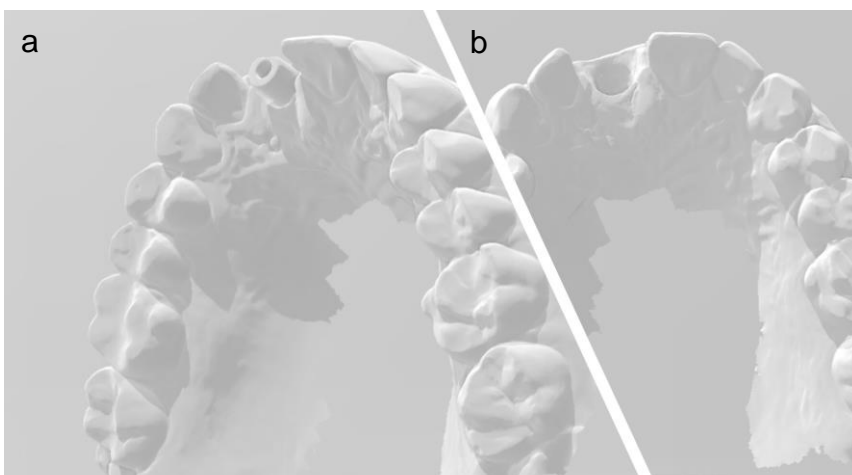


Figure 9: Digitized maxilla for the rehabilitation of the right central incisor with (a) and without (b) the scan body in situ. The scan on the left provides information regarding the implant position/angulation, and the one on the right offers data on the emergence profile.

1.3 Scientific question(s)

The aim of the studies included in the present thesis, was to investigate four different steps of the digital workflow applied to the implant prosthodontic rehabilitation. Our research group investigated the topics of virtual implant planning (Manuscript 1), implant selection (Manuscript 2), surgical guide manufacturing (Manuscripts 3, 4, and 5), and intraoral implant digitization (Manuscript 6).

The first manuscript evaluated the registration accuracy when decreasing the radiographic field of view (FOV) size for virtual implant planning. The focused question was formulated as follows: **Does reducing the FOV volume for sCAIS impact the trueness and precision of the registration procedure? (Manuscript 1).**

Moreover, the second manuscript focused on implant selection. For this purpose, a CAD/CAM RAI system was investigated. Clinical outcomes and PROMs of 31 patients were retrospectively collected and analyzed. The focused question for this study was, **Are clinical results and PROMs when using a CAD/CAM RAI system comparable to data from the literature regarding prefabricated screw-shaped immediate implants? (Manuscript 2)**

In the third, fourth, and fifth included manuscripts, ME-based sterilizable surgical guides made of polylactic acid (PLA) were evaluated regarding trueness (Manuscript 3), trueness and precision (Manuscript 4), and short-term biocompatibility in the oral environment (Manuscript 5). The scientific questions of the three research projects were,

- **Do the printing technology (test: ME, control: SLA) and the use of metal sleeves affect the trueness of guided implant installation? (Manuscript 3)**
- **Do variables such as planning software and surgical guide design affect the final position of implants installed with ME-based drilling guides? (Manuscript 4)**
- **Does the experimental biocopolyester used to create the surgical guides in Manuscripts 3 and 4 respect, in vitro, the biocompatibility standards for short-term intraoral usage? (Manuscript 5)**

After surgical installation, the exact intraoral implant position must be transferred to the dental lab for fabrication of the prosthetic reconstruction. For this purpose, scan bodies are mounted onto the implants and digitized to deliver the information to the lab within a digital workflow. In the fifth manuscript, we investigated if modern IOS systems were able to digitize the abutment of a one-piece ZrO₂ implant system with the same accuracy as for a standard PEEK scan body mounted onto a bone-level two-piece titanium implant. Furthermore, a virtual tool was created for the accurate reconstruction of incomplete scans of the tested one-piece implant type. The focused question of the research was: **Can we avoid using scan bodies when digitizing one-piece ZrO₂ implants? Furthermore, is it possible to accurately reconstruct incomplete scans of the tested implant (Manuscript 6)?**

2 PERSONAL RESEARCH PROJECTS

2.1 Manuscript 1 – Influence of reducing the radiographic field of view on the accuracy of registration with intraoral surface scans

CBCB or CT scans are used as imaging techniques for computer-aided implant planning, but they also expose patients to a variable amount of ionizing irradiation (87). Therefore, considering the “as low as diagnostically acceptable” (ALADA) and “as low as reasonably achievable” (ALARA) principles, attempts to reduce the irradiation of the head and neck region are necessary (29).

In this non-interventional retrospective pilot study, two operators combined the intraoral scans of 15 patients with three different radiographic FOV volumes: full-arch, quadrant, and adjacent tooth/teeth, performing 657 superimpositions in total. They used a beta version of the implant planning software SMOP (Swissmeda) to perform the registration procedure. The operators comprised a beginner with 1 week of intensive training in dataset registration and a long-time professional in virtual implant planning.

The University Medical Center Freiburg Ethics Committee granted authorization to execute the study (Study number: 20/1205; Decision of the Ethics Committee: 11/24/2020). This study was conducted according to the EQUATOR guidelines (<http://www.equator-network.org>) and the STROBE Statement 2020 for observational studies (<http://www.strobe-statement.org>).

The results of this research were presented as oral communication in the basic research category at the 28th Annual Scientific Meeting of the EAO (Digital Days, online) in 2021, and the abstract was subsequently published in *Clinical Oral Implant Research* (88). Mr. Christoph Beyer also presented the study as a digital poster at the 35th Congress of the German Association of Oral Implantology e.V. (DGI) of 2021 in Wiesbaden, Germany.

The following text corresponds to the abstract of the article:

Pieralli, S., Beyer, C., Wesemann, C., Vach, K., Russe, M. F., Kernen, F., Nelson, K., & Spies, B. C. (2022). *Impact of radiographic field-of-view volume on alignment accuracy during virtual implant planning: A noninterventional retrospective pilot study. Clinical oral implants research, 33(10), 1021–1029. <https://doi.org/10.1111/clr.13983>*

Impact of the radiographic field of view volume on the alignment accuracy during virtual implant planning: A non-interventional retrospective pilot study

Objective

To evaluate the impact of reducing the radiographic field of view (FOV) on the trueness and precision of the alignment, between cone beam computed tomography (CBCT) and intraoral scanning data, for implant planning.

Materials and Methods

Fifteen participants presenting with one of three clinical scenarios: single tooth loss (ST, n=5), multiple missing teeth (MT, n=5), and presence of radiographic artifacts (AR, n=5) were included. CBCT volumes covering the full-arch (FA) were reduced to the quadrant (Q) or the adjacent tooth/teeth (A). Two operators, an expert (exp) in

virtual implant planning and an inexperienced clinician performed multiple superimpositions, with FA-exp serving as a reference. Deviations were calculated at the implants' apex and shoulder level. Thereafter, linear mixed models were adapted to investigate the influence of FOV on the discrepancies.

Results

Evaluation of trueness compared to FA-exp resulted in the largest mean (AR-A: $0.10 \pm 0.33\text{mm}$) and single maximum discrepancy (AR-Q: 1.44mm) when in presence of artifacts. Furthermore, for the ST group, the largest mean error ($-0.06 \pm 0.2\text{mm}$, shoulder) was calculated with the FA-FOV, while for MT, with the intermediate volume ($-0.07 \pm 0.24\text{mm}$, Q). In terms of precision, mean SD intervals were $\leq 0.25\text{mm}$ (A-exp). Precision was influenced by the FOV volume (FA<Q<A) but not by the operators' expertise.

Conclusion

For single posterior missing teeth, an extended FOV did not improve the accuracy of registration. However, in the presence of artifacts or multiple missing posterior teeth, caution is recommended when reducing the FOV.

Impact of radiographic field-of-view volume on alignment accuracy during virtual implant planning: A noninterventional retrospective pilot study

Stefano Pieralli¹ | Christoph Beyer^{1,2} | Christian Wesemann¹ | Kirstin Vach³ | Maximilian F. Russe⁴ | Florian Kernen² | Katja Nelson² | Benedikt C. Spies¹

¹Center for Dental Medicine, Department of Prosthetic Dentistry, Medical Center – University of Freiburg, Faculty of Medicine – University of Freiburg, Freiburg, Germany

²Center of Dental Medicine, Department of Oral and Maxillofacial Surgery, Medical Center – University of Freiburg, Faculty of Medicine – University of Freiburg, Freiburg, Germany

³Medical Center – University of Freiburg, Institute for Medical Biometry and Statistics, Faculty of Medicine – University of Freiburg, Freiburg, Germany

⁴Department of Diagnostic and Interventional Radiology, Medical Center – University of Freiburg, Faculty of Medicine – University of Freiburg, Freiburg, Germany

Correspondence

Stefano Pieralli, Center for Dental Medicine, Department of Prosthetic Dentistry, Medical Center – University of Freiburg, Faculty of Medicine – University of Freiburg, Freiburg, Germany.
Email: stefano.pieralli@uniklinik-freiburg.de

Abstract

Objective: To evaluate the impact of reducing the radiographic field of view (FOV) on the trueness and precision of the alignment between cone beam computed tomography (CBCT) and intraoral scanning data for implant planning.

Materials and Methods: Fifteen participants presenting with one of three clinical scenarios: single tooth loss (ST, $n = 5$), multiple missing teeth (MT, $n = 5$) and presence of radiographic artifacts (AR, $n = 5$) were included. CBCT volumes covering the full arch (FA) were reduced to the quadrant (Q) or the adjacent tooth/teeth (A). Two operators, an expert (exp) in virtual implant planning and an inexperienced clinician, performed multiple superimpositions, with FA-exp serving as a reference. The deviations were calculated at the implant apex and shoulder levels. Thereafter, linear mixed models were adapted to investigate the influence of FOV on discrepancies.

Results: Evaluation of trueness compared to FA-exp resulted in the largest mean (AR-A: 0.10 ± 0.33 mm) and single maximum discrepancy (AR-Q: 1.44 mm) in the presence of artifacts. Furthermore, for the ST group, the largest mean error (-0.06 ± 0.2 mm, shoulder) was calculated with the FA-FOV, while for MT, with the intermediate volume (-0.07 ± 0.24 mm, Q). In terms of precision, the mean SD intervals were ≤ 0.25 mm (A-exp). Precision was influenced by FOV volume (FA < Q < A) but not by operator expertise.

Conclusions: For single posterior missing teeth, an extended FOV does not improve registration accuracy. However, in the presence of artifacts or multiple missing posterior teeth, caution is recommended when reducing FOV.

KEYWORDS

ALADA, ALARA, CBCT, FOV, guided implantology, virtual planning

1 | INTRODUCTION

Prosthetically driven virtual implant planning and guided surgery result in more successful rehabilitations and less complications (Canullo et al., 2016; Schneider et al., 2019; Tattan et al., 2020). Digital reconstruction of the intraoral tissues and ideal digital planning of the implant position necessitates three-dimensional (3D) radiographic images, usually acquired via cone beam computed tomography (CBCT). These tomographic images are exported in DICOM format (Digital Imaging and Communications in Medicine) (Jacobs & Quirynen, 2014) and are superimposed with optically acquired surface datasets (Kernen et al., 2016). The latter ones are obtained with intraoral scanners or by stone cast digitization in the dental laboratory and are usually exported as Standard Tessellation Language (STL) data (Emara et al., 2020; Papaspyridakos et al., 2016).

CBCT is an imaging technology used to visualize bone morphology, as well as soft tissue structures and hollow spaces in the bone, for example, the course of the inferior alveolar nerve canal, and should be limited to the region of interest (ROI) to minimize the size of ionizing irradiation in the head and neck region (Pauwels, 2015). The exposure parameters and size of the field of view (FOV) are related to the absorbed radiation dose and should be carefully selected (da Silva Moura et al., 2019; Harris et al., 2012; McGuigan et al., 2018). In the guidelines for implant imaging proposed by the European Association for Osseointegration (EAO) (Harris et al., 2012), the use of techniques requiring less exposure to radiation for patients was stated as an obligatory development to be addressed in future research. Almost a decade after, specific recommendations for low-dose imaging protocols associated with virtual implant planning are still missing (Yeung et al., 2019). Regardless of the clinical situation, the selected FOV acquired for implant planning with subsequent guided surgery is routinely overextended and includes several anatomical structures located outside the ROI. This appears in contrast to the ALARA (as low as reasonably achievable)/ALADA (as low as diagnostically acceptable) principles (White et al., 2014), and their requirement for careful use of ionizing radiation (Bornstein et al., 2014).

Implant planning software are used to overlay intraoral scan data as STL files with CBCT data in a process called registration (Flügge et al., 2017). The latter ones, in the form of DICOM files, are converted into a 3D image visually comparable to the created STL file using volume rendering technique (VRT) based on grayscale thresholds. In addition, multiplanar image reformation (MPR) is used to match the boundaries of the STL file to the cross-sectional data from CBCT. The registration process can be automatic, based on best-fit algorithms, and/or requires initial manual selection of the corresponding areas/points, usually teeth or other hard tissue reference markers (Kernen et al., 2020). Finally, manual fine-tuning might be required for an ideal matching. While the ideal implant position is determined according to both CBCT and intraoral scanning data, the surgical guide design is solely based on the latter. Therefore, accurate matching is mandatory to avoid implant misplacement (Tahmaseb et al., 2018). Consequently, software-based inaccuracies

resulting from a compromised matching process might subsequently result in hardware-based inaccuracies, for example, due to the manufacturing process of the surgical guide or the implant installation procedure, thereby affecting the outcome (Chen et al., 2020; Raico Gallardo et al., 2017; Zhou et al., 2018).

The importance of reducing FOV volume for virtual implant planning was addressed in a recent conference paper (Singh & Hamilton, 2021). To the best of the authors' knowledge, no previous study has evaluated whether the accuracy of the registration process is affected by FOV extension. A reduction in the FOV could potentially lead to decreased patient irradiation; therefore, an assessment of accuracy in case of different FOV extensions in diverse clinical scenarios is needed.

In this investigation, three different FOV volumes were extracted from 15 clinical CBCT datasets representing three different clinical scenarios and used for superimposition with the intraoral surface data of the selected patients. One partial volume was limited to the quadrant (Q), whereas the other was further reduced to the adjacent (A) tooth/teeth next to the implant site. This study aimed to investigate the effect of three FOV volumes for alignment on the accuracy of the planned implants.

The null hypothesis of the study assumed no difference in terms of matching trueness and precision as a function of the FOV volume or the clinical scenario.

2 | MATERIALS AND METHODS

2.1 | Study design

This investigation was designed as a noninterventional retrospective pilot study and was conducted in accordance with the Declaration of Helsinki. Approval to conduct the study was obtained from the Ethics Committee of the Medical Center, University of Freiburg, Germany (investigation number: 20/1205; ethics committee vote: November 24, 2020). Both the EQUATOR guidelines (<http://www.equator-network.org>) and Strobe-statement 2020 for observational studies (<http://www.strobe-statement.org>) were adhered to in the study. All participants signed an informed consent form and approved the use of their clinical data.

The eligibility criteria included patients with a single missing tooth (ST) or multiple adjacent missing teeth (MT) in the posterior region. In addition, participants presenting with sources of radiographic metal strip artifacts (AR) originating from implants and/or full-coverage restorations located in the proximity of the implant site were included as the third group.

2.2 | Data collection

Three-dimensional radiographic and surface datasets of 15 patients used for implant planning at the Department of Oral and Maxillofacial Surgery, University of Freiburg, Germany, between

2019 and 2020 were retrospectively collected. Intraoral digitization was performed by one experienced operator (F.K.) using a scanning device (TRIOS 3, 3Shape), whereas CBCT scans were performed by medical technicians using one device (Morita Accuimot 170, J. Morita GmbH) with the following settings: FOV: 170mm×50mm (diameter×height), circulation time: 14.5 s, tube voltage: 120kV, and current intensity: 32mA. The FOV volume for each patient scan included the entire jaw as the standard procedure. Thereafter, the original DICOM dataset was exported directly from the imaging software (i-Dixel, J. Morita GmbH), integrated within the CBCT device, into the beta version (99.00.9) of an implant planning system (Version 2.17.1 SMOP, Swissmeda AG), and merged with the STL file of the corresponding intraoral scan. A single 4.1mm×10mm bone-level implant (Straumann® Bone Level [BL], Straumann AG) was virtually positioned in the edentulous area of each included clinical case and subsequently used as a landmark for the measurement of discrepancies (Figure 1).

2.3 | Radiographic subsample volumes and registration process

To generate volumes with a reduced FOV, an additional “cropping function” of the planning software (Swissmeda AG) was developed. For this purpose, a portion of the alveolar ridge of the original radiographic dataset was selected and all voxels along this segment were used to define the partial volume. For each clinical case, two reduced

volumes from the original FA were created: One was limited to the quadrant (Q), and one was reduced to the tooth/teeth (A) adjacent to the planned implant site. All FOV extensions were exported with the same coordinates to allow for further comparison.

Each FOV volume (FA, Q, A) of the 15 clinical cases was uploaded as a separate file and merged with the STL data incorporating the implant 10 times by an inexperienced operator who had received basic training in dataset alignment and had no expertise before this investigation (C.B.) (Figure 2). An experienced user (J.B.), a long-time professional in the field of virtual implant planning and dataset superimposition, performed 10 alignments for every FOV partial volume of two randomly selected cases each of the ST, MT, and AR. In addition, one-time matching was conducted by J.B. for each FOV size in all remaining cases ($n = 9$). Overall, the accepted reference for trueness was the combination expert-FA of each included clinical case.

2.4 | Calculation of discrepancies

After matching, all surface scans were exported as STL files from the implant planning system and imported into a three-dimensional inspection software (Geomagic Control X, 3D Systems), maintaining the same coordinates (Figure 3). A best-fit algorithm was used to align the imported datasets using several reference points located on the outer part of the STL files, such as teeth and mucosa. The submerged implants included in the STL files were initially not visible from the

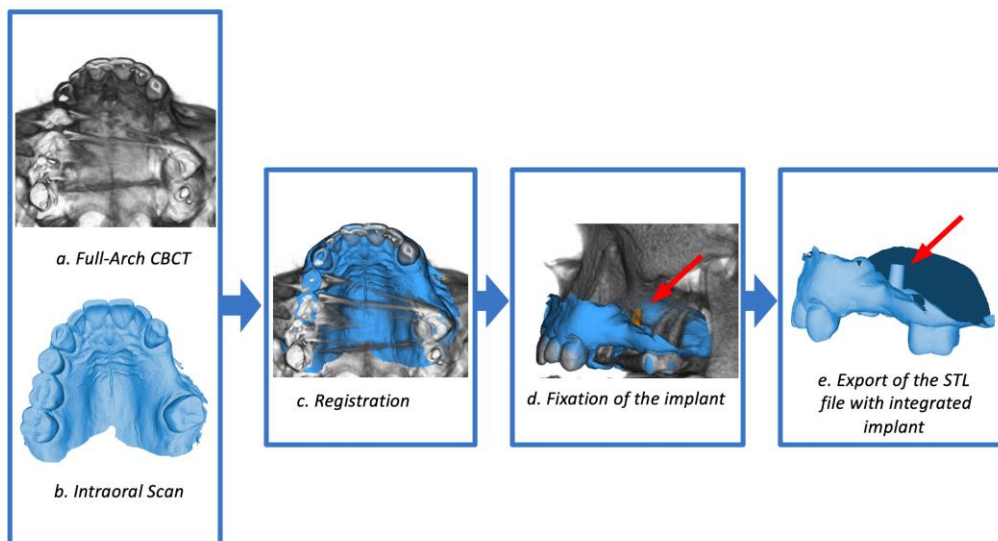


FIGURE 1 Creation of an STL file with integrated landmark in form of a 4.1×10mm oral implant for each case. A CBCT scan (DICOM) covering the full arch (a) and the corresponding intraoral scan (STL) (b) were matched (c) using an implant planning software. An implant was positioned (d) and served, subsequently, as reference for the measurement of discrepancies. Finally, the STL file with integrated implant was exported (e) and used as reference for all further registration processes with different FOV volumes.

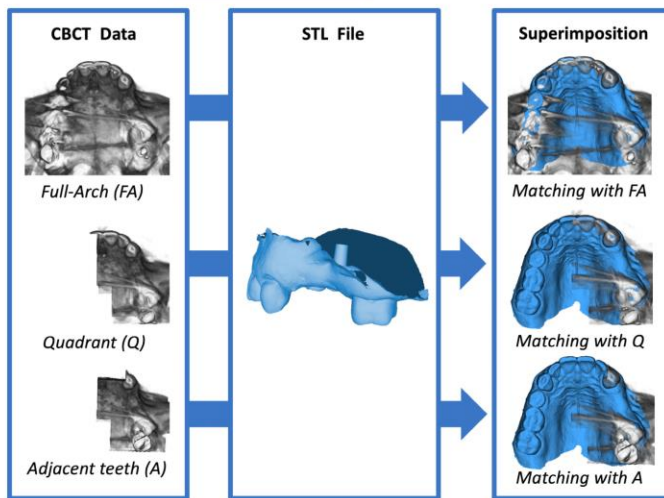


FIGURE 2 All radiographic original and reduced volumes were matched with the same intraoral scan of each clinical case, incorporating an implant, using the implant planning software. After superimposition with the different FOV volumes, the STL file with the new coordinates from the registration was exported and imported in a measuring software for the calculation of discrepancies. Exemplary presentation of a clinical case with artifacts.

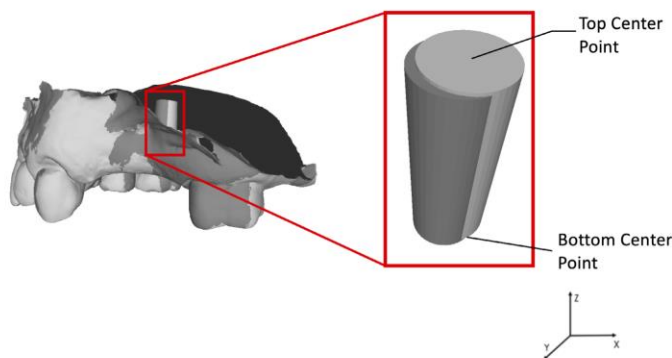


FIGURE 3 After matching with the planning software, each aligned STL file was imported in a measurement software and superimposed with the reference (FA-exp) to assess trueness. For the evaluation of precision, standard deviations were calculated for each coordinate of all situations (ST, MT, AR) and FOVs (FA, Q, A) for both expert and nonexpert. Discrepancies were measured at implant shoulder (top center point) and apex (bottom center point). Exemplary presentation of trueness evaluation.

outside and were therefore not used as a reference for alignment. They later measured the discrepancies between test and reference implants after increasing the translucency of the STL files. One point, positioned at the top center of the implant, was considered the reference for the shoulder, while the other point, located at the bottom center, represented the apex. Both were used as landmarks to measure discrepancies at the horizontal and vertical levels between the aligned datasets (x: sagittal (mesiodistal), y: transverse (buccolingual-palatal), z: vertical (coronoapical)). To assess trueness, exported scan data were aligned 10 times for each FOV size (FA, Q, A) with the corresponding reference (exp-FA), resulting in a total of 450 alignments. To calculate precision, the standard deviation interval for each coordinate (x, y, z) of the superimposed datasets was analyzed for both expert and inexperienced clinicians. For better comprehension, after pooling the clinical situations (ST, MT, AR), the average standard deviation of each FOV volume (FA, Q, A) was calculated for each operator.

2.5 | Statistical methods

With 10 alignments per case, a difference of 1 mm in one of the coordinates (x, y, z) could be detected with a power of 90%, assuming a standard deviation of 0.5. Linear mixed models with random intercepts were fitted for each implant position and coordinate to evaluate the differences between FOV sizes. Scheffé's method was applied to correct for multiple testing, and the probability level for statistical significance was set at $p = .05$. To analyze the precision for each clinical situation (ST, MT, A), 10 repetitions were performed by both expert and nonexpert for two of the five cases of each category (ST, MT, A). Linear mixed models with independent residuals and restricted maximum likelihood techniques were used to compute standard deviations for expert and nonexpert in a pooled setting for all situations. The calculations were performed using the statistical software STATA 17.0 (StataCorp).

3 | RESULTS

3.1 | Outcome data

Fifteen participants (six female and nine male, mean age: 56.8 years) were included, representing three different clinical scenarios (ST, MT, AR; $n = 5$ cases each; ST: 3 maxillae and 2 mandibles, MT: 2 maxillae, and 3 mandibles and AR: 4 maxillae and 1 mandible). The smallest FOV volume, A, resulted in a diameter of 45–60 mm and a height of 35 mm. For trueness assessment, five cases per clinical scenario with $n = 10$ alignments, each by nonexpert and expert, were considered. To evaluate precision, two cases per indication were selected, each examined 10 times by both operators.

3.2 | Trueness assessment

In the ST group, the mean outcomes were significantly affected by the FOV volume (Figure 4). When comparing FA with Q at the implant apex or FA with A at both implant apex and shoulder, significant transverse deviations were found ($p = .02$). No further significance could be calculated (Table 1).

In the MT group, the highest mean deviation compared to the reference was measured at the implant apex in the transverse direction using the FOV volume Q (-0.07 ± 0.24 mm). No significant differences were observed when comparing the three FOV extensions.

When analyzing the mean results of the inexperienced operator within the AR group, significant vertical differences were assessed at the implant shoulder level in favor of the largest (FA) compared to the smallest (A) FOV volume ($p = .02$).

The highest differences compared with the reference measurements were calculated at the implant apex level (Table 2). For the ST group, the highest discrepancy was calculated for the FA-FOV (0.58 mm, transverse). In the MT group, the maximum deviation was measured with the smallest FOV (A: 0.90 mm, sagittal). Scenarios with radiologic artifacts (AR) showed highest discrepancy compared to the reference when using the FOV volume Q (Q: 1.44 mm, vertical).

3.3 | Precision assessment

To obtain an overview of the precision of the different FOV volumes, the individual scenarios were pooled and descriptive statistics were generated.

For all scenarios, the mean SD was ≤ 0.25 mm (A-exp) (Table 3). When considering single coordinates, SD intervals appeared in most cases depending on the FOV volume: $FA < Q < A$. Mean standard deviation intervals did not depend on the operator's expertise (expert vs. inexperienced clinician).

4 | DISCUSSION

The objective of this investigation was to evaluate whether reducing the radiographic FOV influences the accuracy of the registration process with the intraoral surface dataset when virtually planning the implant. To the best of our knowledge, the authors of the present study could not identify any comparable studies in the literature, except for a recent conference paper by Singh and Hamilton (2021). This demonstrates both the lack of data on the topic and the current efforts of other research groups to find viable solutions. The importance of this investigation lies in the fact that it explores a novel method to improve the workflow of virtual implant planning. Reducing the FOV means less irradiation for the patient but also a smaller diagnostic field for the radiologist/clinician and potentially lower costs of the CBCT scans, depending on the clinical case.

The null hypothesis, which presumed no differences at the implant level in terms of accuracy regardless of the FOV extension and clinical situation, had to be partially rejected. According to the ISO standard 5725, accuracy is defined as the combination of both trueness and precision of a system (Boulanger et al., 2012). While trueness relates to the closest representation of the arithmetic mean of multiple measurements to a "true or accepted reference value," precision refers to the consistency and repeatability between the test results and is calculated considering the standard deviation interval.

For this study, given the impossibility of determining the ideal and most accurate superimposition (true value), an accepted reference for trueness was arbitrarily chosen. In everyday practice,

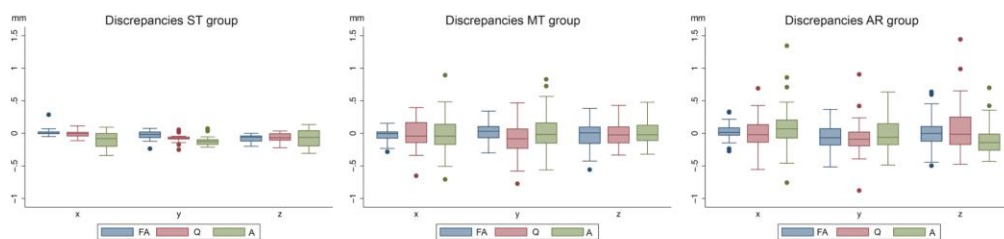


FIGURE 4 Boxplots for discrepancies of the virtual implant apical position in the ST, MT and AR groups. FOV sizes: FA (full arch), Q (quadrant), and a (adjacent). X, sagittal discrepancies; y, transversal discrepancies; z, vertical discrepancies.

TABLE 1 Trueness (mean ± SD) of implant apex/shoulder by clinical situations and FOV significances were highlighted with the same subscript letter

Clin. situation	FOV	Apex (mm)			Shoulder (mm)		
		x	y	z	X	y	z
ST	FA	-0.02 ± 0.09	0.04 ± 0.18 _{a,b}	-0.04 ± 0.15	0.00 ± 0.07	0.05 ± 0.15 _c	-0.06 ± 0.16
	Q	0.01 ± 0.08	-0.03 ± 0.13 _a	-0.04 ± 0.11	0.01 ± 0.07	-0.02 ± 0.11	-0.06 ± 0.12
	A	0.02 ± 0.16	-0.04 ± 0.12 _b	-0.05 ± 0.15	0.02 ± 0.12	0.01 ± 0.11 _c	-0.05 ± 0.15
MT	FA	-0.03 ± 0.09	0.02 ± 0.14	-0.02 ± 0.19	-0.04 ± 0.77	0.01 ± 0.09	-0.02 ± 0.19
	Q	-0.01 ± 0.22	-0.07 ± 0.24	-0.00 ± 0.18	-0.04 ± 0.14	-0.03 ± 0.17	-0.01 ± 0.18
	A	-0.03 ± 0.28	0.01 ± 0.28	0.02 ± 0.19	-0.07 ± 0.18	0.02 ± 0.17	0.01 ± 0.20
AR	FA	0.02 ± 0.12	-0.05 ± 0.22	0.00 ± 0.24	-0.00 ± 0.10	-0.05 ± 0.19	0.00 ± 0.23 _d
	Q	0.00 ± 0.23	-0.06 ± 0.25	0.06 ± 0.36	0.0 ± 0.17	-0.06 ± 0.16	0.05 ± 0.36
	A	0.10 ± 0.33	-0.02 ± 0.25	-0.09 ± 0.25	0.04 ± 0.25	-0.04 ± 0.18	-0.09 ± 0.25 _d

Abbreviations: ST, single tooth; MT, multiple teeth; AR, artifacts; FA, full arch; Q, quadrant; A, adjacent; x, sagittal discrepancies; y, transverse discrepancies; z, vertical discrepancies. [Correction added on 20 August 2022, after first online publication: Table 1 was updated in this current version.]

TABLE 2 Maximum discrepancy of implant apex by clinical situations and FOV

Clin. situation	FOV	Apex (mm)		
		X	y	z
ST	FA	0.29	0.58	0.30
	Q	0.20	0.53	0.21
	A	0.39	0.19	0.40
MT	FA	0.15	0.34	0.39
	Q	0.40	0.47	0.43
	A	0.90	0.84	0.48
AR	FA	0.33	0.37	0.64
	Q	0.70	0.91	1.44
	A	1.34	0.64	0.70

Abbreviations: ST, single tooth; MT, multiple teeth; AR, artifacts; FA, full arch; Q, quadrant; A, adjacent tooth/teeth; x, sagittal discrepancies; y, transverse discrepancies; z, vertical discrepancies.

TABLE 3 Average standard deviations (mm) calculated for expert and inexperienced operator for each coordinate and FOV volume with all clinical scenarios pooled together

	Expert			Inexperienced operator		
	FA	Q	A	FA	Q	A
X	0.14	0.20	0.25	0.07	0.13	0.24
Y	0.11	0.18	0.22	0.11	0.12	0.18
Z	0.22	0.11	0.12	0.11	0.11	0.16

Abbreviations: ST, single tooth; MT, multiple teeth; AR, artifacts; FA, full arch; Q, quadrant; A, adjacent tooth/teeth; x, sagittal discrepancies; y, transverse discrepancies; z, vertical discrepancies.

long-term professional expertise in virtual implant planning and the availability of a high-quality full-arch CBCT scan are considered ideal for dataset registration and served as the reference (FA-exp) in this

study. Nevertheless, the delivery of FA-exp by a single operator may have resulted in high intra-operator bias. A sample size calculation was not possible because of the pilot design of the study; therefore, the number of five patients for each of the three clinical scenarios included was chosen arbitrarily. Power analysis was performed considering the number of alignments ($n = 10$) for each FOV volume ($n = 3$) of each clinical case ($n = 15$), based on the wish to be able to show differences in mean values of two methods of 1 mm size with 90% power. A total of 657 alignments were observed and divided into $n = 450$ by inexperienced users and $n = 207$ by experienced users. Based on the amount of data collected, interpreted, and analyzed, this investigation provides significant findings that are necessary to conduct further studies with a more detailed sample size calculation.

Clinical investigations evaluating the accuracy of guided implant procedures typically involve large FOVs ($\geq 10 \times 10$ cm) (Lou et al., 2021). For this study, three FOV volumes for each of the 15 included clinical cases with single or multiple adjacent missing teeth, with and without the presence of radiographic artifacts, were repeatedly superimposed with the corresponding intraoral scans. Discrepancies were calculated at the level of a virtually positioned bone level implant. Independent of the FOV volume, the highest mean difference from the reference of ≤ 0.1 mm was found. This might question the clinical benefits of using large FOV volumes. Furthermore, under specific circumstances, matching accuracy was found to be significantly affected by FOV volume, for example, in the presence of radiographic artifacts.

Minor mean deviations were assessed using different FOV extensions in this study. However, it should be noted that deviations at the software level sum up with subsequent inaccuracies at the hardware level, for example, during manufacturing of the guide, insertion/fit in the mouth, or drill guidance during implant surgery (Cassetta et al., 2013). Consequently, the calculated maximum deviations may result in clinically relevant discrepancies when followed by further hardware-related inaccuracies that have not yet been specified. In this investigation, the distribution of outliers was

predominantly affected by the clinical scenario (ST < MT < AR) compared with the effect of the FOV volume. Maximum deviations of up to 1.44 mm were measured using the FOV volume Q in the presence of artifacts, which confirms artifact sources as the principal cause of registration errors. For selected clinical scenarios, as for ST, a larger FOV volume did not lead to a significantly more accurate registration process, nor did it show decreased outliers.

Precision was not significantly influenced by the expertise of the operator, suggesting that high reproducibility of registration can be achieved even by non-experienced operators. Furthermore, when pooling the three clinical scenarios evaluated, SD intervals were affected by the FOV volume ($FA < Q < A$), but with minimal differences. This leads to the assumption that the FOV volume may have a negligible influence on the precision of the process, which is in accordance with the preliminary results presented by Singh and Hamilton (2021).

Beam hardening artifacts are the consequence of scattering radiation from high-density objects, such as fixed metal-based prosthetic restorations (Alaidrous et al., 2021) or oral implants (Sancho-Puchades et al., 2015). In their investigation, Flügge et al. (2017) assessed the negative impact of imaging artifacts on the registration accuracy between CBCT and surface scans, and encouraged research on alternative technologies that are potentially less prone to artifact impact, such as magnetic resonance imaging (Flügge et al., 2020).

In the present study, a single CBCT device and intraoral scanner (IOS) were used for all clinical cases to minimize potential confounders linked to the data acquisition process (Güth et al., 2013; Schubert et al., 2019). Other factors that may affect the accuracy of alignment are related to the type and distribution of the anatomical (Flügge et al., 2017) and fiducial (Rangel et al., 2013; Vercruyssen et al., 2014) landmarks used for registration. In this study, no fiducial markers and only anatomical landmarks, such as natural teeth, were used for registration.

A novel methodology for retrospective subsample FOV creation from a single CBCT scan using a test function of a well-documented implant planning software (Kernen et al., 2020; Schneider et al., 2019) was adapted, but potential distortions of the DICOM dataset might have occurred, for example, due to voxel rounding. Generating FOV partial volumes from the raw data included in the CBCT device and not from the exported DICOM file, as was done in this investigation, would have potentially avoided alterations derived from overlapping neighboring radiological structures. However, exporting subvolumes with an identical coordinate system to the original radiographic dataset was not possible. For ethical reasons, performing CBCTs with different FOV extensions in the same patient was not considered as an option.

Protocols for virtual oral implant planning with reduced radiation dose are being investigated and involve using a different number of basic images (de Castro et al., 2021) as well as larger voxels, partial rotations and reduction in mAs (Yeung et al., 2019). This study proposed an alternative for radiation dose reduction based on the use of a smaller FOV, which was reduced to 45 × 35 mm

in this study. If on the one side, reducing the FOV has proven to lead to an reduced effective radiation dose (Jadu et al., 2018), on the other side, an exact quantification of the irradiation variation depending on the FOV extension was not performed and should be further evaluated.

The limitations of the present investigation relate to the pilot design with a limited number of clinical scenarios and software operators. Therefore, their number should be increased in future studies. Clinical indications should be extended, for example, to the anterior region and to cases of partial edentulism with few remaining teeth. Additionally, numerous software operators with different expertise in virtual implant planning should be involved in assessing whether reducing the FOV size significantly compromises the alignment procedure.

Comparisons regarding the implant position (maxilla/mandible) or the time needed for registration by an experienced as well as inexperienced operator were not performed in this study and should be considered in further investigations. Furthermore, a validation process for the adapted method of FOV reduction is still required, and further studies should investigate the feasibility of reducing FOV size with alternative workflows. Future investigations should include different implant planning systems to evaluate their capability to provide accurate registration with smaller FOV volumes. For example, automatic registration can be performed using a best-fit algorithm.

In summary, in this pilot study, accurate registration of CBCT images with a reduced FOV was possible. However, caution is recommended when radiographic artifacts are present. For selected clinical scenarios, such as ST with a low expectation of artifacts, a smaller FOV is worth exploring in prospective clinical settings. The clinical advantages of FOV reduction include lower irradiation of the patient and a more time-efficient examination and diagnosis of the CBCT images by the practitioner or radiologist, as fewer structures located outside the ROI are displayed. Further studies including multiple operators are desirable to investigate the feasibility of FOV reduction in more challenging clinical scenarios to define a threshold for case-specific FOV volume selection.

5 | CONCLUSION

The following suggestions can be made based on the findings of the present study:

- According to the applied reference, the FOV volume can be reduced to adjacent teeth without affecting the registration accuracy at the implant level by more than 0.1 mm on average in the posterior region.
- Clinically relevant maximum discrepancies up to 1.34 mm were registered in the presence of radiographic artifacts and up to 0.90 mm for multiple missing teeth when reducing the FOV volume to the adjacent tooth/teeth.
- A larger FOV does not significantly improve registration accuracy in case of single missing posterior teeth.

AUTHOR CONTRIBUTIONS

Stefano Pieralli: Conceptualization (lead); data curation (lead); investigation (lead); methodology (lead); project administration (lead); software (equal); supervision (lead); validation (lead); visualization (lead); writing – original draft (lead). **Christian Wesemann:** Conceptualization (equal); data curation (equal); investigation (equal); methodology (equal); writing – review and editing (equal). **Kirstin Vach:** Formal analysis (lead); visualization (equal); writing – review and editing (equal). **Florian Kernen:** Investigation (equal); methodology (equal); writing – review and editing (equal). **Katja Nelson:** Conceptualization (lead); writing – review and editing (equal). **Benedikt Christopher Spies:** Conceptualization (lead); data curation (equal); investigation (equal); methodology (lead); project administration (equal); supervision (lead); validation (equal); writing – review and editing (lead).

ACKNOWLEDGMENTS

The authors would like to thank Dr. Stephan Schmälzle from Swissmeda AG (Baar, Switzerland) and Mr. Jens Bingenheimer from stentists-digitale Planungsdienstleistungen (Braunschweig, Germany) for their valuable contribution to this investigation. Open Access funding enabled and organized by Projekt DEAL. Open Access funding enabled and organized by Projekt DEAL.

CONFLICT OF INTEREST

The authors declare that they have no conflict of interest.

DATA AVAILABILITY STATEMENT

The data that support the findings of this study are available from the corresponding author upon reasonable request.

ORCID

Stefano Pieralli  <https://orcid.org/0000-0003-0061-8612>
Kirstin Vach  <https://orcid.org/0000-0001-9278-2203>
Florian Kernen  <https://orcid.org/0000-0002-3067-0756>
Benedikt C. Spies  <https://orcid.org/0000-0003-1702-1679>

REFERENCES

- Alaidrous, M., Finkelman, M., Kudara, Y., Campos, H. C., Kim, Y., & De Souza, A. B. (2021). Influence of zirconia crown artifacts on cone beam computed tomography scans and image superimposition of tomographic image and tooth surface scan: An in vitro study. *The Journal of Prosthetic Dentistry*, 125(4), 684.e681–684.e688. <https://doi.org/10.1016/j.prosdent.2020.06.028>
- Bornstein, M. M., Scarfe, W. C., Vaughn, V. M., & Jacobs, R. (2014). Cone beam computed tomography in implant dentistry: A systematic review focusing on guidelines, indications, and radiation dose risks. *The International Journal of Oral & Maxillofacial Implants*, 29(Suppl), 55–77. <https://doi.org/10.11607/jomi.2014suppl.g1.4>
- Boulanger, M., Johnson, M. E., & Luko, S. N. (2012). Reviews of standards and related material: Statistical standards and ISO, part 1. *Quality Engineering*, 24(1), 94–101. <https://doi.org/10.1080/08982112.2012.623956>
- Canullo, L., Tallarico, M., Radovanovic, S., Delibasic, B., Covani, U., & Rakic, M. (2016). Distinguishing predictive profiles for patient-based risk assessment and diagnostics of plaque induced, surgically and prosthetically triggered peri-implantitis. *Clinical Oral Implants Research*, 27(10), 1243–1250. <https://doi.org/10.1111/clr.12738>
- Cassetta, M., Di Mambro, A., Giansanti, M., Stefanelli, L. V., & Cavallini, C. (2013). The intrinsic error of a stereolithographic surgical template in implant guided surgery. *International Journal of Oral & Maxillofacial Surgery*, 42(2), 264–275. <https://doi.org/10.1016/j.ijom.2012.06.010>
- Chen, Y., Zhang, X., Wang, M., Jiang, Q., & Mo, A. (2020). Accuracy of full-guided and half-guided surgical templates in anterior immediate and delayed implantation: A retrospective study. *Materials (Basel, Switzerland)*, 14(1), 26. <https://doi.org/10.3390/ma14010026>
- da Silva Moura, W., Chiqueto, K., Pithon, G. M., Neves, L. S., Castro, R., & Henriques, J. F. C. (2019). Factors influencing the effective dose associated with CBCT: A systematic review. *Clinical Oral Investigations*, 23(3), 1319–1330. <https://doi.org/10.1007/s00784-018-2561-4>
- de Castro, H. S., Kehrwald, R., Matheus, R. A., Gomes, A. F., & Queiroz, P. M. (2021). Influence of low-dose protocols of CBCT on dental implant planning. *The International Journal of Oral & Maxillofacial Implants*, 36(2), 307–312. <https://doi.org/10.11607/jomi.8773>
- Emara, A., Sharma, N., Halbeisen, F., Msallem, B., & Thieringer, F. (2020). Comparative evaluation of digitization of diagnostic dental cast (plaster) models using different scanning technologies. *Dentistry Journal*, 8, 79. <https://doi.org/10.3390/dj8030079>
- Flügge, T., Derksen, W., Te Poel, J., Hassan, B., Nelson, K., & Wismeijer, D. (2017). Registration of cone beam computed tomography data and intraoral surface scans – A prerequisite for guided implant surgery with CAD/CAM drilling guides. *Clinical Oral Implants Research*, 28(9), 1113–1118. <https://doi.org/10.1111/clr.12925>
- Flügge, T., Ludwig, U., Hövener, J. B., Kohal, R., Wismeijer, D., & Nelson, K. (2020). Virtual implant planning and fully guided implant surgery using magnetic resonance imaging-proof of principle. *Clinical Oral Implants Research*, 31(6), 575–583. <https://doi.org/10.1111/clr.13592>
- Güth, J. F., Keul, C., Stimmelmayer, M., Beuer, F., & Edelhoff, D. (2013). Accuracy of digital models obtained by direct and indirect data capturing. *Clinical Oral Investigations*, 17(4), 1201–1208. <https://doi.org/10.1007/s00784-012-0795-0>
- Harris, D., Horner, K., Gröndahl, K., Jacobs, R., Helmrot, E., Benic, G. I., Bornstein, M. M., Dawood, A., & Quirynen, M. (2012). E.A.O. guidelines for the use of diagnostic imaging in implant dentistry 2011. A consensus workshop organized by the European Association for Osseointegration at the Medical University of Warsaw. *Clinical Oral Implants Research*, 23(11), 1243–1253. <https://doi.org/10.1111/j.1600-0501.2012.02441.x>
- Jacobs, R., & Quirynen, M. (2014). Dental cone beam computed tomography: Justification for use in planning oral implant placement. *Periodontology 2000*, 66(1), 203–213. <https://doi.org/10.1111/prd.12051>
- Jadu, F. M., Alzahrani, A. A., Almutairi, M. A., Al-Amoudi, S. O., Jan, A. M., & Khafaji, M. A. (2018). The effect of varying cone beam computed tomography image resolution and field-of-view centralization on effective radiation dose. *Saudi Medical Journal*, 39(5), 470–475. <https://doi.org/10.15537/smj.2018.5.21658>
- Kernen, F., Benic, G. I., Payer, M., Schär, A., Müller-Gerbl, M., Filippi, A., & Köhl, S. (2016). Accuracy of three-dimensional printed templates for guided implant placement based on matching a surface scan with CBCT. *Clinical Implant Dentistry and Related Research*, 18(4), 762–768. <https://doi.org/10.1111/cid.12348>
- Kernen, F., Kramer, J., Wanner, L., Wismeijer, D., Nelson, K., & Flügge, T. (2020). A review of virtual planning software for guided implant surgery - data import and visualization, drill guide design and manufacturing. *BMC Oral Health*, 20(1), 251. <https://doi.org/10.1186/s12903-020-01208-1>
- Lou, F., Rao, P., Zhang, M., Luo, S., Lu, S., & Xiao, J. (2021). Accuracy evaluation of partially guided and fully guided templates applied to implant surgery of anterior teeth: A randomized controlled trial.

- Clinical Implant Dentistry and Related Research*, 23(1), 117–130. <https://doi.org/10.1111/cid.12980>
- McGuigan, M., Duncan, H., & Horner, K. (2018). An analysis of effective dose optimization and its impact on image quality and diagnostic efficacy relating to dental cone beam computed tomography (CBCT). *Swiss Dental Journal*, 128, 297–316.
- Papaspyridakos, P., Gallucci, G. O., Chen, C. J., Hanssen, S., Naert, I., & Vandenberghe, B. (2016). Digital versus conventional implant impressions for edentulous patients: Accuracy outcomes. *Clinical Oral Implants Research*, 27(4), 465–472. <https://doi.org/10.1111/clr.12567>
- Pauwels, R. (2015). Cone beam CT for dental and maxillofacial imaging: Dose matters. *Radiation Protection Dosimetry*, 165(1–4), 156–161. <https://doi.org/10.1093/rpd/ncv057>
- Raico Gallardo, Y. N., da Silva-Olivio, I. R. T., Mukai, E., Morimoto, S., Sesma, N., & Cordaro, L. (2017). Accuracy comparison of guided surgery for dental implants according to the tissue of support: A systematic review and meta-analysis. *Clinical Oral Implants Research*, 28(5), 602–612. <https://doi.org/10.1111/clr.12841>
- Rangel, F. A., Maal, T. J., Bronkhorst, E. M., Breuning, K. H., Schols, J. G., Bergé, S. J., & Kuijpers-Jagtman, A. M. (2013). Accuracy and reliability of a novel method for fusion of digital dental casts and cone beam computed tomography scans. *PLoS One*, 8(3), e59130. <https://doi.org/10.1371/journal.pone.0059130>
- Sancho-Puchades, M., Hämmerle, C. H., & Benic, G. I. (2015). In vitro assessment of artifacts induced by titanium, titanium-zirconium and zirconium dioxide implants in cone-beam computed tomography. *Clinical Oral Implants Research*, 26(10), 1222–1228. <https://doi.org/10.1111/clr.12438>
- Schneider, D., Sancho-Puchades, M., Mir-Mari, J., Mühlemann, S., Jung, R., & Hämmerle, C. (2019). A randomized controlled clinical trial comparing conventional and computer-assisted implant planning and placement in partially edentulous patients. Part 4: Accuracy of implant placement. *The International Journal of Periodontics & Restorative Dentistry*, 39(4), e111–e122. <https://doi.org/10.11607/prd.4147>
- Schubert, O., Schweiger, J., Stimmelmayer, M., Nold, E., & Güth, J. F. (2019). Digital implant planning and guided implant surgery – Workflow and reliability. *British Dental Journal*, 226(2), 101–108. <https://doi.org/10.1038/sj.bdj.2019.44>
- Singh, A., & Hamilton, A. (2021). EAO-338 / OC-BR-014 | influence of field of view on the precision of registration for guided implant surgery. *Clinical Oral Implants Research*, 32(S22), 16–17. https://doi.org/10.1111/clr.12_13855
- Tahmaseb, A., Wu, V., Wismeijer, D., Coucke, W., & Evans, C. (2018). The accuracy of static computer-aided implant surgery: A systematic review and meta-analysis. *Clinical Oral Implants Research*, 29(S16), 416–435. <https://doi.org/10.1111/clr.13346>
- Tattan, M., Chambrone, L., González-Martín, O., & Avila-Ortiz, G. (2020). Static computer-aided, partially guided, and free-handed implant placement: A systematic review and meta-analysis of randomized controlled trials. *Clinical Oral Implants Research*, 31(10), 889–916. <https://doi.org/10.1111/clr.13635>
- Vercruyssen, M., Cox, C., Coucke, W., Naert, I., Jacobs, R., & Quirynen, M. (2014). A randomized clinical trial comparing guided implant surgery (bone- or mucosa-supported) with mental navigation or the use of a pilot-drill template. *Journal of Clinical Periodontology*, 41(7), 717–723. <https://doi.org/10.1111/jcpe.12231>
- White, S. C., Scarfe, W. C., Schulze, R. K., Lurie, A. G., Douglass, J. M., Farman, A. G., Law, C. S., Levin, M. D., Sauer, R. A., Valachovic, R. W., Zeller, G. G., & Goske, M. J. (2014). The image gently in dentistry campaign: Promotion of responsible use of maxillofacial radiology in dentistry for children. *Oral Surgery, Oral Medicine, Oral Pathology, Oral Radiology*, 118(3), 257–261. <https://doi.org/10.1016/j.oooo.2014.06.001>
- Yeung, A. W. K., Jacobs, R., & Bornstein, M. M. (2019). Novel low-dose protocols using cone beam computed tomography in dental medicine: A review focusing on indications, limitations, and future possibilities. *Clinical Oral Investigations*, 23(6), 2573–2581. <https://doi.org/10.1007/s00784-019-02907-y>
- Zhou, W., Liu, Z., Song, L., Kuo, C. L., & Shafer, D. M. (2018). Clinical factors affecting the accuracy of guided implant surgery—A systematic review and meta-analysis. *The Journal of Evidence-Based Dental Practice*, 18(1), 28–40. <https://doi.org/10.1016/j.jebdp.2017.07.007>

SUPPORTING INFORMATION

Additional supporting information can be found online in the Supporting Information section at the end of this article.

How to cite this article: Pieralli, S., Beyer, C., Wesemann, C., Vach, K., Russe, M. F., Kernen, F., Nelson, K., & Spies, B. C. (2022). Impact of radiographic field-of-view volume on alignment accuracy during virtual implant planning: A noninterventional retrospective pilot study. *Clinical Oral Implants Research*, 33, 1021–1029. <https://doi.org/10.1111/clr.13983>

2.2 Manuscript 2 – Clinical outcomes and Patient-Reported Outcome Measures of CAD/CAM root-analogue implants

Implant selection is a crucial part of implant prosthodontic rehabilitation. Based on available 3D data on hard and soft tissue, dental implants with different designs, dimensions, and materials can be selected. As an alternative to prefabricated threaded implants, RAIs are available for immediate implant free-hand installation. To be ready immediately after tooth extraction, the CAD/CAM RAI is produced in advance based on the segmented CBCT images of the root(s). In this manuscript, clinical results and PROMs of 28 patients rehabilitated with 31 CAD/CAM custom-made RAIs were assessed after a mean follow-up of 18.9 ± 2.4 months after surgery. The study was designed as a retrospective clinical case series. Approval to conduct the investigation was obtained from the Ethical Committee of the Charité—Universitätsmedizin Berlin, Germany (Study number: EA4/140/18).

Dr. Mats W. H. Böse presented this research as a digital poster in the surgery category at the Digital Days Meeting of the EAO, October 8 to 10, 2020. The abstract was published in *Clinical Oral Implants Research* (89).

The following text corresponds to the abstract of the original article:

*Böse, M. W. H., Hildebrand, D., Beuer, F., Wesemann, C., Schwerdtner, P., **Pieralli, S.**, & Spies, B. C. (2020). Clinical Outcomes of Root-Analogue Implants Restored with Single Crowns or Fixed Dental Protheses: A Retrospective Case Series. Journal of clinical medicine, 9(8), 2346. <https://doi.org/10.3390/jcm9082346>*

Clinical Outcomes of Root-Analogue Implants Restored with Single Crowns or Fixed Dental Prostheses: A Retrospective Case Series.

Objective

The objective was to investigate clinical and radiological outcomes of rehabilitations with root-analogue implants (RAIs).

Methods

Patients restored with RAIs, supporting single crowns or fixed dental prostheses, were recruited for follow-up examinations. Besides clinical and esthetical evaluations, X-rays were taken and compared with the records. Patients were asked to evaluate the treatment using Visual Analogue Scales (VAS). For statistical analyses, mixed linear models were used.

Results

A total of 107 RAIs were installed in one dental office. Of these, 31 were available for follow-up examinations. For those remaining, survival has been verified via phone. RAIs were loaded after a mean healing time of 6.6 ± 2.5 months. 12.1 ± 6.9 months after loading, a mean marginal bone loss (MBL) of 1.20 ± 0.73 mm was measured. Progression of MBL significantly decreased after loading ($p = 0.013$). The mean pink and white esthetic score (PES/WES) was 15.35 ± 2.33 at follow-up. A survival rate of 94.4% was calculated after a mean follow-up of 18.9 ± 2.4 months after surgery.

Conclusion

Immediate installation of RAIs does not seem to reduce MBL, as known from the literature regarding screw-type implants and might not be recommended for daily routine. Nevertheless, they deliver esthetically satisfying results.

Article

Clinical Outcomes of Root-Analogue Implants Restored with Single Crowns or Fixed Dental Prostheses: A Retrospective Case Series

Mats Wernfried Heinrich Böse ^{1,*}, Detlef Hildebrand ², Florian Beuer ¹,
Christian Wesemann ¹, Paul Schwerdtner ³, Stefano Pieralli ⁴ and
Benedikt Christopher Spies ⁴

¹ Department of Prosthodontics, Geriatric Dentistry and Craniomandibular Disorders, Institute for Dentistry, Oral and Maxillofacial Surgery, Charité—Universitätsmedizin Berlin, Corporate Member of Freie Universität Berlin, Humboldt-Universität zu Berlin, and Berlin Institute of Health, Campus Benjamin Franklin (CBF), Aßmannshäuser Str. 4–6, 14197 Berlin, Germany; florian.beuer@charite.de (F.B.); christian.wesemann@charite.de (C.W.)

² Private Dental Office Dr. Detlef Hildebrand, Westhafenstraße 1, 13353 Berlin, Germany; hildebrand@dentalforum-berlin.de

³ Institute of Mathematics MA 4–5, Technical University Berlin, Straße des 17. Juni 136, 10623 Berlin, Germany; schwerdt@math.tu-berlin.de

⁴ Department of Prosthetic Dentistry, Center for Dental Medicine, Medical Center—University of Freiburg, Faculty of Medicine—University of Freiburg, Hugstetter Str. 55, 79106 Freiburg, Germany; stefano.pieralli@uniklinik-freiburg.de (S.P.); benedikt.spies@uniklinik-freiburg.de (B.C.S.)

* Correspondence: mats.boese@charite.de; Tel.: +49-(0)30-450-662-516

Received: 1 July 2020; Accepted: 21 July 2020; Published: 23 July 2020



Abstract: The objective was to investigate clinical and radiological outcomes of rehabilitations with root-analogue implants (RAIs). Patients restored with RAIs, supporting single crowns or fixed dental prostheses, were recruited for follow-up examinations. Besides clinical and esthetical evaluations, X-rays were taken and compared with the records. Patients were asked to evaluate the treatment using Visual Analogue Scales (VAS). For statistical analyses, mixed linear models were used. A total of 107 RAIs were installed in one dental office. Of these, 31 were available for follow-up examinations. For those remaining, survival has been verified via phone. RAIs were loaded after a mean healing time of 6.6 ± 2.5 months. 12.1 ± 6.9 months after loading, a mean marginal bone loss (MBL) of 1.20 ± 0.73 mm was measured. Progression of MBL significantly decreased after loading ($p = 0.013$). The mean pink and white esthetic score (PES/WES) was 15.35 ± 2.33 at follow-up. A survival rate of 94.4% was calculated after a mean follow-up of 18.9 ± 2.4 months after surgery. Immediate installation of RAIs does not seem to reduce MBL, as known from the literature regarding screw-type implants, and might not be recommended for daily routine. Nevertheless, they deliver esthetically satisfying results.

Keywords: root-analogue implants; customized implants; CAD/CAM; dental implants; prosthodontics

1. Introduction

Dental implants are successfully used for the replacement of missing and hopeless teeth with a mean survival rate of $94.6 \pm 5.97\%$ after 10 years of clinical service [1]. Concerning the loss of adjacent bone and soft tissues as a result of tooth extraction [2], immediate implant placement has been purported to help reducing resorption processes [3]. However, a generalized recommendation whether immediate, immediate-delayed, or delayed installation of prefabricated screw-shaped implants should

be generally preferred was not scientifically evidenced to date [4,5]. Benefits of immediate surgical procedures are still subject to current investigations [6].

Resorption processes after tooth extraction have been part of scientific research since the twentieth century [7]. With the objective to counteract these processes by replacing extracted roots/teeth with anatomically shaped copies, the Dental Polymer Implant Concept was already introduced in 1969 [8]. Since then, scientific research on root-analogue implants (RAIs) have been conducted repeatedly with variations in used materials and methods in the literature [9–17]. Thereby, the technical possibilities and concepts did indeed allow for the fabrication of root-analogues but not for immediate implant installation in the proper meaning of the word. This resulted in a temporal offset between the removal of the teeth and implant installations. In order to allow for immediate implant installation of RAIs, they needed to be manufactured prior to the extractions. With the help of Digital Imaging and Communication in Medicine (DICOM) data gathered from Cone Beam Computed Tomographies (CBCT), accurate production of RAIs has been made possible prior to surgery [18,19]. However, no long-term clinical data and studies are available, allowing for critical assumptions regarding the former treatment concepts.

In 2013, Natural Dental Implants (NDI Berlin) launched the REPLICATE Immediate Tooth Replacement System on the dental market. Based on the combination of DICOM data and Standard Triangulation/Tessellation Language (STL) data of the intraoral clinical situations, the RAIs were manufactured in a subtractive manner prior to extraction/surgery. Regarding material selection, a one-piece hybrid-version (the endosseous part of the implant is made of titanium and glass-fused to the zirconia abutment) and a one-piece zirconia version was available. The entire endosseous implant surface was enlarged by macro and micro retentions to allow for primary stability during re-installation of the replica. In 2017, a case report described an excellent outcome concerning the clinical and radiographic results [20]. Some authors compared the procedure to the so-called “The Digital One-Abutment/One-Time Concept” [21], another approach aiming to preserve soft and hard tissues using screw-shaped implants. As a result, more clinical data regarding the REPLICATE Immediate Tooth Replacement System was deemed necessary in 2018 [22]. This investigation intended to provide more clinical data and form the basis for further prospective studies on RAIs. The collected data is considered valuable for future investigations and forthcoming developments of root-analogue implant systems. Since the concept of RAIs fulfils the claim for customization and the belief in progressive digitization within dentistry [23], upcoming research on fully individualized implants seems likely.

This retrospective case series was designed to investigate the survival and success rates of rehabilitations with the REPLICATE Immediate Tooth Replacement System seeking for potential clinical, radiological, and social impacts. With a focus on marginal bone loss (MBL) and esthetic outcomes, the objective was to identify advantages and/or disadvantages and provide preliminary data to validate routine clinical applicability. The working hypothesis was that immediate implantations with customized root-analogue implants show comparable clinical, radiographical, and esthetical results to conventional screw-shaped implants.

2. Experimental Section

This study was designed as a clinical retrospective case series. Ethical approval was given by the Ethical Committee of Charité—Universitätsmedizin Berlin, Germany (application number: EA4/140/18). All surgical procedures and follow-up examinations were performed in the private dental office of an experienced dentist focusing on oral surgery in Berlin (author D.H.). D.H. performed all surgical procedures, and the author, M.B., performed all clinical follow-up examinations. All patients received and signed an informed consent form and patient information prior to examinations. In addition to the Case Report Forms (CRFs) completed by the investigator, each participant was asked to assess his own perception of the treatment by applying Visual Analogue Scales (VAS). This research was conducted considering the STROBE statement for observational studies.

To be considered for a treatment with a RAI in the dental office of the study, the patients had to be non-smokers and were not allowed to take any medication affecting the bone metabolism. Regarding the unmaintainable teeth, surrounding soft and hard tissues had to be non-inflammatory, surrounding bone compartments had to be intact, and periodontal gaps had to be visible on CBCTs. The surgeon (D.H.) already conducted the selection of patients during implant consultations, and many RAI surgeries were already performed before the development of the present study. Rejected cases for a RAI treatment were not documented in the dental office. In total, 107 RAIs were inserted between September 2016 and August 2019 in the dental office of the study. Treatments were performed on patients, with an agreement to be treated with a RAI, and met the inclusion criteria. They were referred by their general dentists from all over Germany or introduced themselves on their own initiative. The REPLICATE Immediate Tooth Replacement System had already been approved for the German dental market at the time of all surgeries.

Existing and collected data were anonymized, retrospectively analyzed, and statistically evaluated comparing the patients CRFs and VAS ratings with the detailed records deemed necessary from the manufacturer. Patient inclusion criteria for clinical follow-up examinations in this study were: (1) Treated with the REPLICATE Immediate Tooth Replacement System; (2) completed healing after surgery according to the surgeon; and (3) RAIs restored with single crowns or fixed dental prostheses. All patients treated with a RAI in the dental office refusing to join for follow-up were excluded from the statistical analyses. However, they were included in the calculation of a preliminary overall survival rate in case of confirmation of survival by the patients themselves or the records of the referring dentists. All patients were tried to contact by phone repeatedly by the reception staff of D. H. or the author, M. B. However, only 28 patients treated with 31 RAIs agreed and participated in the follow-up investigations. The reduced study participation compared to total surgeries emphasizes the study practice as part of a dental referral network and the widely dispersed residencies of the treated patients. The dental office was one of a few practices that offered a treatment with this system throughout Germany. Figure 1 provides an overview of this study as a flow diagram.

Detailed planning was required prior to surgical procedures. To fabricate the RAIs, dental impressions with a customized tray and a polyether material (Impregum, 3M Deutschland GmbH, Neuss, Germany), a bite record in habitual occlusion (Futar D, Kettenbach GmbH & Co. KG, Eschenburg, Germany), DICOM data from a CBCT (PAX i-3D, VATECH, Hwaseong-si, Gyeonggi-do, South Korea), completed order forms, and clinical photographs were required by NDI Berlin. Models were fabricated (type IV plaster), digitized with a laboratory scanner, and exported in STL data format. The STL and DICOM data were superimposed by a trained specialist of the manufacturer. Temporary Protective Covers (TPCs), implant portions, abutment portions, and Try-Ins (exact copies of the RAIs to evaluate the fit prior to installation) were virtually designed. Both the design engineer and the dentist checked the design of the datasets. Depending on the dentist's preferences, adjustments to the design were carried out. When approved, the DICOM data were converted into STL datasets and sent to the Computer Aided Manufacturing (CAM)-computers, which generated the Network Common Data Format (NetCDF; nc) to control the milling machines. Regardless of hybrid or all-ceramic RAIs, the surfaces of the implant portions were enlarged using macro and micro retentions. To avoid compression of the alveolar bone, the intra-bony part was individually reduced compared to the original size of the root.

After pre-surgical planning and delivery of the RAIs, immediate installation took place. Hopeless teeth (Figure 2a) were removed as atraumatically as possible to maintain the surrounding bone. Where possible, the Benex Extraction-System (Benex Extraction-System, Helmut Zepf Medizintechnik GmbH, Seitlingen-Oberflacht, Germany) was used (Figure 2b), facilitating atraumatic vertical tooth removal with a reported mean success rate of 83% [24]. If planned and necessary, the bone compartments were adjusted on an individual basis. Before unpacking and insertion of the final RAI, the anticipated fit in the extraction socket was evaluated by using the Try-Ins (Figure 2c,d). All implant surfaces were wetted with Plasma Rich Growth Factors (PRGFs; BTI Biotechnology Institute, San Antonio,

Spain). Since PRGFs might promote bone regeneration, it was used for augmentation of the voids [25]. Thereafter, the RAIs were carefully placed into position with a hammer and a mallet (Figure 2e–g). Subsequent to surgery, supplied TPCs were adhesively attached to one or both adjacent teeth, depending on the design (Figure 2h,i). A gap of approximately 0.6 mm between the TPCs and the abutments of the RAIs served as load protection. To investigate the state of healing, examinations usually took place 3–6 month after surgery, whereas the temporaries were carefully removed, and X-rays were taken. After successful osseointegration (Figure 2j), conventional impressions of the abutment for the manufacturing of the final restorations were made. The prosthetic restorations of the RAIs were delivered in the study center and in the referring dental offices (Figure 2l).

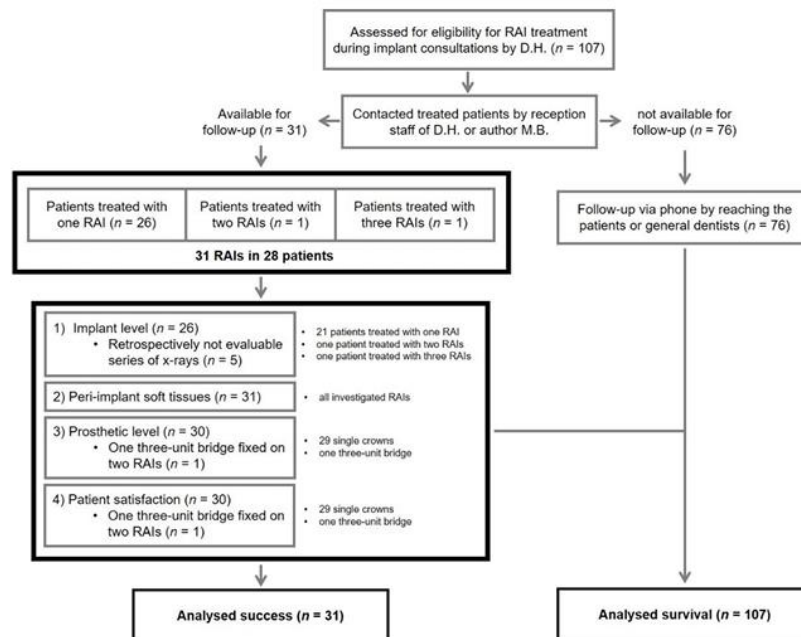


Figure 1. Flow diagram regarding study design and distribution; *n*: number of root-analogues/evaluated data within the different stages of the present study.

When setting up this retrospective evaluation, follow-up examinations were scheduled as soon as possible in consultation with the patients. The CRFs included an update of the anamnesis, surgical, prosthetic, and implant-specific parameters. Radiographs and clinical photographs of the restorations were taken at the follow-up examinations. VAS’ were used for the assessment of patient-reported outcomes. Referring to a systematic review published in 2012, success was determined including 4 superordinate categories: (1) Implant level; (2) Peri-implant soft tissue; (3) Prosthetic level; (4) and Patient satisfaction; this considers the complexity of rehabilitations with implant supported restorations [26].



Figure 2. Exemplary workflow of a restoration with the REPLICATE Immediate Tooth Replacement System: (a) Tooth (24/UL4) not maintainable with longitudinal fracture; (b) Inserted Benex Extraction-System (Benex Extraction-System, Helmut Zepf Medizintechnik GmbH, Seitlingen-Oberflacht, Germany); (c) extracted root and Try-In; (d) Try-In in the alveolus with Plasma Rich Growth Factors (PRGF) at the buccal junction; (e) root-analogue implant (RAI) in its opened sterile packaging; (f) RAI with placement assistance compared to the Try-In; (g) installation of the RAI; (h) Temporary Protective Covers (TPC) before bonding; (i) bonded TPC as load protection; (j) healed RAI with interfering gingiva; (k) contralateral natural teeth; (l) restored RAI and adjacent teeth.

To evaluate success at the implant level radiographs were evaluated at three different times: (1) Surgery (T0); (2) (prior to) Loading (T1); and (3) Follow-up examination (T2). All relevant radiographs were analyzed with ImageJ, an open source image processing program designed for scientific multidimensional images (developed by Wayne Rasband). To calculate the bone loss, defined reference points of the digital RAI constructions (provided by NDI Berlin) were transferred to the radiographs and converted using parallels and the rule of three (Figure 3a–e). All points were defined and checked by the surgeon (D.H.) and the investigator (M.B.). They were independently measured by a single external private lecturer with experience in clinical studies to reduce subjective bias. Considering the measured bone loss, criteria according to Albrektsson et al. [27] and success criteria on the implant level (pain, bone loss < 1.5 mm at first year, annual bone loss < 0.2 mm thereafter, radiolucency, mobility, infection) [26] were used to evaluate clinical evidence of successful osseointegration. Furthermore the following parameters were investigated regarding their impact on bone loss: (1) Gender (male vs female); (2) Age; (3) Implant region (anterior vs posterior); (4) Implant location (maxilla vs mandible); (5) Implant material (hybrid vs all-ceramics); (6) Length of the one-piece implant; (7) Length of the root portion; (8) Length of the abutment portion; (9) Size of implant surface area; (10) Bone quality documented by the surgeon [28]; (11) Difficulty of the operation according to the surgeon (grouped into: easy, intermediate and complicated); and (12) number of roots.

To assess peri-implant soft tissues, the modified plaque (mPI) and bleeding indices (mBI) according to Mombelli et al. [29] and the width of keratinized gingiva (KG) were adopted as criteria at follow-up examinations. Both for mPI (scale 0–3) and mBI (scale 0–3), 0 and 1 were counted as success, whilst 2 and 3 were considered not successful. The keratinized gingiva had to maintain a width of at least 1.5 mm [26] for a rating as success.

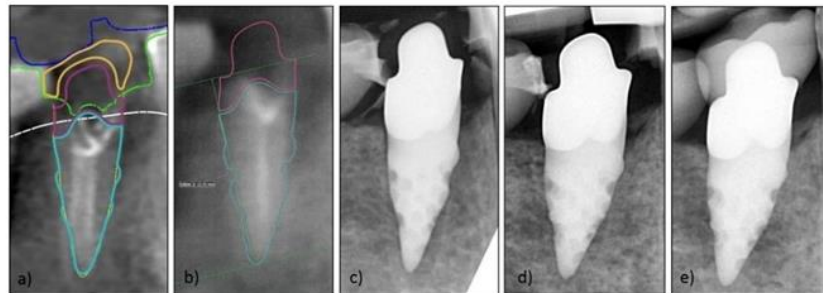


Figure 3. Exemplary series of X-rays for marginal bone loss (MBL) measurement: (a) visualized RAI construction by Natural Dental Implants (NDI); (b) initial image for measurement of bone loss; (c) X-ray post-implantation; (d) X-ray after healing time (before impression for loading); (e) X-ray after loading.

The Pink and White Esthetic Score (PES/WES) [30] and the modified United States Public Health Service (USPHS) criteria (Table 1) [31] were used to allow for standardized assessment of the esthetic outcome and a success rating at the prosthetic level. For both PES and WES, the threshold for clinical acceptability was set at 6 [30] and regarded successful in this study. The 7 modified USPHS criteria: (1) Fracture of veneering ceramic; (2) Fracture of framework; (3) Occlusal roughness; (4) Marginal integrity; (5) Contour of reconstruction; (6) Esthetics of reconstruction; and (7) Discoloration of reconstruction, were applied to every reconstruction and each rated as Alpha (A: within a range of excellence), Beta (B: minor deviations from the ideal), Charlie (C: clinically unacceptable defects that could be intraorally repaired to a clinically acceptable level), or Delta (D: irreparable problem of clinical relevance).

Table 1. Modified United States Public Health Service (USPHS) criteria for the analysis of single crowns and fixed dental prostheses [31,32].

	Alpha (A)	Bravo (B)	Charlie (C)	Delta (D)
Fracture of veneering ceramic	No fracture	Minor chipping (polishable)	Major chipping (up to framework)	Fracture (loss of reconstruction)
Fracture of framework	No fracture	-	-	Fracture (loss of reconstruction)
Occlusal roughness	No roughness	Slight roughness ($\varnothing < 2$ mm)	Obvious roughness ($\varnothing > 2$ mm)	Reconstruction needs to be replaced
Marginal integrity	No visible or soundable gap	Marginal gap slightly soundable	Explorer penetrates a significant crevice	Reconstruction needs to be replaced
Contour of reconstruction	Perfectly contoured	Slightly under-/overcontoured	Pronounced under-/overcontoured	Reconstruction unacceptable
Esthetics of reconstruction	Good esthetics	Slight mismatch in color	Severe color mismatch	Reconstruction unacceptable
Discoloration of reconstruction	No discolorations	discoloration		

Patient-reported outcomes were assessed by applying VAS. Assessment of appearance and chewing ability was included in the evaluation. The patients were asked to label a point on a line that corresponded with their personal satisfaction. The line was 10 cm in length, without scale, and every millimeter corresponded to 1% of satisfaction (i.e., 10 cm corresponded to 100%). The left endpoint represented poor satisfaction (0%), whereas the point at the right end represented excellent satisfaction (100%). Finally, the patient’s markings were measured with a ruler. A rating of 80% or more resulted in a rating as success.

For a successful RAI, all of the 4 superordinate criteria: (1) Implant level; (2) Peri-implant soft tissues; (3) Prosthetic level; and (4) Patient satisfaction, had to be classified successful themselves, following the above defined criteria.

Surgeries of a single practitioner (D.H.) were evaluated. In order to reduce bias, follow-ups were not conducted by the surgeon, but by another independent practitioner (M.B.). In addition, MBL measurements were carried out by an independent private lecturer with experience in clinical studies. The data collection was therefore performed preferably independently and without financial support from the implant company. When compiling the examination parameters, care was taken to use parameters that were as objective and scientifically accepted as possible. Due to the small indication group for a treatment with a RAI, the objective to provide preliminary data and the scarcity of documented data sets in the literature, all possible data sets were evaluated, despite their heterogeneity.

Using 2-sided 95% confidence intervals, a total sample size of 31 RAIs was investigated. For the key clinical data (surgical and RAI-specific parameters, peri-implant soft tissue parameters, MBL, PES, WES, PES/WES), the means, minima, maxima, and standard deviations were calculated. The focus of statistical analysis was the progression of bone loss over time and parameters that may have an impact on it. To compensate for heterogeneous measurement intervals, the mean gradient of the bone loss during time interval 1 (from surgery until loading) and time interval 2 (from loading until examination) were individually computed for each patient. For final comparison, a dependent t-test for paired samples of the mean gradients in the different intervals was used.

To detect parameters potentially affecting the outcome, Welch's *t*-tests on the data grouped by gender, implant region, implant location, implant material, difficulty of the operation and number of roots, were performed. Difficulty of the operation and number of roots were included in Welch's *t*-tests, since only 2 different entries were made in the evaluation of the CRFs. The Pearson's Correlation Coefficient between the total bone loss, age, length of the one-piece implant, root portion: Length, abutment portion: Length, implant surface, and bone quality were computed. Additionally, the Pearson's Correlation was applied to investigate the coefficient among the total bone loss, esthetics (VAS), PES, WES, and PES/WES. Testing was adjusted to the quantity and quality of evaluable data (i.e., just 26 series of X-rays were evaluated). Survival and success rates were specified with calculation of percentages.

All statistical tests were performed with SciPy (SciPy developers), a Python-based ecosystem of open-source software for mathematics, science, and engineering. The level of significance was set at $p < 0.05$.

3. Results

3.1. Demographic Data and Additional Information

One hundred and seven RAI-surgeries were performed between September 2016 and August 2019 in the dental office of this study. Survival of implants was verified at follow-up examinations or, in case of a refused participation, by phone via the patients themselves or the records of the general dentists (see also Figure 1). A hundred and one root-analogues were still in situ at the time of the study after a mean observation period of 18.9 ± 2.4 months. Six RAIs failed, of which 4 did not show osseointegration in the healing period and 2 were lost after prosthetic delivery. This resulted in a survival rate of 94.4%.

A total of 28 patients, consisting of 11 males and 17 females, were recruited for follow-up examinations. One study participant was treated with two and another participant with three RAIs, resulting in a total number of 31 retrospectively examined and restored root-analogues (Table 2).

Table 2. RAI distribution and region.

	Posterior (P)					Anterior (A)					Posterior (P)				
FDI	17	16	15	14	13	12	11	21	22	23	24	25	26	27	
<i>n</i> (maxilla)	1	1	3	0	0	1	6	5	0	1	3	1	0	0	
<i>n</i> (mandible)	0	2	2	1	0	0	0	0	0	0	1	3	0	0	
FDI	47	46	45	44	43	42	41	31	32	33	34	35	36	37	
<i>n</i> (region)	10					13					8				

FDI: Scheme according to the World Dental Federation; *n*: number of placed root-analogues in the respective position or region (anterior or posterior).

The mean age was 55.3 ± 14.2 years at surgeries and 56.6 ± 14.1 years at follow-up examinations. Implant placements of the study participants were performed between September 2016 and September 2018. Loading took place between August 2017 and August 2019. Twenty-five hybrid and 6 all-ceramics RAIs were restored with 29 single crowns and one three-unit fixed dental prostheses after a mean healing time of 6.6 ± 2.5 month. Follow-up examinations took place 17.5 ± 6.4 months after surgery and 10.8 ± 7.0 month after loading. Patient and RAI characteristics are shown in Tables 3 and 4 including *p*-values related to the impact of the different parameters on MBL.

Table 3. Patient characteristics and *p*-values for investigated influence on MBL.

Parameter	Frequency <i>n</i> (%)	<i>p</i> -Value
Gender		
female	17 (61)	0.260
male	11 (39)	
Age		
mean (in years)	55.3/56.6 ¹	0.869
range (in years)	31–82/33–83 ¹	
Implant region		
anterior	13 (42)	0.571
posterior	18 (58)	
Implant location		
maxilla	22 (71)	0.691
mandible	9 (29)	
Implant material		
hybrid	25 (81)	0.483
all-ceramics	6 (19)	
Bone quality		
I	1 (3)	0.898
II	10 (32)	
III	14 (45)	
IV	6 (19)	
Difficulty of the operation		
easy	0 (0)	0.690
intermediate	21 (68)	
complicated	10 (32)	
Number of roots		
single rooted	25 (81)	0.091
multi rooted	6 (19)	

¹ first data concerning the date of surgery, second data concerning the date of examination.

Table 4. RAI characteristics and *p*-values for investigated influence on MBL.

	Length of the One-Piece Implant (in mm)	Root Portion: Length (in mm)	Abutment Portion: Length (in mm)	Implant Surface (in cm ²)
<i>n</i>	31	31	31	25 ¹
Min	12.41	7.49	3.18	101
Max	26.30	14.79	14.86	442
SD	3.12	1.86	2.41	83
Mean	19.19	10.96	8.43	213
<i>p</i> -values	0.709	0.870	0.717	0.078

n: number of root-analogues included in calculations; ¹ the implant surfaces of 6 all-ceramic RAIs could not be provided by NDI Berlin.

3.2. Implant Level

Of 31 RAIs, 26 were radiographically evaluated. Detailed information regarding the data used for measurements of the MBL are shown in Table 5. Before loading of the RAIs the mean MBL was calculated to be 0.82 ± 0.54 mm at T1 (T0-T1). At follow-up examinations the mean MBL was 1.20 ± 0.73 mm at T2 (T0-T2). Between loading (T1) and follow-up (T2), the MBL was 0.40 ± 0.41 mm (T1-T2). Bone resorption after surgery was recorded in every patient. Comparing T0-T1 with T1-T2 (Figure 4), a statistically significant reduced progression of bone resorption could be determined ($p = 0.013$).

Table 5. Marginal bone loss and time difference from surgery (T0) to loading (T1) and the follow-up examination (T2).

RAIs	Surgery (T0) (in mm)	Loading (T1) (in mm)	Examination (T2) (in mm)	T0-T1 (in Days)	T1-T2 (in Days)	T0-T2 (in Days)	JIAP (in mm)
1	0.00	-0.50	-1.30	276	350	626	-1.00
2	0.00	-1.35	-1.55	276	350	626	-1.00
3	0.00	-0.20	-0.50	260	350	610	-1.00
4	0.00	-1.10	-1.30	281	272	553	0.00
5	0.00	-0.90	-0.90	155	418	573	-1.50
6	0.00	-1.10	-2.20	86	509	595	-1.00
7	0.00	-0.50	-0.75	86	663	749	-1.00
8	0.00	-1.10	-1.25	153	750	903	-1.00
9	0.00	-0.30	-0.45	126	34	160	-1.00
10	0.00	-0.75	-1.00	254	358	612	-1.00
11	0.00	-1.70	-1.70	343	260	603	0.00
12	0.00	-0.60	-0.85	291	369	660	-1.00
13	0.00	-1.70	-2.85	92	488	580	-1.00
14	0.00	-0.75	-1.40	132	182	314	-1.00
15	0.00	-0.95	-2.55	266	503	769	-0.75
16	0.00	-0.55	-0.85	228	32	260	-1.00
17	0.00	-0.40	-0.55	151	107	258	-1.00
18	0.00	-0.30	-0.75	135	34	169	-1.00
19	0.00	-0.40	-0.60	182	338	520	-1.00
20	0.00	-0.80	-1.15	124	50	174	-1.00
21	0.00	-0.35	-0.50	97	459	556	-1.00
22	0.00	-2.50	-2.90	99	598	697	-1.25
23	0.00	-0.45	-1.40	99	598	697	-1.25
24	0.00	-0.80	-0.80	102	584	686	-1.00
25	0.00	-0.65	-1.10	91	636	727	0.00
26	0.00	-0.15	-0.15	141	288	429	-1.00
	Min	-0.15	-0.15	86.00	32.00	160.00	-1.5
	Max	-2.50	-2.90	343.00	750.00	903.00	0.00
	SD	0.54	0.73	78.91	208.77	202.03	0.36
	Mean	-0.82	-1.20	173.56	368.46	542.54	-0.91

JIAP: the prior to surgery planned iso- or subcrestal junction between the implant and abutment portion of the RAIs; only 26 of 31 RAIs showed a retrospectively evaluable series of X-rays at follow-up; negative values indicate a loss of bone in relation to marginal bone levels at surgery.

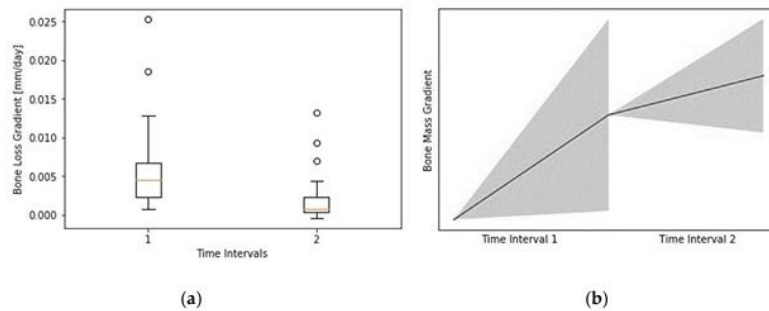


Figure 4. (a) Bone loss gradient in mm/day from surgery to loading (T0-T1; Time Interval (1) and loading to examination (T1-T2; Time Interval (2)); (b) visualization of the box plot without any possible axis labeling based on the calculation of the gradients due to heterogeneous follow-up intervals. Created with SciPy (SciPy developers).

Potential affecting parameters show no statistically significant influence on MBL and are shown in Tables 3 and 4. The junction between the implant and abutment portions (JIAP) of the RAIs were planned iso- or subcrestally while designing the root-analogues prior to surgery (see also Table 5). Since the majority of JIAP were planned 1 mm subcrestally, a statistical evaluation of the influence of JIAP position on MBL was not reasonable. Adopting the afore explained criteria, 80.8% of the evaluable RAIs ($n = 21$) were successful regarding the implant level (Table 6). Pearson’s Correlation Coefficients are documented in Table 7.

Table 6. Success criteria based on included parameters.

	Implant Level		Soft tissue Parameters		Prosthetic Level		Patient Satisfaction		Overall Rating	
	<i>n</i>	%	<i>n</i>	%	<i>n</i>	%	<i>n</i>	%	<i>n</i>	%
<i>n</i>	26	83.9	31	100.0	30	100.0	30	100.0	31	100.0
Success	21	80.8	30	96.8	25	83.3	27	90.0	20	64.5

n: number of evaluated RAIs, respectively, reconstructions; only 26 RAIs could be included in the evaluation of MBL; 31 RAIs were investigated regarding soft tissue parameters; due to 29 single crowns and 1 fixed dental prosthesis, the number of investigated reconstructions and patient satisfaction was 30.

Table 7. Pearson’s Correlation Coefficients.

	Esthetic (VAS)	PES	PES/WES	WES	Total Bone Loss (T0-T2)
Esthetic (VAS)	1.000000	0.335767	0.358691	0.164237	0.074137
PES	0.335767	1.000000	0.666582	0.137687	−0.089390
PES/WES	0.358691	0.666582	1.000000	0.685310	0.012887
WES	0.164237	0.137687	0.685310	1.000000	0.096554
Total bone loss (T0-T2)	0.074137	−0.089390	0.012887	0.096554	1.000000

3.3. Peri-Implant Soft Tissues

The level of presurgical planned restoration margins was ranging from 0.0 mm ($n = 1$), 1.0 mm ($n = 13$), 0.5–1.5 mm ($n = 5$) to ≥ 1.5 mm ($n = 12$) subgingival. All 31 root-analogues were evaluated regarding the peri-implant soft tissues at follow-up as shown in Table 8. The mean mPI was documented to be 0.6 ± 0.5 , the mean mBI was 0.6 ± 0.7 , and the mean KG was 3.9 ± 1.7 mm. This resulted in a success rate of 96.8% ($n = 30$) on the soft tissue level, as shown in Table 6.

Table 8. Peri-implant soft tissue parameters.

	mPI	mBI	KG (in mm)
<i>n</i>	31	31	31
Min	0	0	1.5
Max	1	3	9
SD	0.5	0.7	1.7
Mean	0.6	0.6	3.9

n: number of included root-analogues in calculations; mPI: the modified plaque index [29] mBI: the modified bleeding index [29]; KG: width of buccal keratinized gingiva.

3.4. Prosthetic Level

The total values of PES (mean 7.45 ± 1.50) and WES (mean 7.90 ± 1.74) resulted in a mean score of 15.35 ± 2.33 for PES/WES (Table 9). Including the criteria regarding the prosthetic level, a success rate of 83.3% ($n = 25$) was found (Table 6). Additionally, evaluation of the modified USPHS criteria for the analysis of single crowns and fixed dental prostheses was documented in detail in Table 10. Pearson’s Correlation Coefficients evaluating PES, WES, and PES/WES show no strong dependencies and can be found in Table 7.

3.5. Patient Satisfaction

The esthetic appearance of the reconstructions ($n = 30$) was rated $91.6 \pm 17.5\%$ on the VAS. A slightly lower mean value of $89.1 \pm 18.9\%$ was evaluated regarding the ability to chew. As previously defined, considering both parameters resulted in a success rate of 90.0% ($n = 27$; Table 6) regarding the patient satisfaction. Due to three participants, rating (1) The satisfaction with the appearance and/or (2) The ability to chew as unsatisfactory were counted as failure. Of those, two described discomfort while chewing and one was not pleased with the appearance of the single crown. Pearson’s Correlation Coefficients looking at esthetics (VAS) were again specified in Table 7.

3.6. Overall Survival and Success

Taking the predefined criteria in all 4 categories into account, a success rate of 64.5% ($n = 20$, based on 31 RAIs) and a survival rate of 94.4% (based on 107 RAIs) was determined 17.5 ± 6.4 months after RAI surgeries (Table 6).

Table 9. Detailed Pink Esthetic Score (PES) and White Esthetic Score (WES) for each RAI investigated [30].

RAIs	PES					WES							Total PES + WES
	Mesial Papilla	Distal Papilla	Curvature of Facial Mucosa	Level of Facial Mucosa	Root Convexity/Soft Tissue Color and Texture	Total PES	Tooth Form	Outline/Volume	Color (Hue/Value)	Surface Texture	Translucency/Characterization	Total WES	
1	1	2	2	1	2	8	2	2	2	2	2	10	18
2	1	2	2	1	2	8	2	2	2	2	2	10	18
3	2	2	1	1	1	7	1	1	2	2	2	8	15
4	2	2	2	2	2	10	2	2	2	1	2	9	19
5	1	2	1	2	1	7	1	1	1	1	1	5	12
6	2	2	2	1	1	8	1	1	1	1	1	5	13
7	2	2	2	1	1	8	1	1	1	2	1	6	14
8	0	0	2	2	1	5	1	1	2	2	1	7	12
9	1	1	2	2	2	8	2	2	1	1	2	8	16
10	2	1	2	2	2	9	2	2	1	1	1	7	16
11	2	1	2	2	2	9	2	2	1	1	1	7	16
12	2	2	1	1	1	7	1	1	2	1	1	6	13
13	2	2	1	2	2	9	1	1	1	1	2	6	15
14	1	2	1	1	1	6	1	1	2	2	2	8	14
15	1	1	1	1	1	5	1	1	1	2	2	7	12
16	1	0	2	1	2	6	2	2	2	2	2	10	16
17	2	1	2	2	2	9	2	2	1	2	1	8	17
18	0	2	2	1	2	7	2	1	1	1	2	7	14
19	2	0	1	1	1	5	1	1	1	1	1	5	10
20	1	1	2	2	2	8	2	2	2	2	2	10	18
21	1	0	2	2	2	7	2	2	2	2	2	10	17
22	1	1	1	1	2	6	2	2	2	2	2	10	16
23	1	1	1	1	2	6	2	2	2	2	2	10	16
24	1	1	2	2	1	7	1	1	2	2	2	8	15
25	1	2	2	2	2	9	2	2	2	2	2	10	19
26	0	0	1	1	2	4	2	2	1	2	2	9	13
27	2	1	2	2	1	8	1	1	2	1	1	6	14
28	2	2	2	2	1	9	2	2	2	2	2	10	19
29	1	2	2	2	1	8	2	2	1	2	1	8	16
30	2	2	1	2	2	9	1	1	1	2	1	6	15
31	2	2	2	2	1	9	2	2	1	2	2	9	18
Min	0	0	1	1	1	4	1	1	1	1	1	5	10
Max	2	2	2	2	2	10	2	2	2	2	2	10	19
SD	0.66	0.75	0.49	0.51	0.51	1.50	0.50	0.51	0.51	0.49	0.50	1.74	2.33
Mean	1.35	1.35	1.65	1.55	1.55	7.45	1.58	1.55	1.52	1.65	1.61	7.90	15.35

Table 10. Results applying modified USPHS criteria as mentioned in Table 1 at follow-up.

	Alpha (A)	Bravo (B)	Charlie (C)	Delta (D)
Fracture of veneering ceramic	29 (96.7%)	0	1 (3.3%)	0
Fracture of framework	30 (100.0%)	0	0	0
Occlusal roughness	26 (86.7%)	4 (13.3%)	0	0
Marginal integrity	9 (30.0%)	17 (56.7%)	4 (13.3%)	0
Contour of reconstruction	22 (73.3%)	8 (26.7%)	0	0
Esthetics of reconstruction	24 (80.0%)	6 (20.0%)	0	0
Discoloration of reconstruction	30 (100.0%)	0	0	0

30 included restorations due to 29 single crowns and 1 three-unit fixed dental prostheses.

4. Discussion

Immediate implantations with customized root-analogue implants show comparable results to conventional, screw-shaped implants after a short observation period. It seems that there are advantages in terms of soft tissues and esthetics, but disadvantages in terms of bone loss and restoration margins. However, the database is very small, and the calculations of success and survival rates should be interpreted with care. When discussing the present findings, the limitations of this study, especially regarding the limited sample size, should be kept in mind and conclusions mainly regarded as a tendency. A prospective study design should have been preferred. At the time this study was developed, available data needed to be evaluated retrospectively. However, due to the small indication group for treatment with a RAI and little data described in the literature, it was decided that the presented outcomes should be of interest to the field. Including this study there are too little studies available to be able to make a final comparison between RAIs and screw-shaped implants. Despite the fact that NDI Berlin ceased its business operations on 31 January 2020, the authors expect future developments and investigations regarding RAIs.

Studies on root-analogue implants and potential advantages appear repeatedly in the literature. As the procedure is not established in clinical routine, only case reports with different follow-up intervals [14–17,20,22] or literature reviews exploring the subject [33] are available. Recently, an article reviewing the historical development of RAIs was published [34]. The primary goal of this retrospective case series was to collect comprehensive data and give preliminary survival and success rates for rehabilitations supported by root-analogue implants. Therefore, regularly used scientific parameters, as described in a review in 2012 [26], were examined. Considering the extensive recruitment area and the referral structure of the dental office of the study, the largest possible patient group treated with the *REPLICATE Immediate Tooth Replacement System* was acquired for follow-ups. To the knowledge of the authors, such an extensive and detailed analysis of RAIs has not been described in the literature yet.

For screw-shaped implants, standardized manufacturer’s specifications (e.g., the pitch distance of the threads) are available for radiological analysis of bone loss. As RAIs are fully customized, there are no such standardized values. Therefore, the manufacturer was asked to give individual implant-specific details (e.g., implant length, abutment length, etc.) and precisely specified distances from distinctive RAI points (Figure 3b). This enabled the calculation of MBL as it is performed for screw-shaped implants [35,36]. A control group is missing due to the retrospective study design and high specificity of the treatment. The assessment of bone loss based on two-dimensional X-rays was applied in numerous precedent publications, but findings should be handled with care due to potential artefacts and dimensional limitations of the projection [37,38]. Because of the retrospective study design, no standardized radiographs with customized X-ray holders were available, and measurements should be interpreted with care.

The loss of bone was measured referring to the marginal bone level after installation of the RAIs (T0). Evaluating the radiographs, the absolute loss was measured, even if JIAP was located subcrestally and a bone loss was therefore already expected and considered. This corresponded to the transition between the polished and rough parts of the implant. Due to very homogeneous location of this

transition zone (1 mm subcrestal in 73.1%), its influence on bone remodeling was not statistically evaluated. However, it can be assumed that the bone remodeling is more pronounced in these RAIs, as there are studies, in which screw-shaped implants with a subcrestal rough-smooth border show higher bone remodeling in the first 6 months after installation, than screw-shaped implants with an epicrestal (or close to the crest) rough-smooth border [39,40]. In reference to this, immediate implant placements with screw-shaped implants are usually also performed ~1 mm subcrestally [41], whereby MBL measurements are often carried out with regard to the rough-smooth border after completed healing and before loading. Using prosthetic delivery and loading of the implant as baseline, a mean of 0.40 ± 0.41 mm of bone was lost within a mean of 10.8 ± 7.0 month of service, ranging within the accepted amount of bone loss due to bone remodeling processes [42,43]. Applying the success criteria of the present study, this remodeling processes from installation of the RAIs to final loading were included and resulted in a success rate of 80.8% ($n = 21$) on the implant level. In this study, none of the patient-reported, surgical or RAI-specific parameters had a statistically significant influence on the MBL. However, regarding the limited sample size, the presented data should be interpreted with care. In conclusion, no advantages of RAIs compared to screw-shaped implants by means of bone level stability seem to be apparent. Bone loss observed appears to be comparable to conventional immediate implant surgery with screw-shaped implants and does not seem to further counteract the bony resorption or remodeling processes. These results were documented after a short observation period and should be interpreted as a tendency regarding the methodology. Nevertheless, as well with RAIs, greater bone loss seems to be expected during the healing phase compared to the phase after loading, as it is the case with screw-shaped implants.

To evaluate the success of implant-supported rehabilitations the assessment of the peri-implant soft tissues is inevitable. An evaluation of these, e.g., in form of bleeding on probing (BoP), in combination with peri-implant bone loss is necessary to rule out an undesirable complication of implants, peri-implantitis [1,44].

The RAIs included in the present investigation were mostly designed with subgingival cementation margins ranging from 0.5–1.5 mm (96.8%). But even if a subgingival restoration margin of more than 0.5 mm increases the risk of undetected cement [45], potentially resulting in gingival inflammation, this study revealed favorable results regarding peri-implant soft tissues. Only for one single RAI, a mBI > 2 has been documented. The buccal KG was >1.5 mm at all RAIs and despite oral hygiene was not always categorized optimal, the mPI never exceeded a rating of 2. In the short-term, it seems that the lower success rate regarding MBL detected at RAIs does not have a negative effect on the peri-implant soft tissue stability and health. This may be due to the transition of the abutment to the root portion (shape analogue and same width), compared to screw-shaped implants (strong, hardly cleanable, and probeable rejuvenation). In consequence, the fully anatomical imitation with RAIs might be considered advantageous regarding the susceptibility for peri-implantitis [46].

Finally, implants serve as support to the attempt to restore esthetics and function. To investigate the esthetics and possible complications, objective criteria were necessary to assess success at the prosthetic level. A feasible and comprehensive esthetic score for comparing results regarding rehabilitations with implants is constantly being discussed in the scientific community [47]. For an objective evaluation of the esthetic appearance, the PES/WES [30] as a reproducible instrument [48] and the modified USPHS criteria, which had already been used in other clinical studies to evaluate single crown restorations on implants [32], were used for classification. It should be considered that the PES/WES was originally developed for the evaluation of implant restorations in the esthetic area to be compared with contralateral natural teeth. In the present study, however, only 41.9% ($n = 13$) of the RAIs were in the esthetic area. Thirty-five and a half percent ($n = 11$) of the contralateral teeth were natural teeth, and 64.5% were restored. In such cases, results can be both false positive and false negative, therefore affecting the outcome. Due to the detailed sub-parameters within the PES/WES, however, it still provides a comprehensible and reproducible result. A mean of 15.35 ± 2.33 for PES/WES represents a favorable result compared to previous studies adopting these criteria [30,49]. According to

the modified USPHS criteria, six out of seven criteria provided satisfactory results, predominantly being rated with no (A) or minor complications (B). However, marginal integrity was found to be noteworthy. Many of the restorations were documented to show a slightly soundable marginal gap and for some restorations the explorer even penetrated a significant crevice. Concerning marginal integrity, there seems to be a trend towards increased difficulty to provide conventionally copied RAIs with accurately fitting single crowns or fixed dental prostheses compared to other one-piece implants investigated in studies using the USPHS criteria [32]. Nevertheless, none of the restorations had to be replaced and, regarding the evaluation of the peri-implant soft tissues, does not seem to have a negative influence. A sufficient margin design is nevertheless desirable in order not to provide an exposed surface for possible complications, e.g., promotion of peri-implantitis. If a new fabrication of the restoration is indicated and the abutment portion of the respective RAIs has not been manipulated after the installation, a matching of the new impressions with the existing digital data sets of the abutment portion should be considered. Due to the difficulties described above, this might help to optimize the transition at the preparation margin.

Apart from the preferably objective evaluation of the procedure, each participant was asked to mark VAS for a subjective assessment. The individual sensation at rest or in function, i.e., when biting or chewing nutrition, was rated by the participants with an average of 89.1%. Furthermore, the personal esthetic perception was evaluated with an average of 91.6%. Two participants were not satisfied with “the ability to chew” and have described a different feeling compared to their natural teeth. No pain, mobility, or other clearly defined criteria for failure were evident. Twice, the appearance of the restorations in terms of color and translucency were rated below the defined threshold of 80%. This resulted in 3 unsatisfied patients, since one patient rated both parameters below the threshold for success. Two of these RAIs were located in the anterior region and 1 was located in the posterior region. They were evaluated with 12/12/13 points according to the PES/WES and received AAACBBA/CABCBA/AAABAAA ratings according to the USPHS criteria. The below-average assessment of the PES/WES is thus consistent with the patient-specific assessment. An interpretation of the modified USPHS criteria can also be reconciled with it. This supports the assumption that the criteria used in this study represent a reproducible method for assessing esthetics and complications and are close to individual patient evaluations. Thus, the investigated success rate of 90.0% regarding patient satisfaction is sustained by the pre-discussed objective parameters. The esthetic deficits and marginal discrepancies can be corrected by making new restorations using new impressions. For this purpose, the existing digital data sets should be considered as mentioned above and an additional focus on fittings should be carried out before the final cementation.

Patient satisfaction, esthetics and durability of the prosthetic outcome, soft tissue stability and health, and susceptibility for bone resorptions were considered relevant parameters for the determination of implant success. In terms of MBL, no advantage was found in comparison to screw-shaped implants. The strengths of the procedure seem to be mainly in the esthetic result and maintenance of healthy peri-implant soft tissues. Combining the four applied criteria for success resulted in an overall success rate of 64.5%. This is within the range of success rates of other scientific articles that have classified the implant success based on a combination of 4 superordinate criteria [50–52]. It is well known and reported that overall success decreases with an increasing number of included criteria [26]. Most research is limited to an examination of the implant level and especially the MBL.

It seems that the present findings are in line with the observations by Esposito and collaborators, likewise reporting a reduced success rate but highly satisfying esthetic results for immediately installed implants [53,54]. In contrast to conventional procedures, installing screw-shaped implants, one potential benefit might be considered the circumstance that no further augmentation techniques, such as a connective tissue grafts or guided bone regeneration, were required to achieve a comparably and esthetically pleasing result. Nevertheless, prospective long-term data are necessary for a final evaluation of RAIs. Most importantly, the influence of JIAP location on marginal bone remodeling

and a more reliable evaluation of the resorption processes (three-dimensional or standardized radiographs) would be of interest. In addition, the development of a standardized success score for implant-supported reconstructions would be helpful to compare the findings of different studies in a more comprehensive manner.

Finally, treatment with RAIs is only suitable for a small group of patients with extractions planned in the near future. The alveolar bone needs to be intact and no extensive osteolysis and/or inflammatory processes in the implant region can be present. If possible, artefact-causing reconstructions in CBCTs potentially resulting in inaccuracies when production of the RAIs, such as metal, should be removed in advance. In general, it requires a very cautious approach by an experienced surgeon and destruction of the surrounding tissues during extraction can make RAI installation impossible. In such a case, planning efforts prior to surgery were useless, and the about 15% higher costs compared to screw-shaped implants (including bone and soft tissue augmentations) cannot be justified.

5. Conclusions

Immediate installation of RAIs does not seem to counteract the known marginal bone resorption processes after tooth extraction when compared to immediate installation of screw-shaped implants reported in the literature. However, at least after a short-time observation period, RAIs were found to maintain peri-implant soft tissue conditions and resulted in a predictable and highly satisfying esthetic outcome. For a more reliable analysis, mid- to long-term prospective studies are required. Given the small indication group and the limited data and advantages, it seems that the application of RAIs bears no relation to necessary efforts and expenses so far. The calculated survival rate for RAIs (94.4%) within the collected follow-up data after less than two years should be viewed critically when comparing to a survival rate of 94.6% considering 10-year follow-up data of screw-shaped implants [1]. During the completion of this study, NDI Berlin ceased its business on 31 January 2020. This and the failure to establish RAIs in dentistry within several years can be an indicator for its not yet convincing results.

Author Contributions: Conceptualization, M.W.H.B., D.H., F.B. and B.C.S.; Data curation, M.W.H.B., D.H., C.W., P.S. and B.C.S.; Formal analysis, M.W.H.B., C.W., P.S., S.P. and B.C.S.; Investigation, M.W.H.B. and D.H.; Methodology, M.W.H.B., F.B., C.W., P.S., S.P. and B.C.S.; Project administration, M.W.H.B.; Resources, M.W.H.B., D.H., C.W. and P.S.; Software, C.W. and P.S.; Supervision, B.C.S.; Validation, M.W.H.B., D.H., F.B., C.W., P.S., S.P. and B.C.S.; Visualization, M.W.H.B., C.W., P.S. and B.C.S.; Writing—original draft, M.W.H.B.; Writing—review & editing, F.B., S.P. and B.C.S. All authors have read and agreed to the published version of the manuscript.

Funding: We acknowledge support from the German Research Foundation (DFG) and the Open Access Publication Funds of Charité—Universitätsmedizin Berlin.

Acknowledgments: This investigation was supported by clinical data from the dental office of Detlef Hildebrand in Berlin, Germany and product specific data provided by NDI Berlin in Berlin, Germany.

Conflicts of Interest: The authors declare no conflict of interest.

References

1. Moraschini, V.; Poubel, L.D.C.; Ferreira, V.F.; Barboza, E.D.S. Evaluation of survival and success rates of dental implants reported in longitudinal studies with a follow-up period of at least 10 years: A systematic review. *Int. J. Oral Maxillofac. Surg.* **2015**, *44*, 377–388. [\[CrossRef\]](#)
2. Tan, W.L.; Wong, T.L.T.; Wong, M.C.M.; Lang, N.P. A systematic review of post-extraction alveolar hard and soft tissue dimensional changes in humans. *Clin. Oral Implant. Res.* **2011**, *23*, 1–21. [\[CrossRef\]](#)
3. Bholra, M.; Neely, A.L.; Kolhatkar, S. Immediate Implant Placement: Clinical Decisions, Advantages, and Disadvantages. *J. Prosthodont.* **2008**, *17*, 576–581. [\[CrossRef\]](#)
4. Esposito, M.; Grusovin, M.G.; Polyzos, I.P.; Felice, P.; Worthington, H.V. Timing of implant placement after tooth extraction: Immediate, immediate-delayed or delayed implants? A Cochrane systematic review. *Eur. J. Oral Implant.* **2010**, *3*, 189–205.
5. Clementini, M.; Tiravia, L.; De Risi, V.; Orgeas, G.V.; Mannocci, A.; De Sanctis, M. Dimensional changes after immediate implant placement with or without simultaneous regenerative procedures. *J. Clin. Periodontol.* **2015**, *42*, 666–677. [\[CrossRef\]](#)

6. Arora, H.; Khzam, N.; Roberts, D.; Bruce, W.L.; Ivanovski, S. Immediate implant placement and restoration in the anterior maxilla: Tissue dimensional changes after 2-5 year follow up. *Clin. Implant. Dent. Relat. Res.* **2017**, *19*, 694–702. [[CrossRef](#)]
7. Pietrovovski, J.; Massler, M. Alveolar ridge resorption following tooth extraction. *J. Prosthet. Dent.* **1967**, *17*, 21–27. [[CrossRef](#)]
8. Hodosh, M.; Povar, M.; Shklar, G. The dental polymer implant concept. *J. Prosthet. Dent.* **1969**, *22*, 371–380. [[CrossRef](#)]
9. Lundgren, D.; Rylander, H.; Andersson, M.; Johansson, C.; Albrektsson, T. Healing-in of root analogue titanium implants placed in extraction sockets. An experimental study in the beagle dog. *Clin. Oral Implant. Res.* **1992**, *3*, 136–144. [[CrossRef](#)]
10. Kohal, R.; Hürzeler, M.B.; Mota, L.F.; Klaus, G.; Caffesse, R.G.; Strub, J.R. Custom-made root analogue titanium implants placed into extraction sockets. An experimental study in monkeys. *Clin. Oral Implant. Res.* **1997**, *8*, 386–392. [[CrossRef](#)]
11. Kohal, R.; Klaus, G.; Gieloff, B.; Hürzeler, M.B.; Strub, J.R. Wurzelanalogue Titanimplantate (Bio-Design-Implantate) für die Sofortimplantation-Das Re-Implant-System. *Implantologie* **1996**, *4*, 99–115.
12. Strub, J.R.; Klaus, G.; Ferrareso, F.; Kohal, R. The Re Implant® System for Immediate Implant Placement. *J. Esthet. Restor. Dent.* **1997**, *9*, 187–196. [[CrossRef](#)] [[PubMed](#)]
13. Kohal, R.; Klaus, G.; Strub, J.R. Klinische Untersuchung eines neuen dentalen Sofort-Implantatsystems. Das ReImplant-System. *Dtsch. Zahnärztliche Z.* **2002**, *57*, 495–497.
14. Pirker, W.; Kocher, A. Immediate, non-submerged, root-analogue zirconia implant in single tooth replacement. *Int. J. Oral Maxillofac. Surg.* **2008**, *37*, 293–295. [[CrossRef](#)]
15. Pirker, W.; Kocher, A. Immediate, non-submerged, root-analogue zirconia implants placed into single-rooted extraction sockets: 2-year follow-up of a clinical study. *Int. J. Oral Maxillofac. Surg.* **2009**, *38*, 1127–1132. [[CrossRef](#)]
16. Pirker, W.; Kocher, A. Root analog zirconia implants: True anatomical design for molar replacement—A case report. *Int. J. Periodontics Restor. Dent.* **2011**, *31*, 663–668.
17. Pirker, W.; Wiedemann, D.; Lidauer, A.; Kocher, A. Immediate, single stage, truly anatomic zirconia implant in lower molar replacement: A case report with 2.5 years follow-up. *Int. J. Oral Maxillofac. Surg.* **2011**, *40*, 212–216. [[CrossRef](#)]
18. Moin, D.A.; Hassan, B.; Mercelis, P.; Wismeijer, D. Designing a novel dental root analogue implant using cone beam computed tomography and CAD/CAM technology. *Clin. Oral Implant. Res.* **2011**, *24*, 25–27. [[CrossRef](#)]
19. Mangano, C.; Cirotti, B.; Sammons, R.L.; Mangano, C. Custom-made, root-analogue direct laser metal forming implant: A case report. *Lasers Med Sci.* **2012**, *27*, 1241–1245. [[CrossRef](#)]
20. Pour, R.; Randelzhofer, P.; Edelhoff, D.; Prandtner, O.; Rafael, C.; Liebermann, A. Innovative Single-Tooth Replacement with an Individual Root-Analog Hybrid Implant in the Esthetic Zone: Case Report. *Int. J. Oral Maxillofac. Implant.* **2017**, *32*. [[CrossRef](#)]
21. Beuer, F.; Groesser, J.; Schweiger, J.; Hey, J.; Güth, J.-F.; Stimmelmayer, M. The Digital One-Abutment/One-Time Concept. A Clinical Report. *J. Prosthodont.* **2015**, *24*, 580–585. [[CrossRef](#)] [[PubMed](#)]
22. Schubert, O.; Beuer, F.; Güth, J.-F.; Nold, E.; Edelhoff, D.; Metz, I. Two digital strategies in modern implantology—Root-analogue implants and the digital one-abutment/one-time concept. *Int. J. Comput. Dent.* **2018**, *21*, 115–131. [[PubMed](#)]
23. Sanz, M.; Nogueurol, B.; Sanz-Sánchez, I.; Hammerle, C.H.F.; Schliephake, H.; Renouard, F.; Sicilia, A.; Steering Committee; Cordaro, L.; Jung, R. European Association for Osseointegration Delphi study on the trends in Implant Dentistry in Europe for the year 2030. *Clin. Oral Implant. Res.* **2019**, *30*, 476–486. [[CrossRef](#)]
24. Muska, E.; Walter, C.; Knight, A.; Taneja, P.; Bulsara, Y.; Hahn, M.; Desai, M.; Dietrich, T. Atraumatic vertical tooth extraction: A proof of principle clinical study of a novel system. *Oral Surg. Oral Med. Oral Pathol. Oral Radiol.* **2013**, *116*, e303–e310. [[CrossRef](#)] [[PubMed](#)]
25. Okada, H.; Takahashi, K.; Ogura, N.; Tomoki, R.; Ito, K.; Kondoh, T. Plasma rich in growth factors stimulates proliferation, migration, and gene expression associated with bone formation in human dental follicle cells. *J. Dent. Sci.* **2016**, *11*, 245–252. [[CrossRef](#)]
26. Papaspyridakos, P.; Chen, C.-J.; Singh, M.; Weber, H.-P.; O Gallucci, G. Success criteria in implant dentistry: A systematic review. *J. Dent. Res.* **2011**, *91*, 242–248. [[CrossRef](#)]

27. Albrektsson, T.; Zarb, G.; Worthington, P.; Eriksson, A.R. The long-term efficacy of currently used dental implants: A review and proposed criteria of success. *Int. J. Oral Maxillofac. Implant.* **1986**, *1*, 11–25.
28. Bra-Nemark, P.-I.; Zarb, G.A.; Albrektsson, T.; Rosen, H.M. Tissue-Integrated Prostheses. Osseointegration in Clinical Dentistry. *Plast. Reconstr. Surg.* **1986**, *77*, 496–497. [[CrossRef](#)]
29. Mombelli, A.; Oosten, M.A.C.; Schürch, E.; Land, N.P.; Lang, N.P. The microbiota associated with successful or failing osseointegrated titanium implants. *Oral Microbiol. Immunol.* **1987**, *2*, 145–151. [[CrossRef](#)]
30. Belsler, U.C.; Grütter, L.; Vailati, F.; Bornstein, M.M.; Weber, H.-P.; Buser, D. Outcome Evaluation of Early Placed Maxillary Anterior Single-Tooth Implants Using Objective Esthetic Criteria: A Cross-Sectional, Retrospective Study in 45 Patients With a 2- to 4-Year Follow-Up Using Pink and White Esthetic Scores. *J. Periodontol.* **2009**, *80*, 140–151. [[CrossRef](#)]
31. Schmalz, G.; Ryge, G. Reprint of Criteria for the clinical evaluation of dental restorative materials. *Clin. Oral Investig.* **2005**, *9*, 215–232. [[CrossRef](#)] [[PubMed](#)]
32. Spies, B.C.; Kohal, R.; Balmer, M.; Vach, K.; Jung, R.E. Evaluation of zirconia-based posterior single crowns supported by zirconia implants: Preliminary results of a prospective multicenter study. *Clin. Oral Implant. Res.* **2016**, *28*, 613–619. [[CrossRef](#)] [[PubMed](#)]
33. Pessanha-Andrade, M.; Sordi, M.B.; Henriques, B.; Silva, F.; Teughels, W.; Souza, J.C. Custom-made root-analogue zirconia implants: A scoping review on mechanical and biological benefits. *J. Biomed. Mater. Res. Part B Appl. Biomater.* **2018**, *106*, 2888–2900. [[CrossRef](#)] [[PubMed](#)]
34. Pour, R.S.; Rafael, C.F.; Engler, M.L.P.D.; Edelhoff, D.; Klaus, G.; Prandtner, O.; Berthold, M.; Liebermann, A. Historical development of root analogue implants: A review of published papers. *Br. J. Oral Maxillofac. Surg.* **2019**, *57*, 496–504. [[CrossRef](#)] [[PubMed](#)]
35. Galindo-Moreno, P.; León-Cano, A.; Ortega-Oller, I.; Monje, A.; O'valle, F.; Catena, A. Marginal bone loss as success criterion in implant dentistry: Beyond 2 mm. *Clin. Oral Implant. Res.* **2014**, *26*, e28–e34. [[CrossRef](#)]
36. Degidi, M.; Daprile, G.; Piattelli, A. Marginal bone loss around implants with platform-switched Morse-cone connection: A radiographic cross-sectional study. *Clin. Oral Implant. Res.* **2016**, *28*, 1108–1112. [[CrossRef](#)]
37. A Malloy, K.; Wadhvani, C.; McAllister, B.; Wang, M.; A Katancik, J. Accuracy and Reproducibility of Radiographic Images for Assessing Crestal Bone Height of Implants Using the Precision Implant X-ray Locator (PIXRL) Device. *Int. J. Oral Maxillofac. Implant.* **2017**, *32*, 830–836. [[CrossRef](#)]
38. Walton, T.R.; Layton, D. Intra- and inter-examiner agreement when assessing radiographic implant bone levels: Differences related to brightness, accuracy, participant demographics and implant characteristics. *Clin. Oral Implant. Res.* **2018**, *29*, 756–771. [[CrossRef](#)]
39. Hartman, G.A.; Cochran, D.L. Initial Implant Position Determines the Magnitude of Crestal Bone Remodeling. *J. Periodontol.* **2004**, *75*, 572–577. [[CrossRef](#)]
40. Hermann, J.S.; Cochran, D.L.; Nummikoski, P.V.; Buser, D. Crestal Bone Changes Around Titanium Implants. A Radiographic Evaluation of Unloaded Nonsubmerged and Submerged Implants in the Canine Mandible. *J. Periodontol.* **1997**, *68*, 1117–1130. [[CrossRef](#)]
41. Capelli, M.; Testori, T.; Galli, F.; Zuffetti, F.; Motroni, A.; Weinstein, R.; Del Fabbro, M. Implant–Buccal Plate Distance as Diagnostic Parameter: A Prospective Cohort Study on Implant Placement in Fresh Extraction Sockets. *J. Periodontol.* **2013**, *84*, 1768–1774. [[CrossRef](#)] [[PubMed](#)]
42. Misch, C.E.; Perel, M.L.; Wang, H.-L.; Sammartino, G.; Galindo-Moreno, P.; Trisi, P.; Steigmann, M.; Rebaudi, A.; Palti, A.; Pikos, M.A.; et al. Implant Success, Survival, and Failure: The International Congress of Oral Implantologists (ICOI) Pisa Consensus Conference. *Implant. Dent.* **2008**, *17*, 5–15. [[CrossRef](#)] [[PubMed](#)]
43. Pjetursson, B.E.; Zarauz, C.; Strasding, M.; Sailer, I.; Zwahlen, M.; Zembic, A. A systematic review of the influence of the implant-abutment connection on the clinical outcomes of ceramic and metal implant abutments supporting fixed implant reconstructions. *Clin. Oral Implant. Res.* **2018**, *29*, 160–183. [[CrossRef](#)] [[PubMed](#)]
44. Heitz-Mayfield, L.J.A.; Aaboe, M.; Araujo, M.; Carrión, J.B.; Cavalcanti, R.; Cionca, N.; Cochran, D.; Darby, I.; Funakoshi, E.; Gierthmuehlen, P.C.; et al. Group 4 ITI Consensus Report: Risks and biologic complications associated with implant dentistry. *Clin. Oral Implant. Res.* **2018**, *29*, 351–358. [[CrossRef](#)]
45. Linkevicius, T.; Vindasiute, E.; Puisys, A.; Linkeviciene, L.; Maslova, N.; Puriene, A. The influence of the cementation margin position on the amount of undetected cement. A prospective clinical study. *Clin. Oral Implant. Res.* **2012**, *24*, 71–76. [[CrossRef](#)]

46. Hashim, D.; Cionca, N.; Combescure, C.; Mombelli, A. The diagnosis of peri-implantitis: A systematic review on the predictive value of bleeding on probing. *Clin. Oral Implant. Res.* **2018**, *29*, 276–293. [[CrossRef](#)]
47. Arunyanak, S.P.; Pollini, A.; Ntounis, A.; Morton, D. Clinician assessments and patient perspectives of single-tooth implant restorations in the esthetic zone of the maxilla: A systematic review. *J. Prosthet. Dent.* **2017**, *118*, 10–17. [[CrossRef](#)]
48. Tettamanti, S.; Millen, C.; Gavric, J.; Buser, D.; Belser, U.C.; Bragger, U.; Wittneben, J.-G. Esthetic Evaluation of Implant Crowns and Peri-Implant Soft Tissue in the Anterior Maxilla: Comparison and Reproducibility of Three Different Indices. *Clin. Implant. Dent. Relat. Res.* **2015**, *18*, 517–526. [[CrossRef](#)]
49. Gallucci, G.O.; Grütter, L.; Nedir, R.; Bischof, M.; Belser, U.C. Esthetic outcomes with porcelain-fused-to-ceramic and all-ceramic single-implant crowns: A randomized clinical trial. *Clin. Oral Implant. Res.* **2010**, *22*, 62–69. [[CrossRef](#)]
50. Gallucci, G.O.; Doughtie, C.B.; Hwang, J.W.; Fiorellini, J.P.; Weber, H.-P. Five-year results of fixed implant-supported rehabilitations with distal cantilevers for the edentulous mandible. *Clin. Oral Implant. Res.* **2009**, *20*. [[CrossRef](#)]
51. Romeo, E.; Lops, D.; Margutti, E.; Ghisolfi, M.; Chiapasco, M.; Vogel, G. Long-term survival and success of oral implants in the treatment of full and partial arches: A 7-year prospective study with the ITI dental implant system. *Int. J. Oral Maxillofac. Implant.* **2004**, *19*, 247–259.
52. Romeo, E.; Tomasi, C.; Finini, I.; Casentini, P.; Lops, D. Implant-supported fixed cantilever prosthesis in partially edentulous jaws: A cohort prospective study. *Clin. Oral Implant. Res.* **2009**, *20*, 1278–1285. [[CrossRef](#)] [[PubMed](#)]
53. Esposito, M.; Grusovin, M.G.; Polyzos, I.P.; Felice, P.; Worthington, H.V. Interventions for replacing missing teeth: Dental implants in fresh extraction sockets (immediate, immediate-delayed and delayed implants). *Cochrane Database Syst. Rev.* **2010**, *9*, CD005968. [[CrossRef](#)] [[PubMed](#)]
54. Esposito, M.; Zucchelli, G.; Cannizzaro, G.; Checchi, L.; Barausse, C.; Trullenque-Eriksson, A.; Felice, P. Immediate, immediate-delayed (6 weeks) and delayed (4 months) post-extractive single implants: 1-year post-loading data from a randomised controlled trial. *Eur. J. Oral Implant.* **2017**, *10*, 11–26.



© 2020 by the authors. Licensee MDPI, Basel, Switzerland. This article is an open access article distributed under the terms and conditions of the Creative Commons Attribution (CC BY) license (<http://creativecommons.org/licenses/by/4.0/>).

2.3 Manuscript 3 – Trueness of implant installation using sterilizable surgical guides fabricated in office by material extrusion

Performing sCAIS allows for higher accuracy compared to free-hand surgery (90). To date, CAD/CAM surgical guides are mainly created by SLA or DLP technique (67). The main drawbacks of both methods are the high production costs and the time-consuming postprocessing procedures. To overcome such limits, surgical guides made by ME might represent a viable option. In this study, surgical guides created by ME were compared in terms of trueness of implant installation to market-available SLA-based ones. In addition, the impact of using metal sleeves was assessed. All surgical guides were steam sterilized before use.

Dr. Valentin Hromadnik presented this study as a digital poster in the basic research category at the 26th Annual Scientific Meeting of the EAO in 2019 in Lisbon, Portugal. The abstract was published in *Clinical Oral Implants Research* (91). Furthermore, the research was awarded with the prize for “best preclinical investigation” at the 33rd. Annual Scientific Meeting of the DGI in 2019 in Hamburg, Germany.

The following text corresponds to the abstract of the article:

Pieralli, S., Spies, B. C., Hromadnik, V., Nicic, R., Beuer, F., & Wesemann, C. (2020). *How Accurate Is Oral Implant Installation Using Surgical Guides Printed from a Degradable and Steam-Sterilized Biopolymer?* *Journal of clinical medicine*, 9(8), 2322. <https://doi.org/10.3390/jcm9082322>

How Accurate Is Oral Implant Installation Using Surgical Guides Printed from a Degradable and Steam-Sterilized Biopolymer?

Objective

3D printed surgical guides are used for prosthetically-driven oral implant placement. When manufacturing these guides, information regarding suitable printing techniques and materials as well as the necessity for additional, non-printed stock parts such as metal sleeves is scarce. The aim of the investigation was to determine the accuracy of a surgical workflow for oral implant placement using guides manufactured by means of fused deposition modeling (FDM) from a biodegradable and sterilizable biopolymer filament. Furthermore, the potential benefit of metal sleeve inserts should be assessed.

Methods

A surgical guide was designed for the installation of two implants in the region of the second premolar (SP) and second molar (SM) in a mandibular typodont model. For two additive manufacturing techniques (stereolithography [SLA]: reference group, FDM: observational group) $n = 10$ surgical guides, with (S) and without (NS) metal sleeves, were used. This resulted in 4 groups of 10 samples each (SLA-S/NS, FDM-S/NS). Target and real implant positions were superimposed and compared using a dedicated software. Sagittal, transversal, and vertical discrepancies at the level of the implant shoulder, apex and regarding the main axis were determined. MANOVA with posthoc Tukey tests were performed for statistical analyses.

Results

Placed implants showed sagittal and transversal discrepancies of < 1 mm, vertical discrepancies of < 0.6 mm, and axial deviations of $\leq 3^\circ$. In the vertical dimension, no

differences between the four groups were measured ($p \leq 0.054$). In the sagittal dimension, SLA groups showed decreased deviations in the implant shoulder region compared to FDM ($p \leq 0.033$), whereas no differences in the transversal dimension between the groups were measured ($p \leq 0.054$). The use of metal sleeves did not affect axial, vertical, and sagittal accuracy, but resulted in increased transversal deviations ($p = 0.001$).

Conclusion

Regarding accuracy, biopolymer-based surgical guides manufactured by means of FDM present similar accuracy than SLA. Cytotoxicity tests are necessary to confirm their biocompatibility in the oral environment.

Article

How Accurate Is Oral Implant Installation Using Surgical Guides Printed from a Degradable and Steam-Sterilized Biopolymer?

Stefano Pieralli ¹, Benedikt Christopher Spies ^{1,*}, Valentin Hromadnik ², Robert Nicic ², Florian Beuer ² and Christian Wesemann ^{2,3}

¹ Department of Prosthetic Dentistry, Center for Dental Medicine, Medical Center—University of Freiburg, Faculty of Medicine—University of Freiburg, 79106 Freiburg, Germany; stefano.pieralli@uniklinik-freiburg.de

² Department of Prosthodontics, Humboldt-Universität zu Berlin, and Berlin Institute of Health, Charité—Universitätsmedizin Berlin, corporate member of Freie Universität Berlin, Geriatric Dentistry and Craniomandibular Disorders, 14197 Berlin, Germany; valentin.hromadnik@charite.de (V.H.); robert.nicic@charite.de (R.N.); florian.beuer@charite.de (F.B.); christian.wesemann@charite.de (C.W.)

³ Department of Orthodontics, Humboldt-Universität zu Berlin, and Berlin Institute of Health, Charité—Universitätsmedizin Berlin, corporate member of Freie Universität Berlin, Dentofacial Orthopedics and Pedodontics, Aßmannshäuser Str. 4-6, 14197 Berlin, Germany

* Correspondence: benedikt.spies@uniklinik-freiburg.de; Tel.: +49-761-270-49060

Received: 23 June 2020; Accepted: 17 July 2020; Published: 22 July 2020



Abstract: 3D printed surgical guides are used for prosthetically-driven oral implant placement. When manufacturing these guides, information regarding suitable printing techniques and materials as well as the necessity for additional, non-printed stock parts such as metal sleeves is scarce. The aim of the investigation was to determine the accuracy of a surgical workflow for oral implant placement using guides manufactured by means of fused deposition modeling (FDM) from a biodegradable and sterilizable biopolymer filament. Furthermore, the potential benefit of metal sleeve inserts should be assessed. A surgical guide was designed for the installation of two implants in the region of the second premolar (SP) and second molar (SM) in a mandibular typodont model. For two additive manufacturing techniques (stereolithography [SLA]: reference group, FDM: observational group) $n = 10$ surgical guides, with (S) and without (NS) metal sleeves, were used. This resulted in 4 groups of 10 samples each (SLA-S/NS, FDM-S/NS). Target and real implant positions were superimposed and compared using a dedicated software. Sagittal, transversal, and vertical discrepancies at the level of the implant shoulder, apex and regarding the main axis were determined. MANOVA with posthoc Tukey tests were performed for statistical analyses. Placed implants showed sagittal and transversal discrepancies of <1 mm, vertical discrepancies of <0.6 mm, and axial deviations of $\leq 3^\circ$. In the vertical dimension, no differences between the four groups were measured ($p \leq 0.054$). In the sagittal dimension, SLA groups showed decreased deviations in the implant shoulder region compared to FDM ($p \leq 0.033$), whereas no differences in the transversal dimension between the groups were measured ($p \leq 0.054$). The use of metal sleeves did not affect axial, vertical, and sagittal accuracy, but resulted in increased transversal deviations ($p = 0.001$). Regarding accuracy, biopolymer-based surgical guides manufactured by means of FDM present similar accuracy than SLA. Cytotoxicity tests are necessary to confirm their biocompatibility in the oral environment.

Keywords: accuracy; additive manufacturing; biodegradability; computer-aided design; dental implants; fused deposition modelling; medical device; lignin; surgical guides

1. Introduction

Implant-supported single crowns (SCs) and multi-unit fixed dental prostheses (FDPs) present a predictable treatment option for patients with missing or hopeless natural teeth [1,2]. However, biological and technical complications can be associated with malpositioned implants or poorly designed superstructures [3–5]. Backward planning, as available in digital workflows, can be considered an effective tool to avoid implant malposition [6,7].

An implant planning software allows to import acquired radiographical and surface data and to visualize the final outcome, thereby facilitating to define the ideal implant site according to a virtual set-up and the anatomical characteristics of the patient [8,9]. Based on the virtually planned implant position, a surgical drilling guide can be manufactured, e.g., by 3D printing [10,11] and adapted to the clinical workflow without a typical learning curve [12]. Printing technology based on computer aided design and manufacturing (CAD-CAM) allows to create objects by adding consecutive layers [13]. Surgical guides made from resin-based materials using the stereolithography (SLA) or digital light processing (DLP) technique are mostly used in daily clinical routine [14] also for skeletal anchorage purposes [15]. Using SLA for printing, multiple layers of fluid resin are successively photopolymerized by selective ultraviolet (UV) laser radiation ($\lambda = 350\text{--}450\text{ nm}$) allowing the creation of highly accurate objects [16] with fine grained complex geometries [17]. However, increased manufacturing costs and time-consuming post processing procedures are necessary for manufacturing SLA printed surgical guides, and potential debris by means of detached resin particles are likely to affect the surgical site. Additional non-printable stock articles such as metal guidance in the form of sleeves or drill handles are frequently used to avoid wear and debris of the guide and incorrect drilling paths [18].

To date, multiple 3D printing technologies available on the market are suitable for additive manufacturing of dental devices such as surgical guides [19], among these fused deposition modelling (FDM) represents a straightforward and cost-effective method [20]. This technique allows extrusion of melted thermoplastic filaments through a mobile nozzle with subsequent deposition on a hot plate according to the planned CAD dataset, requiring a minimal postprocessing sequence [21,22]. Despite the favorable characteristics of this technique, accuracy of the final object is still a topic of controversial discussion and seems to be highly dependent of the printing process and the raw material used [23].

Among other filaments, FDM technology allows for additive manufacturing of biopolymers such as lignin and polylactides (PLA), a biodegradable filament used for tissue engineering purposes in various fields of regenerative medicine and dentistry [24–26]. Despite environmental advantage in terms of biodegradability, recent studies showed improvements of the mechanical properties by changing the layups of the fibers of subsequent layers [20]. Since FDM printed surgical guides made of lignin and PLA might represent a cost-effective, sterilizable, and environmental-friendly alternative to surgical guides made of SLA printed resins, this study aimed to compare SLA and FDM printed guides in terms of the accuracy when used for implant positioning.

The purpose of this investigation was to measure the accuracy of a guided workflow for implant placement by comparing the discrepancies between the virtually planned (target) and finally realized position of oral implants at the level of the apex, shoulder, and the implant axis. The influence of the manufacturing technology (SLA and FDM) and a potential benefit of inserted metal sleeves were evaluated on the basis of two implants installed to support a three-unit FDP in a mandibular model.

The null hypothesis assumed no significant horizontal or vertical discrepancies between target and realized implant position, irrespective of the 3D printing method and the use of metal guidance at both implant positions.

2. Experimental Section

2.1. Reference Model

A typodont model (IMP1001-UL-SP-DM, Nissin, Kyoto, Japan) revealing a removable edentulous alveolar ridge located in the posterior part of the lower left quadrant was used to install two two-piece titanium oral implants in the region of the second premolar and molar (SP and SM), respectively. To allow multiple implant placement, the removable alveolar ridge of the model was digitized using an intraoral scanner (IOS) (TRIOS 3, 3shape, Copenhagen, Denmark), adjusted in an inspection-software (Fusion 360, Autodesk, San Rafael, CA, USA) and 3D printed from a ABS filament (DuraPro ABS black, ExdruDr, Lauterach, Austria) by means of FDM, with an 1.5 mm outermost layer printed in compact form (100%) and an infill of 75%. This aimed to mimic cortical and spongy bone.

2.2. Digital Implant Planning

To simulate a clinical workflow, a cone-beam computer tomography (CBCT) (Veraviewepocs 3-D R100, J. Morita Corp., Osaka, Japan) of the reference model was performed. The mandible was removed from the occludator by a medical technical assistant prior to radiography to avoid metal-induced artifacts (field of view: 8 cm × 8 cm, circulation time: 9.4 s, tube voltage: 80 kV and current intensity: 1 mA). The corresponding virtual dataset (Digital Imaging and Communications in Medicine, DICOM) was subsequently imported in an implant planning software (SMOP, Swissmeda AG, Baar, Switzerland) and superimposed with the surface data (standard tessellation language, STL) obtained with an IOS (TRIOS 3, 3shape) of the reference model by a professional in the field of digital design. To avoid distortions, a standardized scan path, under ceiling lighting was followed during the acquisition of the STL data. Thereafter, a three-unit FDP (ranging from the SP to the SM) was designed by a master dental technician (R.N.) using a CAD software (Dental Designer, 3shape) and imported into the implant-planning software (Figure 1).

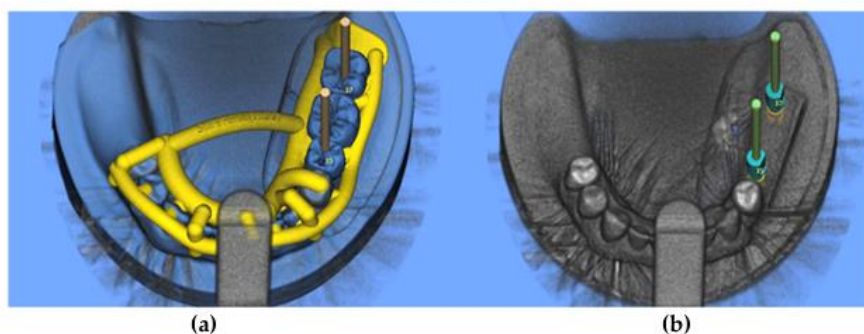


Figure 1. Digital implant planning: (a) design of the surgical guide, (b) virtual application of scan bodies (target position).

Two two-piece titanium implants were virtually positioned and parallelized in the afore mentioned regions to allow for transocclusal screw-retention of the FDP. Thereafter, implant positions (referred to by virtual scan bodies) were exported as STL file (“target position”). Finally, a surgical template for guided implant installation was designed (J.B.). For sleeveless (N.S.) insertion, the diameter of the drilling holes of the surgical guides was digitally adapted to an inner diameter of 4.6 mm in order to match the inner diameter of the used titanium sleeves (S) (Guide System Guiding sleeve, REF.: J3734.3803, Camlog).

2.3. 3D Printing of Surgical Guides

For each of the four groups (FDM-S, FDM-NS, SLA-S, SLA-NS) 10 surgical guides were additively manufactured and steam sterilized in an autoclave (15 min, 121 °C) (Webeco, Serie EC, Selmsdorf, Germany). Two different 3D printing technologies were evaluated in this investigation. SLA (Form 2, Dental SG Resin, Formlabs, Boston, MA, USA) was used to manufacture surgical guides made of medical class 1 resin (Dental SG Resin, Formlabs) certified for dental use (EN-ISO 10993-1:2009/AC:2010, USP Class VI) by printing 0.05 mm thin layers. The average printing time of each sample was 50 min. This allowed simultaneous printing of multiple units followed by a post-processing sequence consisting of a 5 min rinsing in alcohol (99% isopropanol), air-drying, and 30 min light curing ($\lambda = 405$ nm) at 60 °C. Finally, printing supports were removed, and smooth surface finishing was performed. The FDM printed surgical guides (Prusa i3 MK3, Prague, Czech Rep.) were manufactured using an experimental biofilament based on lignin with a layer thickness of 0.06 mm, a printing temperature of 220 °C and a print bed temperature of 60 °C. The average printing time was 60 min. Apart of removing the support-structures and polishing, no further post-processing was needed for FDM printed surgical guides. Finally, the guides were steam-sterilized as the SLA printed guides mentioned afore.

2.4. Surgical Protocol

The surgical guides were used for the insertion of 80 two-piece regular platform tapered titanium implants (3.8 × 9 mm; CAMLOG® SCREW-LINE Promote plus, REF.: K1052.3809; Camlog, Basel, Switzerland) in the removable part of the mandible model following a standardized drilling protocol. In the first instance, a pilot drill with a diameter of 2 mm (Guide System Pilot drill set, REF.: J5063.4309; Camlog) (800 rounds per minute, RPM) provided with calibrated depth control was used. Subsequent, two successive yellow-color coded drills (Guide System Surgery-set SCREW-LINE, REF.: J5065.3809; Camlog) designated for the installation of 3.8 mm wide implants of this type were provided with metal sleeves and used to progressively enlarge the implant site (500 RPM). Finally, a cortical bone drill expanded the implant site (Guide System Form drill SCREW-LINE, Cortical bone, REF.: J5068.3809; Camlog) (500 RPM) and manual tapping (15 RPM) was performed. All implants were inserted by hand (<15 RPM) and provided with scan bodies (CAMLOG® Scanbodies, REF.: K2610.3810, Camlog), made of polyetheretherketon (PEEK). To simulate a clinical setting, drilling and implant insertion procedures were performed using a dental simulator manikin phantom head by one single operator (V.H.).

2.5. Data Acquisition

The digitization process of the scan bodies was conducted by means of a 3D LED scanner (D2000, 3shape) showing a precision of 5 µm/8 µm (ISO 12836/implant). The resulting STL files were subsequently imported in an inspection software (Geomagic Control X, 3-D Systems; Rock Hill, CA, USA) and aligned with the target implant position. For this purpose, the actual 3D position of the scan bodies was used as reference and superimposed to the target position by performing an initial 7-point alignment followed by a best-fit superimposition according to Gauss (Figure 2). Thereafter, sagittal, transversal and vertical discrepancies were measured at both the implant apex and implant shoulder level using a linear 2-point measurement. Similarly, deviations of the main axis were assessed.

2.6. Statistical Analysis

For the statistical analysis, data were tested for normal distribution (Kolmogorow–Smirnow test) and variance homogeneity (Levene test). Afterwards multivariate analyses of variance (MANOVA) with post hoc Tukey tests were calculated for the independent variables 3D printing technology (SLA, FDM) and use of sleeve (S, NS) at both implant positions (SP and SM). The statistical analysis was calculated with a statistical software program (IBM SPSS Statistics, v22.0, IBM Corp). The significance level was set at $\alpha = 0.05$.

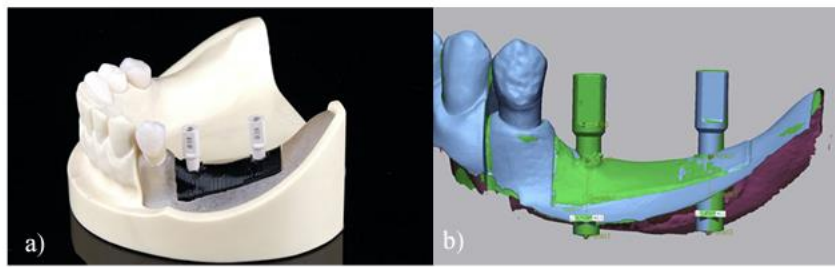


Figure 2. Digitization of the scan bodies: (a) Scan bodies in situ (implant final position), (b) Superimposition of planned and final position.

3. Results

A total of 80 implants were inserted by using four different groups ($n = 10$) of surgical guides (SLA-S, SLA-NS, FDM-S, FDM-NS). Compared to target, all installed implants showed maximum vertical (z) deviations of <0.6 mm and horizontal (x, y) deviations of <1.0 mm (Figure 3). A maximum angular discrepancy referring to the main axis of 3.02° was calculated (Figure 4). Mean and descriptive statistics can be found in Table 1. MANOVA revealed significant transversal (y) differences at the apex ($p = 0.001$), sagittal (x) and transversal (y) differences at the shoulder level ($p = 0.001$) and axial differences ($p = 0.033$) between the groups (Table 2).

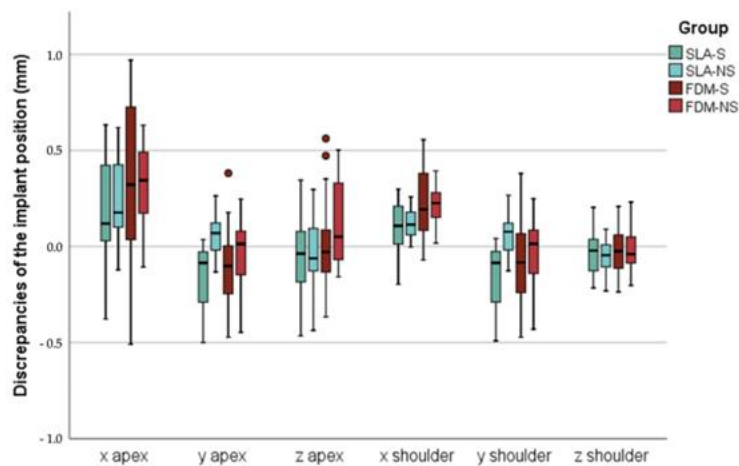


Figure 3. Boxplots of minimum, maximum, interquartile range, median, and outliers for discrepancies of the implant position at implant apex and shoulder level. SLA: stereolithography, FDM: fused deposition modeling, S: metal sleeve, NS: no metal sleeve, x: sagittal discrepancies, y: transversal discrepancies, z: vertical discrepancies.

3.1. Sagittal Discrepancies (X)

No significant deviations were measured at the apical level of the implants between the groups ($p = 0.05$). However, at the implant shoulder, significant sagittal differences were found in the SM region ($p = 0.001$). Both SLA groups showed decreased discrepancies compared with FDM ($p \leq 0.033$). The use of a metal sleeve did not affect the accuracy of implant insertion for both SLA ($p = 0.992$) or FDM ($p = 0.482$).

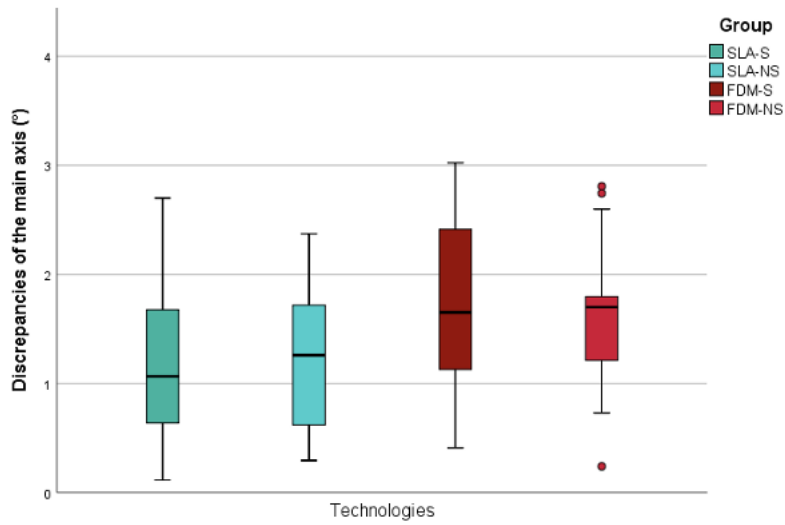


Figure 4. Boxplots of minimum, maximum, interquartile range, median, and outliers for discrepancies of the implant main axis. SLA: stereolithography, FDM: fused deposition modeling, S: metal sleeve, NS: no metal sleeve, x: sagittal discrepancies, y: transversal discrepancies, z: vertical discrepancies.

3.2. Transversal Discrepancies (Y)

Mean transverse discrepancies at the apical level were found to be 0.4 ± 0.2 mm with deviations ranging from 0.1 to 0.9 mm. Apically, both printing technologies showed comparable results, but sleeveless insertion revealed lower deviations in the SP region for both SLA ($p = 0.001$) and FDM ($p = 0.201$). Similarly, minor differences between the printing technologies were found at the implant shoulder, but again sleeveless insertion increased the accuracy for both SLA ($p = 0.001$) and FDM ($p = 0.001$) in the SP region.

3.3. Vertical Deviations (z)

Irrespective of the group, the mean vertical deviation resulted in 0.2 ± 0.1 mm at the apex level and 0.1 ± 0.1 mm at the shoulder level. Overall maximum vertical discrepancies ranged between 0.1 and 0.6 mm at the apex level, and 0.1 and 0.2 mm at the shoulder level. MONAVA showed neither apical ($p \geq 0.054$) nor at implant shoulder level ($p \geq 0.352$) differences between the groups in both implant regions.

3.4. Main Axis Deviations

No significant axial differences between the groups were found in the SP region ($p = 0.409$) with mean deviations ranging between $1.3 \pm 0.9^\circ$ (SLA-S) and $1.9 \pm 0.8^\circ$ (FDM-S). Likewise, comparable results between the groups were measured in the area of SM. Only the group with the smallest mean deviations of 0.8 ± 0.5 (SLA-NS) differed significantly from the largest deviations of 1.7 ± 0.9 (FDM-S) ($p = 0.020$).

Table 1. Mean ± standard deviation of the discrepancies at the implant apex and shoulder level and the main axis.

Position	Technology	Guidance	Apex (mm)			Shoulder (mm)			Axis (°)	
			x	y	z	x	y	z		
35	SLA	S	0.3 ± 0.2	-0.2 ± 0.2	-0.1 ± 0.2	0.1 ± 0.1	-0.2 ± 0.2	-0.1 ± 0.1	1.3 ± 0.9	
		NS	0.3 ± 0.2	0.1 ± 0.1	-0.1 ± 0.2	0.1 ± 0.1	0.1 ± 0.1	-0.1 ± 0.1	1.6 ± 0.5	
	FDM	S	0.2 ± 0.4	-0.3 ± 0.1	0.1 ± 0.3	0.1 ± 0.2	-0.3 ± 0.1	0 ± 0.1	1.9 ± 0.8	
		NS	0.3 ± 0.2	-0.1 ± 0.2	0.2 ± 0.3	0.2 ± 0.1	-0.1 ± 0.2	0 ± 0.1	1.9 ± 0.8	
	37	SLA	S	0.1 ± 0.3	-0.1 ± 0.1	0.0 ± 0.2	0.1 ± 0.1	-0.1 ± 0.1	0.0 ± 0.1	1.2 ± 0.6
			NS	0.1 ± 0.2	0.0 ± 0.1	0.0 ± 0.2	0.1 ± 0.1	-0.1 ± 0.1	0.0 ± 0.1	0.8 ± 0.5
FDM		S	0.4 ± 0.4	0.0 ± 0.2	-0.1 ± 0.1	0.3 ± 0.1	0.1 ± 0.2	0.0 ± 0.1	1.7 ± 0.9	
		NS	0.3 ± 0.2	0.1 ± 0.1	0.1 ± 0.2	0.2 ± 0.1	0.1 ± 0.1	0.0 ± 0.1	1.3 ± 0.4	

SLA: stereolithography, FDM: fused deposition modeling, S: metal sleeve, NS: no metal sleeve, x: sagittal discrepancies, y: transversal discrepancies, z: vertical discrepancies.

Table 2. Results of MANOVA with post hoc pairwise comparisons in case of $p < 0.05$.

		MANOVA Significance	Position	Multiple Comparisons		Tukey Test Significance
				Group (A)	Group (B)	
Apex	x	0.050	35	SLA-NS	SLA-S	0.001
	y	0.001			FDM-S	0.001
					FDM-NS	0.045
	z	0.054				
Shoulder	x	0.001	37	SLA-S	FDM-S	0.001
					FDM-NS	0.017
					FDM-S	0.001
	y	0.001	35	SLA-NS	FDM-NS	0.033
					SLA-S	0.001
					FDM-S	0.001
	z	0.352	37	SLA-S	FDM-NS	0.035
Axis		0.033	37	SLA-NS	FDM-S	0.020

MANOVA: multivariate analysis of variance, SLA: stereolithography, FDM: fused deposition modeling, S: metal sleeve, NS: no metal sleeve, x: sagittal discrepancies, y: transversal discrepancies, z: vertical discrepancies.

4. Discussion

The aim of this investigation was to assess the accuracy of guided implant positioning by using a simplified and more economic additive CAM method, namely FDM, and compare it to SLA. A total of 80 two-piece titanium implants were positioned and digitized. Significant differences between final and planned implant position resulted comparing FDM and SLA, and the null hypothesis was partially rejected. Regardless of the study group, maximum vertical deviations of <0.6 mm, horizontal deviation of <1 mm and axial deviation of $\leq 3.02^\circ$ were measured.

In this study implants were placed in vitro in a typodont model, which does not fully reflect the clinical situation. Especially differences between natural bone and resin blocks as implant site can affect implant installation. The rationale was therefore to create a bi-layered alveolar bone architecture by creating blocks with 1.5 mm external layers printed in compact form with 100% infill (cortical bone) and an internal part with 75% infill, simulating a porous scaffold (spongiosa). As proof of concept, three different internal densities of infill (50%, 75%, and 100%) were used to perform test implant placements at study conceptualization by five experienced clinicians. Eligibility criteria were a resistance to drilling comparable to the posterior mandible (2/3 bone quality) [27] and implant insertion torque < 30 Ncm (recommended for this implant system). Blocks with 75% internal infill fulfilled both above mentioned criteria and were adapted.

The final implant position was assessed by digitization of the scan body and superimposing the planned and final implant position. This approach has already been described in vitro [28] and in vivo [29,30]. In a recent RCT, a postoperative CBCT, with the same field of view of the diagnostic one, was conducted to evaluate the accuracy of guided implant positioning as an alternative method [31] showing comparable results to digitization of scan bodies [32].

Implant planning software are CAD systems which virtually recreate the intraoral circumstances for planification purposes. Comparable to other implant software, the one used in this investigation (SMOP) enables to match a 3D radiographic dataset with digitized surface geometries [33]. X-ray data for 3D virtual planning purposes are produced by CBCT and saved as voxel based volumetric DICOM files, whereas the intraoral scans and the wax up/set up of the final restoration are saved as surface polygons in STL format. According to the results of a prospective controlled clinical investigation by Schnutenhaus et al. manual alignment between CBCT and model scan data performed using afore mentioned software can lead to mean deviations of 0.2 mm [34]. However, matching CBCT and surface scans and 3D printing surgical guides using SMOP lead to a more accurate implant positioning compared to surgical guides which use physical positioners to transfer the coordinates of the planned drilling slots [35]. Since dental surfaces are considered ideal for matching purposes, a sufficient number of teeth with few restoration-induced artifacts are needed for manual matching procedures and avoid the use of an x-ray template as reference [8].

Producing surgical guides by FDM was found to be more cost-effective and less time consuming than using SLA. Considering the FDM printing equipment used in this study, a sleeveless surgical guide can be produced with material costs 0.5–1 € compared to 10–20 € if produced by means of SLA. Furthermore, 50 min printing time and additional 35 min post-processing (5 min washing + 30 min light curing) were needed to manufacture an SLA printed surgical guide. An FDM printed surgical guide was fabricated in 65 min (60 min printing time + 5 min post processing).

For this investigation a typodont model of a mandible with unilateral shortened dental arch beginning from the SP was used to plan a screw retained three-unit implant supported FDP (SP–SM). Implants in both locations showed comparable deviations. In a clinical study no difference between implants placed using free ending surgical guides in a shortened dental arch compared with mesial and distal tooth-supported surgical guides in an interrupted arch was measured [36]. This is consistent with the study results of Schnutenhaus et al. evaluating the accuracy of implant position as a function of the remaining teeth [37]. The wide basal configuration designed for mucosal-supported areas seems to balance the soft tissue resilience (snow-shoe principle).

Surgical guides with (S) and without sleeves (NS) showed an equal drill-slot gap (intrinsic error) [38] and the advantage of using metal guidance for implant placement was questioned. In this investigation the use of metal sleeves (S) did not result in more accurate implant positioning compared to NS for both the printing methods. The avoidance of metal sleeves reduced costs (one package containing two-sleeves costs 33 €), production time and error potentials (luting of the sleeve into the slot). Laederach et al. evaluated several systems provided with metal guidance in terms of accuracy of final implant position and could show significant deviations comparing centric and eccentric drilling procedures [39]. On one side, the use of metal guidance does not seem to prevent the clinician from eccentric drilling paths. On the other hand, horizontal drifting of the rotating drill from the metallic slot leads to overheating of the drill and metallic debris, both potentially detrimental for the implant site [40,41]. Metallic particles in the surrounding tissue of the implant are discussed as a potential cofactor for perimplantitis [42]. A sleeveless system that allows for hand-piece guidance rather than drill guidance, thereby avoiding direct contact of rotating components with the surgical guide, is available on the market but information regarding its accuracy is still scarce [43]. In contrast, the approach of this study was to produce surgical guides from a printable and potentially biodegradable biopolymer as proof of concept. A biodegradable material that is suitable for additive manufacturing is PLA. However, pure PLA transforms into the glass phase during autoclave sterilization at temperatures of 121 °C and will potentially deform/lose dimensional accuracy. Likewise overheating due to contact with the drill could lead to deformation of the material. For this reason, a novel lignin-containing filament was investigated for the production of medical products. Lignin is a cross-linked phenolic polymer that occurs in the cell walls of plants and is thermally stable up to 165 °C [44].

Main limitation of the present investigation consisted in the in vitro design, which might have led to more accurate results compared to clinical reality. However, the experimental 3D printable biofilament is not yet allowed for clinical use. Potential bias might be related to the identical design of the surgical guides and the single operator positioning the implants. In addition, changing the manufacturing parameters (e.g., thickness of the layers, printing temperature) could have resulted in a different outcome. To the best knowledge of the authors, this was the first attempt to use the investigated biopolymer to fabricate cost effective, degradable, and sterilizable surgical guides for accurate implant positioning by FDM.

In this study, the lignin drilling templates produced by FDM allowed a reduction of the production costs of 50% even if metallic sleeves are used. However, metal sleeves did not lead to a more accurate implant position. Production of FDM-NS surgical guides resulted the most cost-effective (0.5–1 € per unit) and SLA-S the most expensive (40–50 € per unit). Therefore, further research should address the cytotoxicity of the biofilament for medical use approval and the potential biodegradability of lignin debris in the peri-implant area. Clinical trials are needed to confirm the high accuracy in terms of implant positioning of the evaluated surgical guides as well as the intraoral fit and fracture resistance.

5. Conclusions

According to the outcome of this in vitro study, the following conclusions can be drawn:

- Implant placement using FDM and SLA printed surgical guides resulted in comparable accuracy of implant position.
- Both investigated implant positions (SP, SM) showed comparable deviations.
- The use of metal sleeves for surgical guides did not improve the final accuracy of the implant position.

Author Contributions: Conceptualization: S.P., C.W., and B.C.S.; methodology, V.H., S.P., R.N.; validation, F.B., S.P., C.W., and B.C.S.; formal analysis, C.W.; data curation, V.H., R.N., S.P.; writing—original draft preparation, S.P.; writing—review and editing, C.W., B.C.S. and F.B.; visualization, C.W.; supervision, F.B. and B.C.S. All authors have read and agreed to the published version of the manuscript.

Funding: The article processing charge was funded by the Baden-Wuerttemberg Ministry of Science, Research and Art and the University of Freiburg in the funding program Open Access Publishing.

Acknowledgments: The authors would like to thank Jens Bingenheimer (stentists—digitale Planungsdienstleistungen, Braunschweig, Germany) for the matching procedures and the design of the surgical guide.

Conflicts of Interest: The authors declare no conflict of interest.

References

- Rabel, K.; Spies, B.C.; Pieralli, S.; Vach, K.; Kohal, R.J. The clinical performance of all-ceramic implant-supported single crowns: A systematic review and meta-analysis. *Clin. Oral Implants Res.* **2018**, *29* (Suppl. 18), 196–223. [[CrossRef](#)] [[PubMed](#)]
- Pieralli, S.; Kohal, R.J.; Rabel, K.; von Stein-Lausnitz, M.; Vach, K.; Spies, B.C. Clinical outcomes of partial and full-arch all-ceramic implant-supported fixed dental prostheses. A systematic review and meta-analysis. *Clin. Oral Implants Res.* **2018**, *29* (Suppl. 18), 224–236. [[CrossRef](#)]
- De Kok, I.J.; Duqum, I.S.; Katz, L.H.; Cooper, L.F. Management of Implant/Prosthetic Complications. *Dent. Clin. North. Am.* **2019**, *63*, 217–231. [[CrossRef](#)] [[PubMed](#)]
- Chen, S.T.; Buser, D. Esthetic outcomes following immediate and early implant placement in the anterior maxilla—A systematic review. *Int. J. Oral Maxillofac. Implants* **2014**, *29* (Suppl. g3.3), 186–215. [[CrossRef](#)] [[PubMed](#)]
- Canullo, L.; Tallarico, M.; Radovanovic, S.; Delibasic, B.; Covani, U.; Rakic, M. Distinguishing predictive profiles for patient-based risk assessment and diagnostics of plaque induced, surgically and prosthetically triggered peri-implantitis. *Clin. Oral Implants Res.* **2016**, *27*, 1243–1250. [[CrossRef](#)] [[PubMed](#)]
- Burkhardt, F.; Strietzel, F.P.; Bitter, K.; Spies, B.C. Guided implant surgery for one-piece ceramic implants: A digital workflow. *Int. J. Comput. Dent.* **2020**, *23*, 73–82.
- Pozzi, A.; Polizzi, G.; Moy, P.K. Guided surgery with tooth-supported templates for single missing teeth: A critical review. *Eur. J. Oral Implantol.* **2016**, *9* (Suppl. 1), S135–S153.
- Flugge, T.; Derksen, W.; Te Poel, J.; Hassan, B.; Nelson, K.; Wismeijer, D. Registration of cone beam computed tomography data and intraoral surface scans—A prerequisite for guided implant surgery with CAD/CAM drilling guides. *Clin. Oral Implants Res.* **2017**, *28*, 1113–1118. [[CrossRef](#)]
- Pieralli, S.; Gintaute, A.; Beuer, F.; Spies, B.C. Digital and Orthodontically Driven Implant Planning: A Multidisciplinary Case History Report. *Int. J. Prosthodont* **2019**, *32*, 214–216. [[CrossRef](#)]
- Bencharit, S.; Staffen, A.; Yeung, M.; Whitley, D., 3rd; Laskin, D.M.; Deeb, G.R. In Vivo Tooth-Supported Implant Surgical Guides Fabricated With Desktop Stereolithographic Printers: Fully Guided Surgery Is More Accurate Than Partially Guided Surgery. *J. Oral Maxillofac. Surg.* **2018**, *76*, 1431–1439. [[CrossRef](#)]
- Henprasert, P.; Dawson, D.V.; El-Kerdani, T.; Song, X.; Couso-Queiruga, E.; Holloway, J.A. Comparison of the Accuracy of Implant Position Using Surgical Guides Fabricated by Additive and Subtractive Techniques. *J. Prosthodont.* **2020**. Online ahead of print. [[CrossRef](#)] [[PubMed](#)]
- Cassetta, M.; Altieri, F.; Giansanti, M.; Bellardini, M.; Brandetti, G.; Piccoli, L. Is there a learning curve in static computer-assisted implant surgery? A prospective clinical study. *Int. J. Oral Maxillofac. Surg.* **2020**. [[CrossRef](#)] [[PubMed](#)]
- Aimar, A.; Palermo, A.; Innocenti, B. The Role of 3D Printing in Medical Applications: A State of the Art. *J. Healthc. Eng.* **2019**, *2019*, 5340616. [[CrossRef](#)] [[PubMed](#)]
- Revilla-Leon, M.; Sadeghpour, M.; Ozcan, M. An update on applications of 3D printing technologies used for processing polymers used in implant dentistry. *Odontology* **2019**. [[CrossRef](#)] [[PubMed](#)]
- Cassetta, M.; Altieri, F.; Di Giorgio, R.; Barbato, E. Palatal orthodontic miniscrew insertion using a CAD-CAM surgical guide: Description of a technique. *Int. J. Oral Maxillofac. Surg.* **2018**, *47*, 1195–1198. [[CrossRef](#)]
- Patzelt, S.B.; Bishti, S.; Stampf, S.; Att, W. Accuracy of computer-aided design/computer-aided manufacturing-generated dental casts based on intraoral scanner data. *J. Am. Dent. Assoc.* **2014**, *145*, 1133–1140. [[CrossRef](#)]
- Quan, H.; Zhang, T.; Xu, H.; Luo, S.; Nie, J.; Zhu, X. Photo-curing 3D printing technique and its challenges. *Bioact. Mater.* **2020**, *5*, 110–115. [[CrossRef](#)]

18. Tallarico, M.; Kim, Y.J.; Cocchi, F.; Martinolli, M.; Meloni, S.M. Accuracy of newly developed sleeve-designed templates for insertion of dental implants: A prospective multicenters clinical trial. *Clin. Implant. Dent. Relat Res.* **2019**, *21*, 108–113. [[CrossRef](#)]
19. Rungrojwittayakul, O.; Kan, J.Y.; Shiozaki, K.; Swamidass, R.S.; Goodacre, B.J.; Goodacre, C.J.; Lozada, J.L. Accuracy of 3D Printed Models Created by Two Technologies of Printers with Different Designs of Model Base. *J. Prosthodont.* **2020**, *29*, 124–128. [[CrossRef](#)]
20. Kiendl, J.; Gao, C. Controlling toughness and strength of FDM 3D-printed PLA components through the raster layup. *Compos. Part B Eng.* **2019**, *180*. [[CrossRef](#)]
21. Mazzanti, V.; Malagutti, L.; Mollica, F. FDM 3D Printing of Polymers Containing Natural Fillers: A Review of their Mechanical Properties. *Polymers* **2019**, *11*. [[CrossRef](#)] [[PubMed](#)]
22. Ngo, T.; Kashani, A.; Imbalzano, G.; Nguyen, K.; Hui, D. Additive manufacturing (3D printing): A review of materials, methods, applications and challenges. *Compos. Part B Eng.* **2018**, *143*. [[CrossRef](#)]
23. Li, H.; Wang, T.; Sun, J.; Yu, Z. The effect of process parameters in fused deposition modelling on bonding degree and mechanical properties. *Rapid Prototyp. J.* **2018**, *24*, 80–92. [[CrossRef](#)]
24. Giammona, G.; Craparo, E.F. Biomedical Applications of Polylactide (PLA) and Its Copolymers. *Molecules* **2018**, *23*, 980. [[CrossRef](#)]
25. Ceccarelli, G.; Presta, R.; Lupi, S.M.; Giarratana, N.; Bloise, N.; Benedetti, L.; Cusella De Angelis, M.G.; Rodriguez, Y.B.R. Evaluation of Poly(Lactic-co-glycolic) Acid Alone or in Combination with Hydroxyapatite on Human-Periosteal Cells Bone Differentiation and in Sinus Lift Treatment. *Molecules* **2017**, *22*, 2109. [[CrossRef](#)]
26. Oledzka, E.; Pachowska, D.; Orłowska, K.; Kolmas, J.; Drobniewska, A.; Figat, R.; Sobczak, M. Pamidronate-Conjugated Biodegradable Branched Copolyester Carriers: Synthesis and Characterization. *Molecules* **2017**, *22*, 1063. [[CrossRef](#)]
27. Lekholm, U.; Zarb, G.A. Patient selection and preparation. In *Tissue Integrated Prostheses: Osseointegration in Clinical Dentistry*; Quintessence Publishing Co.: Chicago, IL, USA, 1985; pp. 199–209.
28. Herschdorfer, L.; Negreiros, W.M.; Gallucci, G.O.; Hamilton, A. Comparison of the accuracy of implants placed with CAD-CAM surgical templates manufactured with various 3D printers: An in vitro study. *J. Prosthet Dent.* **2020**. [[CrossRef](#)]
29. Skjervén, H.; Riis, U.H.; Herlofsson, B.B.; Ellingsen, J.E. In Vivo Accuracy of Implant Placement Using a Full Digital Planning Modality and Stereolithographic Guides. *Int. J. Oral Maxillofac. Implants* **2019**, *34*, 124–132. [[CrossRef](#)]
30. Derksen, W.; Wismeijer, D.; Flugge, T.; Hassan, B.; Tahmaseb, A. The accuracy of computer-guided implant surgery with tooth-supported, digitally designed drill guides based on CBCT and intraoral scanning. A prospective cohort study. *Clin. Oral Implants Res.* **2019**, *30*, 1005–1015. [[CrossRef](#)] [[PubMed](#)]
31. Younes, F.; Cosyn, J.; De Bruyckere, T.; Cleymaet, R.; Bouckaert, E.; Eghbali, A. A randomized controlled study on the accuracy of free-handed, pilot-drill guided and fully guided implant surgery in partially edentulous patients. *J. Clin. Periodontol.* **2018**, *45*, 721–732. [[CrossRef](#)]
32. Skjervén, H.; Olsen-Bergem, H.; Ronold, H.J.; Riis, U.H.; Ellingsen, J.E. Comparison of postoperative intraoral scan versus cone beam computerised tomography to measure accuracy of guided implant placement—A prospective clinical study. *Clin. Oral Implants Res.* **2019**, *30*, 531–541. [[CrossRef](#)] [[PubMed](#)]
33. Kurt, B.R. Template guided surgery with the open-access software “smop”. *Swiss Dent. J.* **2014**, *124*, 305–323. [[PubMed](#)]
34. Schnutenhaus, S.; Groller, S.; Luthardt, R.G.; Rudolph, H. Accuracy of the match between cone beam computed tomography and model scan data in template-guided implant planning: A prospective controlled clinical study. *Clin. Implant. Dent. Relat Res.* **2018**, *20*, 541–549. [[CrossRef](#)] [[PubMed](#)]
35. Kernen, F.; Benic, G.I.; Payer, M.; Schar, A.; Müller-Gerbl, M.; Filippi, A.; Kuhl, S. Accuracy of Three-Dimensional Printed Templates for Guided Implant Placement Based on Matching a Surface Scan with CBCT. *Clin. Implant. Dent. Relat Res.* **2016**, *18*, 762–768. [[CrossRef](#)] [[PubMed](#)]
36. Behneke, A.; Burwinkel, M.; Behneke, N. Factors influencing transfer accuracy of cone beam CT-derived template-based implant placement. *Clin. Oral Implants Res.* **2012**, *23*, 416–423. [[CrossRef](#)]
37. Schnutenhaus, S.; Edelmann, C.; Rudolph, H.; Dreyhaupt, J.; Luthardt, R.G. 3D accuracy of implant positions in template-guided implant placement as a function of the remaining teeth and the surgical procedure: A retrospective study. *Clin. Oral Investig.* **2018**, *22*, 2363–2372. [[CrossRef](#)]

38. Cassetta, M.; Di Mambro, A.; Giansanti, M.; Stefanelli, L.V.; Cavallini, C. The intrinsic error of a stereolithographic surgical template in implant guided surgery. *Int. J. Oral Maxillofac. Surg.* **2013**, *42*, 264–275. [[CrossRef](#)]
39. Laederach, V.; Mukaddam, K.; Payer, M.; Filippi, A.; Kuhl, S. Deviations of different systems for guided implant surgery. *Clin. Oral Implants Res.* **2017**, *28*, 1147–1151. [[CrossRef](#)]
40. Kim, Y.; Ju, S.; Kim, M.; Park, M.; Jun, S.; Ahn, J. Direct Measurement of Heat Produced during Drilling for Implant Site Preparation. *Appl. Sci.* **2019**, *9*, 1898. [[CrossRef](#)]
41. Van der Cruyssen, F.; Vasconcelos, K.; Verhelst, P.-J.; Shujaat, S.; Delsupehe, A.-M.; Hauben, E.; Orhan, K.; Politis, C.; Jacobs, R. Metal debris after dental implant placement: A proof-of-concept study in fresh frozen cadavers using MRI and histological analysis. *Int. J. Oral Implantol.* **2019**, *12*, 349–356.
42. Fretwurst, T.; Nelson, K.; Tarnow, D.P.; Wang, H.-L.; Giannobile, W.V. Is Metal Particle Release Associated with Peri-implant Bone Destruction? An Emerging Concept. *J. Dental Res.* **2018**, *97*, 259–265. [[CrossRef](#)] [[PubMed](#)]
43. Schnutenhaus, S.; von Koenigsmarck, V.; Blender, S.; Ambrosius, L.; Luthardt, R.G.; Rudolph, H. Precision of sleeveless 3D drill guides for insertion of one-piece ceramic implants: A prospective clinical trial. *Int. J. Comput. Dent.* **2018**, *21*, 97–105. [[PubMed](#)]
44. Martone, P.T.; Estevez, J.M.; Lu, F.; Ruel, K.; Denny, M.W.; Somerville, C.; Ralph, J. Discovery of Lignin in Seaweed Reveals Convergent Evolution of Cell-Wall Architecture. *Curr. Biol.* **2009**, *19*, 169–175. [[CrossRef](#)] [[PubMed](#)]



© 2020 by the authors. Licensee MDPI, Basel, Switzerland. This article is an open access article distributed under the terms and conditions of the Creative Commons Attribution (CC BY) license (<http://creativecommons.org/licenses/by/4.0/>).

2.4 Manuscript 4 – Impact of planning software and template design on the accuracy of implant installation using surgical guides created by material extrusion

In the previous manuscript, the authors focused on the manufacturing method for surgical guide fabrication. Surgical guides with an open-frame design were manufactured by ME (test) and SLA (control) and compared in terms of the trueness of implant installation. In Manuscript 4, the focus was set on the computer-aided design part of the surgical guide creation process. Two planning software types and two surgical guide designs were applied to create surgical guides by ME. The main outcomes were the trueness and precision of implant positioning. All surgical guides underwent steam sterilization at 121 °C and 2 bar for 60 min before use.

The investigation was presented as an oral communication in the basic research category at the Annual Scientific Meeting of the EAO in 2022 in Geneva, Switzerland. The abstract was published in *Clinical Oral Implants Research* (92). Furthermore, this investigation was also displayed as a poster presentation at the 36th. Annual Scientific Meeting of the DGI in 2022 in Hamburg, Germany.

The following text corresponds to the abstract of the article:

Rothlauf, S., Pieralli, S.*, Wesemann, C., Burkhardt, F., Vach, K., Kernen, F., & Spies, B. C. (2023). Influence of planning software and template design on the accuracy of static computer assisted implant surgery performed using guides fabricated with material extrusion technology: An in vitro study. Journal of dentistry, 132, 104482. Advance online publication. <https://doi.org/10.1016/j.jdent.2023.104482>*

* Authors contributed equally

Influence of planning software and template design on the accuracy of static computer assisted implant surgery performed using guides fabricated with material extrusion technology: An in vitro study.

Objectives

This in vitro study aimed to assess the influence of the planning software and design of the surgical template on both trueness and precision of static computer assisted implant surgery (sCAIS) performed using guides fabricated using material extrusion (ME).

Methods

Three-dimensional radiographic and surface scans of a typodont were aligned using two planning software (coDiagnostiX, CDX; ImplantStudio, IST) to virtually position the two adjacent oral implants. Thereafter, surgical guides were fabricated with either an original (O) or modified (M) design with reduced occlusal support and were sterilized. Forty surgical guides were used to install 80 implants equally distributed amongst four groups: CDX-O, CDX-M, IST-O, and IST-M. Thereafter, the scan bodies were adapted to the implants and digitized. Finally, inspection software was used to assess discrepancies between the planned and final positions at the implant shoulder and main axis level. Multilevel mixed-effects generalised linear models were used for statistical analyses ($p = 0.05$).

Results

In terms of trueness, the largest average vertical deviations (0.29 ± 0.07 mm) were assessed for CDX-M. Overall, vertical errors were dependant on the design ($O < M$; $p \leq 0.001$). Furthermore, in horizontal direction, the largest mean discrepancy was 0.32 ± 0.09 mm (IST-O) and 0.31 ± 0.13 mm (CDX-M). CDX-O was superior compared to

IST-O ($p = 0.003$) regarding horizontal trueness. The average deviations regarding the main implant axis ranged between $1.36 \pm 0.41^\circ$ (CDX-O) and $2.63 \pm 0.87^\circ$ (CDX-M). In terms of precision, mean standard deviation intervals of ≤ 0.12 mm (IST-O and –M) and $\leq 1.09^\circ$ (CDX-M) were calculated.

Conclusion

Implant installation with clinically acceptable deviations is possible with ME surgical guides. Both evaluated variables affected trueness and precision with negligible differences.

Reference to the full-text: Rothlauf, S.*, Pieralli, S.*, Wesemann, C., Burkhardt, F., Vach, K., Kernen, F., & Spies, B. C. (2023). Influence of planning software and template design on the accuracy of static computer assisted implant surgery performed using guides fabricated with material extrusion technology: An in vitro study. *Journal of dentistry*, 132, 104482. Advance online publication. <https://doi.org/10.1016/j.jdent.2023.104482>

2.5 Manuscript 5 – Cytotoxicity of polymers intended for the additive manufacturing of surgical guides by material extrusion

Surgical guides come into direct contact with intraoral hard and soft tissues during implant surgery. Since the experimental biocopolyester filament used in Manuscripts 3 and 4 was not certified for clinical usage, our research group conducted a preliminary study to test, in vitro, its potential cytotoxicity in the oral environment. A further polypropylene-based material meant for ME was included in the analysis, and a medically certified resin for SLA printing served as the control group. The aim of the study was to evaluate, in vitro, the short-term intraoral biocompatibility by assessing the biological risk on human gingival keratinocytes (HGK) according to ISO 10993-5:2009 and ISO 10993-12:2021. Furthermore, markers were used in quantitative real-time PCR (qRT-PCR) for the expression analysis of the following genes: ANXA5, CASP8, and CASP9 for apoptosis and IL1B, IL6, and TNF for inflammation.

This research was presented as a digital poster in the basic research category at the 28th Annual Scientific Meeting of the EAO (Digital Days) in 2021, and the abstract was published in *Clinical Oral Implant Research* (93). Dr. Felix Burkhardt presented the study at the Deutsche Implantologentag / 35th DGI-Kongress in 2021 in Wiesbaden, Germany, and was awarded the prize for “best preclinical investigation.”

The following text corresponds to the abstract of the article:

Burkhardt, F., Spies, B. C., Wesemann, C., Schirmeister, C. G., Licht, E. H., Beuer, F., Steinberg, T., & Pieralli, S. (2022). Cytotoxicity of polymers intended for the extrusion-based additive manufacturing of surgical guides. Scientific reports, 12(1), 7391. <https://doi.org/10.1038/s41598-022-11426-y>

Cytotoxicity of polymers intended for the extrusion-based additive manufacturing of surgical guides

Objective

Extrusion-based printing enables simplified and economic manufacturing of surgical guides for oral implant placement. Therefore, the cytotoxicity of a biocopolyester (BE) and a polypropylene (PP), intended for the fused filament fabrication of surgical guides was evaluated.

Methods

For comparison, a medically certified resin based on methacrylic esters (McE) was printed by stereolithography (n = 18 each group). HGKs were exposed to eluates of the tested materials and an impedance measurement, and a tetrazolium assay (MTT) were performed. Modulations in gene expression were analyzed by quantitative PCR. One-way ANOVA with post-hoc Tukey tests were applied.

Results

None of the materials exceeded the threshold for cytotoxicity (< 70% viability in MTT) according to ISO 10993-5:2009. The impedance-based cell indices for PP and BE, reflecting cell proliferation, showed little deviations from the control, while McE caused a reduction of up to 45% after 72 h. PCR analysis after 72 h revealed only marginal modulations caused by BE while PP induced a down-regulation of genes encoding for

inflammation and apoptosis ($p < 0.05$). In contrast, the 72 h McE eluate caused an up-regulation of these genes ($p < 0.01$).

Conclusion

All evaluated materials can be considered biocompatible *in vitro* for short-term application. However, long-term contact to McE might induce (pro-)apoptotic/(pro-)inflammatory responses in HGK.



OPEN

Cytotoxicity of polymers intended for the extrusion-based additive manufacturing of surgical guides

Felix Burkhardt^{1✉}, Benedikt C. Spies¹, Christian Wesemann^{1,4}, Carl G. Schirmeister^{2,3}, Erik H. Licht³, Florian Beuer⁴, Thorsten Steinberg⁵ & Stefano Pieralli¹

Extrusion-based printing enables simplified and economic manufacturing of surgical guides for oral implant placement. Therefore, the cytotoxicity of a biocopolyester (BE) and a polypropylene (PP), intended for the fused filament fabrication of surgical guides was evaluated. For comparison, a medically certified resin based on methacrylic esters (ME) was printed by stereolithography (n = 18 each group). Human gingival keratinocytes (HGK) were exposed to eluates of the tested materials and an impedance measurement and a tetrazolium assay (MTT) were performed. Modulations in gene expression were analyzed by quantitative PCR. One-way ANOVA with post-hoc Tukey tests were applied. None of the materials exceeded the threshold for cytotoxicity (<70% viability in MTT) according to ISO 10993-5:2009. The impedance-based cell indices for PP and BE, reflecting cell proliferation, showed little deviations from the control, while ME caused a reduction of up to 45% after 72 h. PCR analysis after 72 h revealed only marginal modulations caused by BE while PP induced a down-regulation of genes encoding for inflammation and apoptosis ($p < 0.05$). In contrast, the 72 h ME eluate caused an up-regulation of these genes ($p < 0.01$). All evaluated materials can be considered biocompatible in vitro for short-term application. However, long-term contact to ME might induce (pro-)apoptotic/(pro-)inflammatory responses in HGK.

Prosthetic backward planning in combination with guided implant placement as available in a digital workflow, minimizes the risk of complications and leads to a predictable rehabilitation¹⁻³. Surgical guides are predominantly created by additive manufacturing (AM), as this results in customized and thus convenient aids accompanied by less material wastage and lower production costs compared to the subtractive fabrication e.g., by milling or grinding⁴. AM of surgical guides is primarily conducted by vat photopolymerization (e.g., stereolithography (SLA) or digital light processing (DLP)), based on light curing of liquid resins⁵⁻⁷. Complex and fine-grained objects can be produced by vat photopolymerization, but extensive post-processing procedures such as rinsing, washing and additional light-curing are required to achieve final mechanical properties⁶.

In contrast, material extrusion, also known as fused filament fabrication and under the trademark "fused deposition modeling", is a cost-effective and straightforward three dimensional (3D) printing technology based on the extrusion of a thermoplastic filament through a heated nozzle onto a printing bed⁸. On the one hand, minimal post-processing is required for printed objects by material extrusion, on the other hand, warpage and limited accuracy represent typical limitations of the technique⁹⁻¹¹. Warpage is a result of residual stress accumulation during the cooling phase and depends in particular on the crystallization degree of the polymer, the thermal properties of the filament, and the printing process^{12,13}. However, Pieralli et al. demonstrated in-vitro a similar accuracy for implants inserted with guides by material extrusion and vat photopolymerization¹⁴. An experimental biocopolyester (BE) with improved temperature resistance was used for the manufacturing of the surgical guides as a cost-effective alternative to resins for vat photopolymerization. Low-crystallization biopolymers are already being used in the non-medical field for material extrusion¹⁴. Polylactic acids (PLA) and

¹Department of Prosthetic Dentistry, Faculty of Medicine, Medical Center, Center for Dental Medicine, University of Freiburg, Hugstetter Straße 55, 79106 Freiburg, Germany. ²Freiburg Materials Research Center FMF and Institute for Macromolecular Chemistry, Albert-Ludwigs-University Freiburg, Stefan-Meier-Str. 21, 79104 Freiburg, Germany. ³Basell Sales & Marketing B.V., LyondellBasell Industries, Industriepark Höchst, 65926 Frankfurt, Germany. ⁴Department of Prosthodontics, Geriatric Dentistry and Craniomandibular Disorders, Charité -Universitätsmedizin Berlin, corporate member of Freie Universität Berlin, Humboldt-Universität Zu Berlin and Berlin Institute of Health, Assmanshauser Str. 4-6, 14197 Berlin, Germany. ⁵Division of Oral Biotechnology, Faculty of Medicine, Medical Center, Center for Dental Medicine, University of Freiburg, Hugstetter Straße 55, 79106 Freiburg, Germany. ✉email: felix.burkhardt@uniklinik-freiburg.de

Material	Manufacturer	Matrix
Healthcare PP, <i>Purell</i> type	LyondellBasell Industries B.V., Rotterdam, The Netherlands	Unfilled polypropylene impact copolymer, MFI (230 °C/2.16 kg) = 15 g/10 min
GreenTec PRO	Extrudr, Lauterbach, Austria	Biocopolyester blend
Dental SG Resin	Formlabs, Boston, MA, USA	Bisphenol A dimethacrylate; 7,7,9-trimethyl-4,13-dioxo-3,14-dioxo-5,12-diazahexadecane-1,16-diyl bismethacrylate, phenyl bis(2,4,6-trimethylbenzoyl)-phosphine oxide

Table 1. Brand names, manufacturers, and composition according to the manufacturer.

acrylonitrile butadiene styrene polyamide (ABS)¹⁵ are commonly used for material extrusion, while polyolefins are rarely applied for extrusion-based printing, although they are widely used for plastic production also for medical applications¹³. These high molar mass hydrocarbons are chemically resistant and mechanically durable due to their semi-crystalline properties and are able to undergo steam sterilization as a result of their high Vicat softening temperature^{16–18}. Therefore, polyolefins such as polypropylene (PP) may provide a further cost-effective alternative for the production of accurate sterilizable surgical guides with well-balanced property profiles.

When applied in the form of 3D printed surgical guides, polymers come into direct contact with intraoral hard and soft tissue cells. Monomer release was described from resins intended for the vat photopolymerization of surgical guides¹⁹ and occlusal splints²⁰ while several studies mention possible adverse effects of resin-based materials in the oral environment^{21–23}. Investigations regarding the potential cytotoxicity of substances eluted from extruded materials on human oral cells are sparse. Therefore, a biological risk assessment of BE and PP prior to their intraoral application is mandatory to evaluate potential cytotoxic effects on human tissue-specific cells.

The present study aimed to evaluate the in vitro biocompatibility of the two processed filaments, BE and PP, by using human gingival keratinocytes (HGK) according to the ISO guidelines 10993-5:2009²⁴ and 10993-12:2021²⁵. As a comparison, a commercially available photopolymerizable resin based on methacrylic-esters (ME) and approved for vat photopolymerization of medical devices (class 1) was used. In order to investigate potential cytotoxic effects, interleukin 1 β (*IL1B*), interleukin 6 (*IL6*) and tumor necrosis factor (*TNF*) encoding for inflammation in HGK were investigated. Genes under study included annexin A5 (*ANAX5*), Caspase 8 (*CASP8*), and Caspase 9 (*CASP9*) as representatives of (pro-)inflammation in HGK. The null hypothesis assumed no differences in terms of biocompatibility between BE, PP, and ME.

Material and methods

Investigational materials. An experimental commercially available biocopolyester filament with a diameter of 1.75 mm (BE; GreenTec Pro, Extrudr, Lauterbach, Austria) based on a polylactic acid-based blend with improved temperature resistance and compostability according to EN 13432:2002²⁶ was investigated. In addition, a semi-crystalline polypropylene (PP) filament was extruded from a medical-grade (United States Pharmacopeia (USP) Class VI) injection molding granulate (Healthcare PP, *Purell* type, LyondellBasell Industries B.V., Rotterdam, The Netherlands)²⁷ and examined. The PP filament was fabricated using a twin-screw extruder (Teach-Line™, ZK 25 T, Collin, Ebersberg, Germany) at 180 °C and 45 rpm, with a 3.3 mm die diameter, a water-cooling system, and a winding unit (take-off speed 90 mm s⁻¹). The resulting filament cross-section exhibited dimensions of 2.8 × 2.6 (± 0.05) mm. The dimensions were determined with a micrometer screw at 50 randomly selected points along the filament. For comparison, a commercially available medical Class I photopolymerizable resin (ISO 10993-1:2009 and USP Class VI) based on methacrylic esters (ME; Dental SG Resin, Formlabs, Boston, MA, USA) and intended for the manufacture of surgical guides by SLA was used. Detailed information regarding the composition of the materials are summarized in Table 1.

Preparation of samples and eluates. A standardized test specimen (15 × 15 × 3 mm) was designed using a Computer-Aided Design (CAD) software (Meshmixer 3.5, Autodesk, Inc., San Rafael, CA, USA) and imported as a standard tessellation language (STL) file into the corresponding nesting software. Thereafter, 18 samples were printed for each of the three groups (PP, BE, and ME) according to ISO 10993-12:2021²⁵ which specifies the requirements for sample preparation. Extrusion of both experimental filaments (PP, BE) was performed at a printing speed of 50 mm s⁻¹, layer height of 0.2 mm with 100% infill. AM of PP was conducted at a nozzle temperature of 210 °C and a build plate temperature of 60 °C (Ultimaker S5, Ultimaker B.V., The Netherlands). Specimens of group BE were printed at a nozzle temperature of 220 °C and a build plate temperature of 60 °C (Prusa i3, MK3, Prague, Czech Republic). Two different extrusion-based printers were used for the manufacturing of the samples since they were produced at two different locations. Samples of group ME were produced with a layer thickness of 0.05 mm using an SLA printer (Form 2, Formlabs, Boston, MA, USA) and subsequently post-processed with rinsing in 99% isopropanol for 5 min, air drying and light-curing for 30 min at 60 °C ($\lambda = 405$ nm). Finally, support structures were removed. Samples were cleaned in 75% ethanol for 5 min and rinsed with water before being processed in a washer-disinfector (PG 8536, Miele, Gütersloh, Germany) containing a liquid detergent (neodisher MediClean forte, Dr. Weigert AG, Zug, Switzerland). All specimens were steam sterilized in an autoclave (Webeco, Series EC, Selmsdorf, Germany) at 134 °C for 5 min. For the preparation of the eluates, each sample was immersed in 5 mL keratinocyte growth medium (KG-M1, PromoCell, Heidelberg, Germany) in six well plates (Greiner Bio-One, Frickenhausen, Germany). One-half of the samples was stored at 37 °C, 97% humidity, and 5% CO₂ for 24 h and the other half for 72 h. All eluates were kept at 4 °C and absence of light before application to cell cultures.

Gene	RefSeq (mRNA)	Protein	Function
<i>ANXA5</i>	NM_0011154	Annexin A5	Apoptosis
<i>CASP8</i>	NM_001080124	Caspase 8	Apoptosis
<i>CASP9</i>	NM_001229	Caspase 9	Apoptosis
<i>IL1B</i>	NM_000576	Interleukin 1 β	Inflammation
<i>IL6</i>	NM_000600	Interleukin 6	Inflammation
<i>TNF</i>	NM_000594	Tumor necrosis factor	Inflammation

Table 2. Markers used in qRT-PCR for gene expression analysis.

Cell cultures and cultivation media. Human gingival keratinocytes (HGK) derived from the oral gingiva were used in this study. The Ethics Committee of the University Medical Center Freiburg, Freiburg, Germany approved the collection of tissue samples for the following cell culture experiments (vote no. 411/08) and donors signed an informed consent. All experiments were carried out in accordance with relevant guidelines and regulations. HGK were immortalized with the human papillomavirus type 16 E6/E7 oncogenes²⁸ to obtain a stable cell line with high reproducibility, and cultivated in a low-calcium KG-M1 medium (PromoCell) with kanamycin. Standard cell culture conditions (37 °C; 97% humidity; 5% CO₂) with standard culture flasks up to size T175 (Greiner Bio-One, Frickenhausen, Germany) were used for cultivation. When reaching approximately 80% of confluency, cells were split using trypsin and manual cell scrapers. DMEM3, containing fetal calf serum (FBS, Biochrom AG, Berlin, Germany), was added to stop the enzymatic reaction of trypsin. The cell numbers were determined by an automated Cell Counter (LUNA, Logos Biosystems, Anyang, South Korea). For the conduction of the experiments, HGK were cultured in passages between 36 and 41.

Impedance measurement. According to the manufacturer's instructions, the impedance was measured with a real-time cell analyzing system (RTCA) (iCelligence, ACEA Biosciences, Inc., San Diego, CA, USA). Before adding the cells, 100 μ l of cell medium containing the eluates (and without for the control) were applied to each of the eight wells of the E-plate E8 of the RTCA system, and a background impedance measurement without HGK was taken. Subsequently, 400 μ l medium were applied to each of the wells containing HGK to achieve a density of 1.1×10^4 cells/cm². Plates were incubated with standard cell culture conditions (37 °C; 97% humidity; 5% CO₂) for 5 d. RTCA iCelligence software (ACEA Biosciences) was used for data acquisition and analysis. Tests were conducted with three biological and two technical replicates for each of the evaluated polymers. The cell index (CI) describes the result of the impedance induced by adherent cells to the electron flow and was normalized at the time point of substance addition.

Colorimetric tetrazolium assay (MTT). A quantitative colorimetric assay with tetrazolium salt (3-(4,5-dimethylthiazol-2-yl)-2,5-diphenyltetrazoliumbromid; MTT) (Abcam, Cambridge, UK) was performed in accordance to the ISO guideline 10993-5:2009²⁴ to detect the viability of HGK after incubation with the eluates. This assay is based on the reduction of yellow water-soluble MTT in living cells to blue-violet insoluble formazan. To conduct the MTT assay, 200 μ l medium containing HGK were applied to each well of a 96 well plate (Greiner Bio-One, Frickenhausen, Germany) to obtain a density of 1.4×10^4 cells/cm². Subsequently, the plates were incubated at 37 °C for 24 h to allow cell adherence. Cell culture medium was then replaced with the one containing the eluates and cells were re-incubated at previously described conditions. After removing the eluate medium, 100 μ l MTT solution was added to the cell cultures and incubated for 3 h. Finally, to measure the formazan concentration, a scanning spectrophotometer (Infinite 200 PRO, Tecan, Männedorf, Switzerland) with a wavelength of 590 nm and the compatible data acquisition software were used.

RNA isolation and quantitative real-time PCR (qRT-PCR). For gene expression analysis, HGK were seeded with a density of 3.5×10^4 cells/cm² in 24-well plates (Greiner Bio-One, Frickenhausen, Germany). After adding the 24 h and 72 h eluates, cells were incubated for 72 h at formerly described cell culture conditions, and subsequently lysed with RLT Buffer (Qiagen, Venlo, The Netherlands) and dithiothreitol (Biorad, Berkeley, CA, USA). RNA isolation and purification was performed using the RNeasy mini Kit (Qiagen), while for the analysis of RNA integrity and concentration the Experion RNA Analysis Kit (Biorad) was used. First-strand cDNA was synthesized using the RevertAid First Strand cDNA Synthesis Kit (Thermo Fisher Scientific, Waltham, MA, USA). The quantification of the synthesized cDNA was conducted with the Quant-iT PicoGreen dsDNA Reagent Kit (Life Technologies, Carlsbad, California, USA) and the 200 PRO Microplate Reader (Tecan, Crailsheim, Germany). For each polymerase chain reaction, 5 ng cDNA/ μ l were used for normalization. The qRT-PCR analysis was performed with the RT2 SYBR Green qPCR Mastermix (SABiosciences, Qiagen) on the CFX96 Real-Time PCR Detection System (Biorad) according to the manufacturer's instructions. Commercially available and pre-validated primers (SABiosciences, Qiagen) were used for the expression analysis of HGK relevant genes (Tables 2 and 3). In addition, the unmodulated housekeeping genes glyceraldehyde-3-phosphate dehydrogenase (*GAPDH*), ribosomal protein L13a (*RPL13A*) and ubiquitin C (*UBC*) (all SABiosciences, Qiagen) were used for normalization. The qRT-PCR analysis was performed according to the following temperature profile protocol: 10 min at 95 °C (initial denaturation) followed by 40 cycles of denaturation for 15 s at 95 °C, 30 s at 55 °C (annealing) and 30 s at 72 °C (extension). Relative gene expression levels were calculated using the $2^{-\Delta\Delta CT}$

Gene	Primer sequences (forward sequence)
ANXA5	GTGGCTCTGATGAAACCTCTC
CASP8	AGAAGAGGGTCATCTGGGAGA
CASP9	GTTTGAGGACCTTCGACCAGCT
IL1B	CCACAGACCTCCAGGAGAATG
IL6	AGACAGCCACTCACCTTTCAG
TNF	CTCTTCTGCCTGCTGCACTTG

Table 3. Primer sequences of the investigated genes.

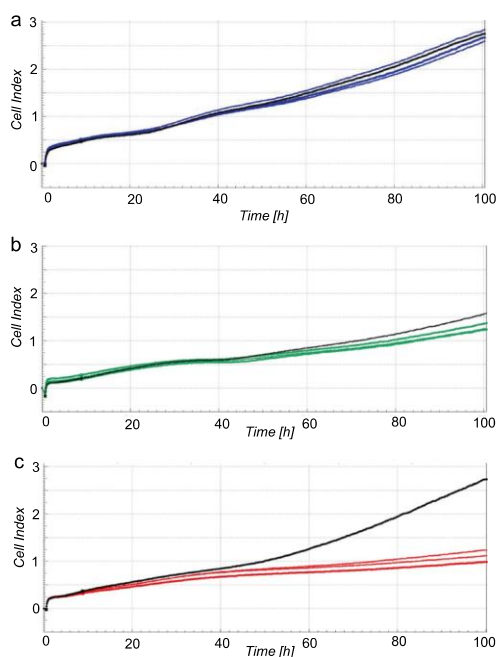


Figure 1. Impedance-based cell index after exposure of HGK to 72 h eluates of PP (a), BE (b), ME (c). The respective non-treated control is visualized in black. Each of the cell indices represents the average of a technical duplicate.

method according to Livak and Schmittgen²⁹ for each biomarker. Data were relative to the housekeeping genes and normalized to the negative control.

Statistical analysis. For statistical analysis, data were tested for homogeneity of variances (Levene test) and analysis of variance (ANOVA) with post-hoc Tukey HSD tests for comparison between the polymers and the negative control. In addition, statistical differences between the evaluated time points were assessed using the Student's t-test and calculations were performed with the software SPSS Statistics (v.22.0, IBM Corp., Armonk, New York, USA). The level of significance was set at $\alpha = 0.05$.

Results

Impedance measurement. A real-time impedance measurement was performed to monitor live cell proliferation, adhesion, and viability of HGK after exposure to the eluates as determined by the CI (Fig. 1). After an incubation period of 24 h, a reduced CI was observed for the 72 h eluates of ME (12% reduction) compared to the untreated control ($p < 0.05$) (Fig. 2a). None of the evaluated 24 h eluates showed a significant regulation of the CI compared to the control after an incubation period of 24 h ($p > 0.05$). After an incubation period of 72 h, both ME eluates (24 h and 72 h eluate) showed a significant inferior CI compared to the control (32% reduction

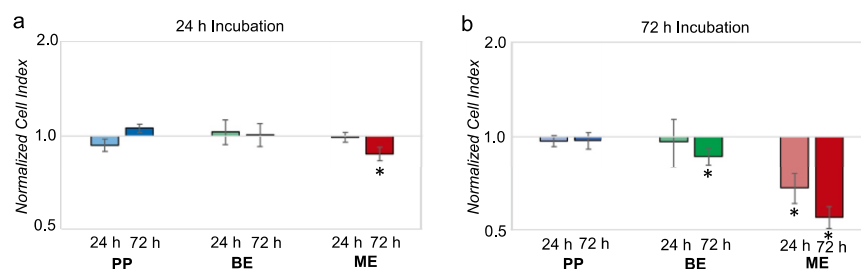


Figure 2. Impedance-based cell index normalized to the non-treated control group after exposure of HGK to eluates of the evaluated polymers (PP, BE, ME) for 24 h (a) and 72 h (b). The first column of each group represents the cell index after incubation with the 24 h eluate and the second column with the 72 h eluate.

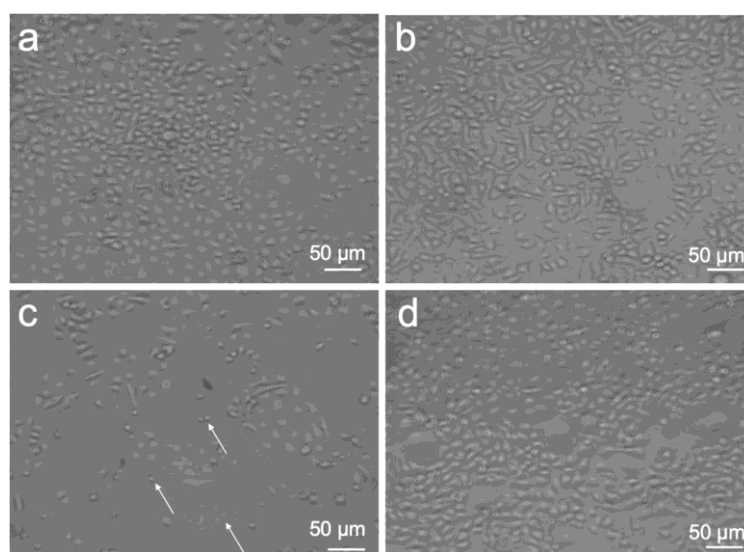


Figure 3. Light microscopic analysis of HGK after incubation with 72 h eluates of PP (a), BE (b), and ME (c) for 72 h in comparison to the non-treated control (d). HGK undergoing apoptosis are shown exemplarily using arrows.

for the 24 h eluate; 45% reduction for the 72 h eluate) ($p < 0.05$) (Figs. 1c, 2b). No significant differences were observed for both PP eluates and the 24 h BE eluate in comparison to the control ($p > 0.05$). However, a reduction of CI of 14% occurred for the 72 h BE eluate compared to the control ($p < 0.05$). The results of the significantly reduced CI after an incubation of 72 h with ME were consistent with the observation under the light microscope (Fig. 3): The cell number was distinctly reduced and the cell morphology was partially apoptotic after incubation with ME (both eluates) for 72 h. In contrast, HGK revealed a confluent cell lawn after incubation with PP and BE for 72 h which had a similar appearance as after incubation with the non-treated control (Fig. 3a,b,d). These observations were consistent with the results of the impedance measurement for PP, L, and the control.

MTT assay. The MTT assay showed a viability of 78% after incubation of HGK with the 24 h PP eluate (Fig. 4). The viability was reduced to 84% after incubation with the 72 h BE eluate. Both ME eluates as well as the 72 h PP and the 24 h BE eluate showed no reduced viability in the MTT assay. In accordance with ISO guideline²⁴, a test specimen exhibits a cytotoxic potential when the viability is reduced to $< 70\%$, which occurred for none of the evaluated polymers or time points.

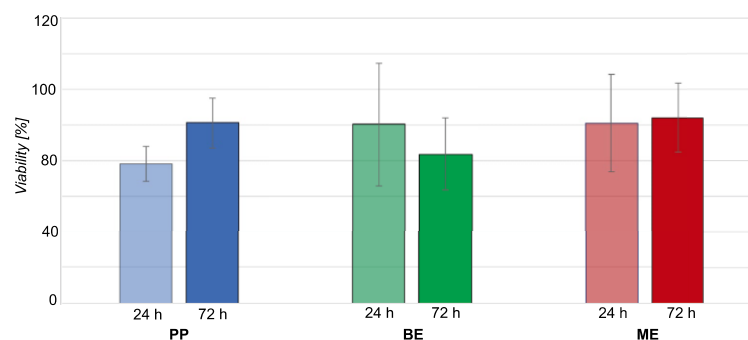


Figure 4. Viability of HGK after exposure to eluates of the tested polymers (PP, BE, ME) in the MTT assay. The first column of each group represents the cell index after incubation with the 24 h eluate and the second column with the 72 h eluate.

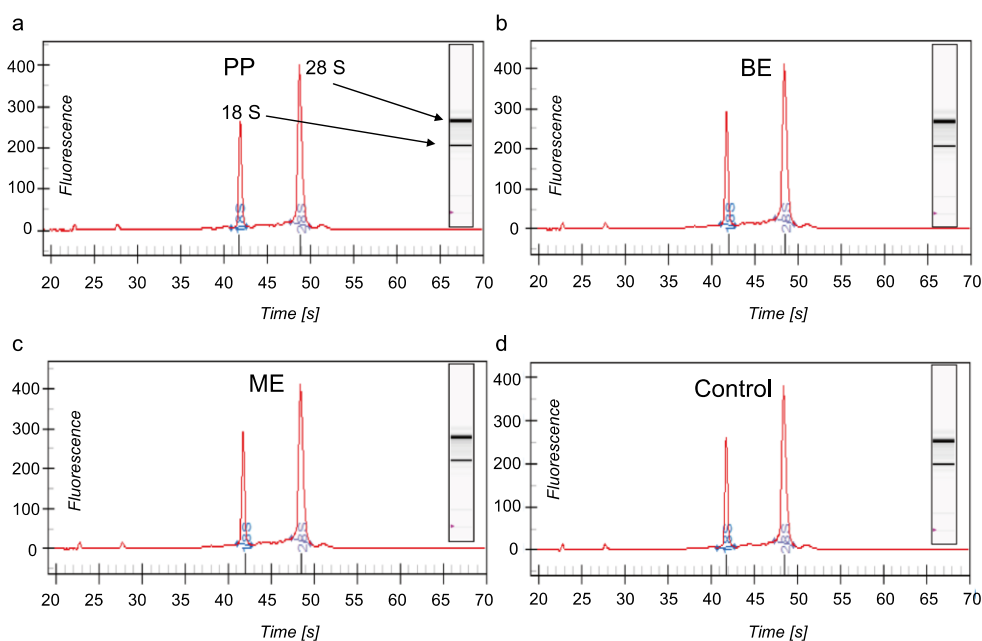


Figure 5. Exemplary electropherograms and virtual gels derived for HGK exposed to PP (a), BE (b), and ME (c) 24 h eluates, as well as unexposed HGK (control, d). In the electropherogram, the two peaks depict the 18S and 28S rRNA (arrows in a). The virtual gel (inserts in a–d) is reconstructed based on the peaks and the total RNA concentration.

Gene expression analysis. A qRT-PCR analysis was performed to investigate possible modulations of relevant genes related to apoptosis and inflammation. Electropherograms and virtual gels (Fig. 5) obtained from the total RNA extraction of HGK, both the unexposed control and after incubation with eluates, showed two distinct peaks for the control 18S and 28S rRNAs. The integrity and amount of total RNA was measured in all groups and considered as appropriate for the qRT-PCR analysis. Figure 6 shows the results of the qRT-PCR

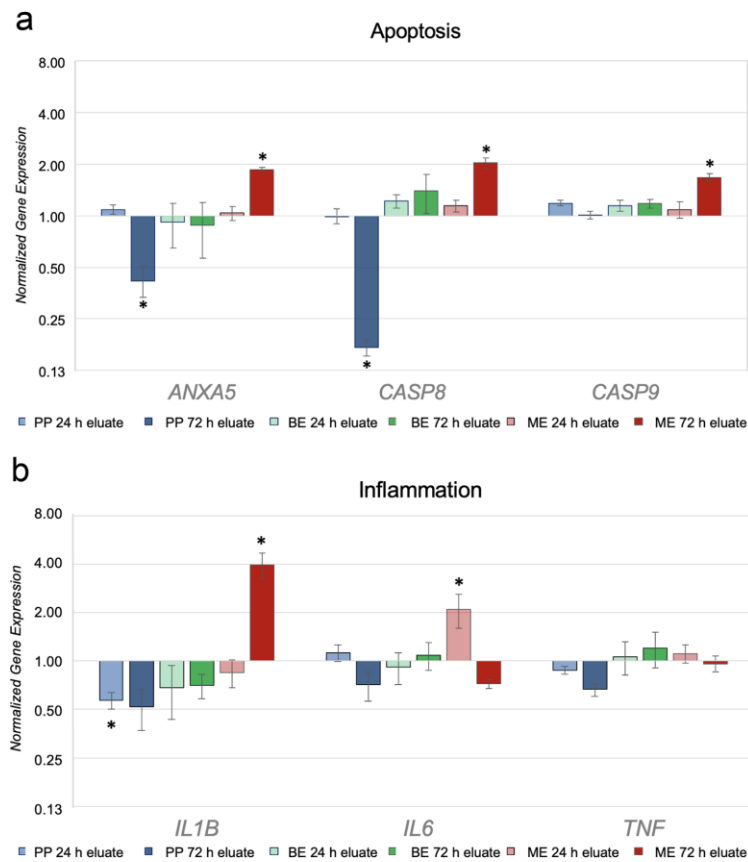


Figure 6. Normalized up-/down-modulation of selected genes of apoptosis (a) and inflammation (b) in HGK exposed to 24 h and 72 h eluates from PP, BE and ME for 72 h referring to the untreated control. Data are normalized to the untreated control cells and the unregulated housekeeping genes *GAPDH*, *RPL13A* and *UBC*. The normalized expression was calculated using the $2^{-\Delta\Delta CT}$ method²⁹. Asterisks (*) indicate significance ($p < 0.05$) compared to the untreated cells.

analysis for distinct biomarkers related to (pro-)apoptotic and (pro-)inflammatory processes after an incubation period of 72 h.

The biomarkers expression of (pro-)apoptosis *ANXA5*, *CASP8*, and *CASP9* resulted in a significant upregulation after incubation with the ME 72 h eluate compared to the control ($p < 0.05$). In contrast, no significant regulation was observed after incubation with the 24 h eluate ($p > 0.05$). The 24 h eluates of the extrusion-based printed specimens PP and BE showed no up-regulation of the respective biomarkers ($p > 0.05$). After incubation with the 72 h PP eluate, a down-modulation of the biomarkers *ANXA5* and *CASP8* were observed ($p < 0.05$). Comparing the eluate time points for each group, significant differences were found for PP and ME for the biomarkers *ANXA5*, *CASP8*, and *CASP9* ($p < 0.05$). No significant modulations were observed for group BE between the two evaluated eluate time points for all investigated biomarkers ($p > 0.05$).

HGK showed an increase of the inflammatory-related biomarker *IL1B* after incubation with the 72 h ME eluate ($p = 0.01$) compared to the non-treated control. In contrast, the 24 h PP eluate caused a significant down-regulation for *IL1B* ($p < 0.05$). The other tested eluates exhibited a tendency toward down-regulation regarding this inflammation marker. After incubation with the 24 h ME eluate, HGK showed an increased expression of the biomarker interleukin 6 (*IL6*) ($p < 0.01$) in comparison to the untreated control, whereas the 72 h eluate of this polymer caused a tendency toward down-regulation. No significant modulations ($p > 0.05$) compared to the control were observed for *IL6* after incubation with the remaining groups. In addition, the biomarker *TNF*

showed no significantly modulated gene expression compared to the control group for the evaluated materials and eluate time points ($p > 0.05$). When comparing 24 h with 72 h eluate time points of group PP, significant differences were observed for the genes *IL6* and *TNF* ($p < 0.05$). Group ME showed significant differences between the two eluate time points for *IL1B* and *IL6* ($p < 0.05$), whereas BE revealed no significant modulations in gene expression of the inflammatory biomarkers between the two eluate times ($p > 0.05$).

Discussion

Numerous materials for resin-based AM of surgical guides are available on the market but the demand for inexpensive and sustainable materials as well as for simple fabrication workflows is increasing³⁰. The objective of the present study was to evaluate the in vitro biocompatibility of two experimental polymers intended for the AM of surgical guides by material extrusion in comparison to a certified light-curable resin used for vat photopolymerization of medical class I surgical guides (ISO 10993-5:2009 and USP Class VI). A commonly used biopolymer for material extrusion in the non-medical field is based on PLA³¹. However, pure PLA is prone to deformation when steam sterilized at temperatures above 121 °C. Therefore, an experimental biocopolyester blend based on PLA, other biopolymers, and calcium carbonate fillers was utilized for optimized temperature resistance. In addition, a semi-crystalline PP was included in the present biocompatibility evaluation. PP belongs to the group of polyolefins which are high-molecular hydrocarbon materials derived from fossil or renewable energy sources³². Due to its semi-crystalline nature, PP appears chemically resistant and withstands steam sterilization. A PP injection molding granulate with certified biocompatibility according to USP class VI was used for the extrusion of the PP filament²⁷. However, material properties might suffer from alteration during the extrusion or printing process leading to potential cytotoxic effects. The null hypothesis of this study assumed no differences in terms of biocompatibility on HGK between the evaluated materials.

HGK were selected based on their anatomical location on the surface of the oral mucosa. Due to the in-vitro short lifetime of primary HGK with resulting limited reproducibility of the experiments, immortalized HGK were chosen. Nevertheless, the differentiation pattern of this cell line is well-preserved, making HGK comparable to the original tissue and particularly suitable for experiments on modulations of gene expression²⁸. The eluates were prepared according to ISO guideline 10993-12:2021, which describes sample preparation and reference materials. Furthermore, the incubation time of 24 h for the MTT assay is defined in ISO standard 10993-5:2009 while the incubation period of 72 h for the qRT-PCR was based on the results of the impedance measurement. The extended incubation period was also used to evaluate materials for long-term intraoral application, such as splints or aligners³³.

RTCA iCelligence™ and MTT assay were used to measure the proliferation and viability of HGK after incubation with the eluates. None of the eluates showed a reduced viability (threshold set at <70%) in the MTT assay according to ISO 10993-5:2009, which was in accordance with the RTCA measurement and cells' morphology after incubation with eluates of both filaments, indicating no cytotoxic effects for PP and L. Solely the 72 h BE eluate showed a slightly reduced CI after several days of incubation. A significantly reduced CI was observed for both ME eluates (24 and 72 h), with HGK also showing a significantly reduced cell density and increased apoptotic appearance under the light microscope. These results did not occur in the MTT assay which might suggest a higher specificity and sensitivity of the RTCA system³⁴. A further advantage of the RTCA system is the comprehensive documentation of cellular proliferation, growth, and morphological changes (not only in terms of viability) over the entire period of the investigation, rather than being limited to individual endpoints. In addition, no formazan products are generated as in the MTT assay (which might interact with the compounds of the eluates and affect the final results)^{35,36}.

To investigate the influence of the eluates on gene expression level of HGK, a qRT-PCR analysis was performed. Potential cytotoxic effects, which might have led to a reduced CI and morphological changes of HGK after incubation with ME for an extended period, were investigated based on relevant biomarkers for (pro-)apoptosis and (pro-)inflammation after 72 h of incubation. The evaluated caspases *CASP8* and *CASP9* are initiator caspases which can induce apoptosis^{37,38}. *ANXA5* binds efficiently to phosphatidylserine and is transported to the outer surface of the plasma membrane in the early apoptosis stage³⁹. Furthermore, *IL1B* is secreted from keratinocytes and fibroblasts and represents a marker for the early inflammatory response^{40,41}. The presence of *IL6* in the inflamed tissue also plays a decisive role in the onset and maintenance of periodontal inflammatory conditions such as periodontitis and gingivitis⁴². The additionally investigated marker *TNF* is a pro-inflammatory cytokine associated to tissue degeneration and able to stimulate osteoclastic activity⁴³. In the present study, an up-regulation of the early apoptosis biomarkers *ANXA5*, *CASP8* and *CASP9* was observed after incubation with the 72 h ME eluate. Since these modulations did not occur for the 24 h eluate, it can be assumed that the release of cytotoxic compounds occurs after a longer period. Polydorou et al.⁴⁴ showed that light-cured composite materials release monomers over a time period of up to 1 year, which might have adverse effects on oral tissues. Released monomers, such as bisphenol A-glycidyl methacrylate (BisGMA) of a methacrylate-based nanohybrid composite resin contained in a related form in the investigated SLA-resin, induced severe apoptosis in HGK after 4 d⁴⁵. Moreover, in human gingival fibroblasts (HGF) apoptosis induced by oxidative stresses was observed after the release of monomers^{22,46}. The tendency toward cytotoxic effects on gene expression level after incubation with the 72 h ME eluates was corroborated with an up-regulation of *IL1B* and *IL6*, with the latter biomarker being regulated by the 24 h eluate. Therefore, the present results suggest that monomers can be released from ME test specimens after an extended period despite elaborated washing and light-curing steps and may induce (pro-)apoptotic/(pro-)inflammatory modulations in HGK. The null hypothesis assuming no differences in cytotoxicity between the evaluated materials was therefore rejected. Resins for vat photopolymerization still contain numerous compounds and photoinitiators in the processed parts that are cytotoxic⁴⁷ and may induce (pro-)apoptotic/(pro-)inflammatory modulations in HGK. This outcome seems in agreement with a similar

study, which assessed low cytotoxic effects of the evaluated SLA-resin in mesenchymal stem cells and showed significantly decreased viability in the MTT assay after an extended incubation period, although the printed resin is classified as biocompatible⁵¹. Zhu et al. questioned the safety of several resins for vat photopolymerization in terms of release of toxic substances in water-based cell culture media⁴⁸. As in our study, cytotoxic effects in form of mortality of aquatic bioindicators were not observed after 24 h but increased dramatically over a prolonged period of up to 72 h⁴⁸. The inconsistencies between official certifications and the observed results might derive from the different incubation periods.

PLA and ABS for extrusion-based AM seem not to induce behavioral abnormalities in zebrafish compared to the evaluated photopolymerizable resins⁴⁸, which is in agreement with our results on gene expression level. None of the extrusion-based materials (PP and BE) showed an up-regulation of the evaluated (pro-)apoptotic/(pro-)inflammatory biomarkers. The significant down-regulation of *ANXA5* and *CASP8* caused by the PP 72 h eluate might even indicate an anti-apoptotic side effect on HGK. These results were enhanced by the activity of the investigated inflammatory markers *IL1B*, *IL6*, and *TNF* which tended toward down-regulation after incubation with PP. These properties are known for polyolefins, which are rarely processed by material extrusion, but are widely used for various medical applications like e.g., tubes, syringes and piezoelectric materials for their high purity and low allergy potential^{32,49}. The fact that BE did not show limitations on gene expression level with regard to its biocompatibility is consistent with the literature^{50,51}. No adverse side effects in terms of biocompatibility for HGK were observed after extrusion-based AM and steam sterilization. This can be attributed to a different chemical structure and the absence of photoinitiators or monomers in filaments intended for material extrusion, differently than for photo-curable 3D printing materials¹⁹. Nevertheless, further studies evaluating other cell cultures as e.g. osteoblasts, are needed. An assessment of cells in the tissue compound, such as by means of interactive cell systems of HGK and HGF, would be necessary to mimic similar in-vivo conditions⁵⁸.

Conclusions

According to the results of this study, all evaluated materials can be considered as biocompatible in vitro for short-term intraoral usage as for guided implant positioning. Furthermore, both experimental filaments showed reduced (pro-)apoptotic/(pro-)inflammatory modulations compared to the investigated SLA-resin. Material extrusion of surgical guides made of PP and BE thus might represent a cost-effective alternative to currently used materials and manufacturing processes.

Data availability

All data generated or analysed during this study are included in this published article.

Received: 25 February 2022; Accepted: 19 April 2022

Published online: 05 May 2022

References

- Dhaese, J., Ackhurst, J., Wismeijer, D., De Bruyn, H. & Tahmaseb, A. Current state of the art of computer-guided implant surgery. *Periodontol* **73**, 121–133 (2017).
- Chen, L., Lin, W.-S., Polido, W. D., Eckert, G. J. & Morton, D. Accuracy, reproducibility, and dimensional stability of additively manufactured surgical templates. *J. Prosthet. Dent.* **122**, 309–314 (2019).
- Burkhardt, F., Strietzel, F. P., Bitter, K. & Spies, B. C. Guided implant surgery for one-piece ceramic implants: a digital workflow. *Int. J. Comput. Dent.* **23**, 73–82 (2020).
- Henprasert, P. et al. Comparison of the accuracy of implant position using surgical guides fabricated by additive and subtractive techniques. *J. Prosthodont.* **29**, 534–541 (2020).
- Herschdorfer, L., Negreiros, W. M., Gallucci, G. O. & Hamilton, A. Comparison of the accuracy of implants placed with CAD-CAM surgical templates manufactured with various 3D printers: An in vitro study. *J. Prosthet. Dent.* **125**, 905–910 (2021).
- Quan, H. et al. Photo-curing 3D printing technique and its challenges. *Bioact. Mater.* **5**, 110–115 (2020).
- Sommacal, B., Savic, M., Filippi, A., Köhl, S. & Thieringer, F. Evaluation of two 3D printers for guided implant surgery. *Int. J. Oral Maxillofac. Implants* **33**, 743–746 (2018).
- Ligon, S. C., Liska, R., Stampfl, J., Gurr, M. & Mülhaupt, R. Polymers for 3D Printing and customized additive manufacturing. *Chem. Rev.* **117**, 10212–10290 (2017).
- Wang, T.-M., Xi, J.-T. & Jin, Y. A model research for prototype warp deformation in the FDM process. *Int. J. Adv. Manuf. Technol.* **33**, 1087–1096 (2007).
- Geng, P. et al. Effect of thermal processing and heat treatment condition on 3D printing PPS properties. *Polymers* **10**, 875 (2018).
- Schirmeister, C. G., Hees, T., Licht, E. H. & Mülhaupt, R. 3D printing of high density polyethylene by fused filament fabrication. *Addit. Manuf.* **28**, 152–159 (2019).
- Fischer, J. M. *Handbook of Molded Part Shrinkage and Warpage* (Elsevier/William Andrew, 2013).
- Stürzel, M., Mihan, S. & Mülhaupt, R. From multisite polymerization catalysis to sustainable materials and all-polyolefin composites. *Chem. Rev.* **116**, 1398–1433 (2016).
- Pieralli, S. et al. How accurate is oral implant installation using surgical guides printed from a degradable and steam-sterilized biopolymer?. *J. Clin. Med.* **9**, 2322 (2020).
- Yang, H., Ji, F., Li, Z. & Tao, S. Preparation of hydrophobic surface on PLA and ABS by fused deposition modeling. *Polymers* **12**, 1539 (2020).
- Malpass, D. B. *Introduction to Industrial Polyethylene: Properties, Catalysts, Processes* (Wiley, 2010).
- Ehrenstein, G. W. *Polymer-Werkstoffe: Struktur-Eigenschaften-Anwendung* (Hanser, 2011).
- Spoerk, M., Holzer, C. & Gonzalez-Gutierrez, J. Material extrusion-based additive manufacturing of polypropylene: A review on how to improve dimensional inaccuracy and warpage. *J. Appl. Polym. Sci.* **137**, 48545 (2020).
- Kessler, A., Reichl, F.-X., Folwaczny, M. & Högg, C. Monomer release from surgical guide resins manufactured with different 3D printing devices. *Dent. Mater.* **36**, 1486–1492 (2020).
- Wedekind, L. et al. Elution behavior of a 3D-printed, milled and conventional resin-based occlusal splint material. *Dent. Mater.* **37**, 701–710 (2021).
- Kreß, S. et al. 3D Printing of cell culture devices: Assessment and prevention of the cytotoxicity of photopolymers for stereolithography. *Materials* **13**, 3011 (2020).

22. Lottner, S., Shehata, M., Hickel, R., Reichl, F.-X. & Durner, J. Effects of antioxidants on DNA-double strand breaks in human gingival fibroblasts exposed to methacrylate based monomers. *Dent. Mater.* **29**, 991–998 (2013).
23. Schweikl, H., Spagnuolo, G. & Schmalz, G. Genetic and cellular toxicology of dental resin monomers. *J. Dent. Res.* **85**, 870–877 (2006).
24. ISO 10993-5:2009. *Biological evaluation of medical devices: Part 5: Tests for in vitro cytotoxicity*. (2009).
25. ISO 10993-12:2021. *Biological evaluation of medical devices: Part 12: Sample preparation and reference materials*. (2021).
26. EN 13432. *Packaging: Requirements for packaging recoverable through composting and biodegradation—Test scheme and evaluation criteria for the final acceptance of packaging*. (2002).
27. Burkhardt, F. *et al.* Pandemic-driven development of a medical-grade, economic and decentralized applicable polyolefin filament for additive fused filament fabrication. *Molecules* **25**, 5929 (2020).
28. Roesch-Ely, M. *et al.* Organotypic co-cultures allow for immortalized human gingival keratinocytes to reconstitute a gingival epithelial phenotype in vitro. *Differentiation* **74**, 622–637 (2006).
29. Livak, K. J. & Schmittgen, T. D. Analysis of relative gene expression data using real-time quantitative PCR and the 2(-Delta Delta C(T)) method. *Methods* **25**, 402–408 (2001).
30. Lüchtenborg, J. *et al.* Implementation of fused filament fabrication in dentistry. *Appl. Sci.* **11**, 6444 (2021).
31. Mazzanti, V., Malagutti, L. & Mollica, F. FDM 3D printing of polymers containing natural fillers: A review of their mechanical properties. *Polymers* **11**, 1094 (2019).
32. Mühlaupt, R. Green polymer chemistry and bio-based plastics: Dreams and reality. *Macromol. Chem. and Phys.* **214**, 159–174 (2013).
33. Kurzmann, C. *et al.* Evaluation of resins for stereolithographic 3D-printed surgical guides: The response of L929 cells and human gingival fibroblasts. *Biomed. Res. Int.* **2017**, 1–11 (2017).
34. Türker-Şener, L., Albeniz, G., Diñç, B. & Albeniz, I. iCELLigence real-time cell analysis system for examining the cytotoxicity of drugs to cancer cell lines. *Ex. Ther. Med.* **14**, 1866–1870 (2017).
35. Garcia, S. N., Gutierrez, L. & McNulty, A. Real-time cellular analysis as a novel approach for in vitro cytotoxicity testing of medical device extracts. *J. Biomed. Mater. Res.* **101A**, 2097–2106 (2013).
36. Stefanowicz-Hajduk, J. & Ochocka, J. R. Real-time cell analysis system in cytotoxicity applications: Usefulness and comparison with tetrazolium salt assays. *Toxicol. Rep.* **7**, 335–344 (2020).
37. Kuida, K. Caspase-9. *Int. J. Biochem. Cell Biol.* **32**, 121–124 (2000).
38. Tummers, B. & Green, D. R. Caspase-8: Regulating life and death. *Immunol. Rev.* **277**, 76–89 (2017).
39. Kang, T. H. *et al.* Annexin A5 as an immune checkpoint inhibitor and tumor-homing molecule for cancer treatment. *Nat. Commun.* **11**, 1137 (2020).
40. Dinarello, C. A. Biologic basis for interleukin-1 in disease. *Blood* **87**, 2095–2147 (1996).
41. Ren, K. & Torres, R. Role of interleukin-1 β during pain and inflammation. *Brain. Res. Rev.* **60**, 57–64 (2009).
42. Bartold, P. M. & Haynes, D. R. Interleukin-6 production by human gingival fibroblasts. *J. Periodont. Res.* **26**, 339–345 (1991).
43. Tervahartiala, T. *et al.* Tumor necrosis factor- α and its receptors, p55 and p75, in gingiva of adult periodontitis. *J. Dent. Res.* **80**, 1535–1539 (2001).
44. Polydorou, O., König, A., Hellwig, E. & Kümmerer, K. Long-term release of monomers from modern dental-composite materials. *Eur. J. Oral Sci.* **117**, 68–75 (2009).
45. Schulz, S. D. *et al.* Human gingival keratinocyte response to substances eluted from Silorane composite material reveal impact on cell behavior reflected by RNA levels and induction of apoptosis. *Dent. Mater.* **28**, e135–e142 (2012).
46. Szczepanska, J. *et al.* 2-Hydroxyethyl methacrylate (HEMA), a tooth restoration component, exerts its genotoxic effects in human gingival fibroblasts through methacrylic acid, an immediate product of its degradation. *Mol. Biol. Rep.* **39**, 1561–1574 (2012).
47. Carve, M. & Wlodkovic, D. 3D-Printed chips: Compatibility of additive manufacturing photopolymeric substrata with iological applications. *Micromachines* **9**, 91 (2018).
48. Zhu, F., Friedrich, T., Nugegoda, D., Kaslin, J. & Wlodkovic, D. Assessment of the biocompatibility of three-dimensional-printed polymers using multispecies toxicity tests. *Biomicofluidics* **9**, 061103 (2015).
49. Klimiec, E., Kaczmarek, H., Królikowski, B. & Kolaszczyński, G. Cellular polyolefin composites as piezoelectric materials: Properties and applications. *Polymers* **12**, 2698 (2020).
50. Imilthan, S. *et al.* Systematic in vitro biocompatibility studies of multimodal cellulose nanocrystal and lignin nanoparticles. *J. Biomed. Mater. Res.* **108**, 770–783 (2020).
51. Geddes, L., Themistou, E., Burrows, J. F., Buchanan, F. J. & Carson, L. Evaluation of the in vitro cytotoxicity and modulation of the inflammatory response by the bioresorbable polymers poly(D, L-lactide-co-glycolide) and poly(L-lactide-co-glycolide). *Acta Biomater.* **134**, 261–275 (2021).

Acknowledgements

The authors thank MDT Robert Nicic (Department of Prosthodontics, Geriatric Dentistry and Craniomandibular Disorders, Charité—Universitätsmedizin Berlin) for his contribution in preparing the samples and MTA Yrgalem Abreah (Center for Dental Medicine, Division of Oral Biotechnology, Faculty of Medicine—University of Freiburg) for her assistance in conducting the cell culture experiments. The article processing charge was funded by the Baden-Wuerttemberg Ministry of Science, Research and Art and the University of Freiburg in the funding program Open Access Publishing.

Author contributions

S.P., B.C.S., C.W. and F.Bu. conceived the ideas; T.S. collected the data; F.Bu., T.S., and S.P. analyzed the data; F.Bu. and S.P. led the writing; B.C.S., C.W., C.G.S., E.H.L., F.Be. and T.S. revised and approved the manuscript; C.W., S.P., E.L., C.G.S. provided the resources; B.C.S. and S.P. supervised the research.

Funding

Open Access funding enabled and organized by Projekt DEAL. This research did not receive any specific grant from funding agencies in the public, commercial, or not-for-profit sectors.

Competing interests

The authors declare no competing interests.

Additional information

Correspondence and requests for materials should be addressed to F.B.

Reprints and permissions information is available at www.nature.com/reprints.

Publisher's note Springer Nature remains neutral with regard to jurisdictional claims in published maps and institutional affiliations.



Open Access This article is licensed under a Creative Commons Attribution 4.0 International License, which permits use, sharing, adaptation, distribution and reproduction in any medium or format, as long as you give appropriate credit to the original author(s) and the source, provide a link to the Creative Commons licence, and indicate if changes were made. The images or other third party material in this article are included in the article's Creative Commons licence, unless indicated otherwise in a credit line to the material. If material is not included in the article's Creative Commons licence and your intended use is not permitted by statutory regulation or exceeds the permitted use, you will need to obtain permission directly from the copyright holder. To view a copy of this licence, visit <http://creativecommons.org/licenses/by/4.0/>.

© The Author(s) 2022

2.6 Manuscript 6 – Accuracy of one-piece zirconia implant scan body–free digitization

Intraoral scans are increasingly finding application in implant prosthodontics. However, standard screw-retained scan bodies are usually not compatible when choosing implants with one-piece design. In fact, at study conceptualization, only conventional impression-taking of the investigated implant was possible.

In Manuscript 6, the feasibility of a scan body–free digitization of a one-piece ZrO₂ implant type (ceramic.implant, vitaclinical, VITA Zahnfabrik, Bad Säckingen, Germany) was investigated in vitro. The comparison included a two-piece bone-level titanium implant with a scan body and a prepared natural tooth. Two scanning systems, Omnicam, software version 5.0.x (Dentsply–Sirona, York, USA), and Trios 3, software version 1.4.7.3 (3shape, Copenhagen, Denmark), were utilized for digitization. Furthermore, a self-developed virtual reconstruction tool was applied to reconstruct partial scans of the implant abutment simulating different clinical situations.

This research was presented as a digital poster in the prosthetics category at the 26th Annual Scientific Meeting of the EAO in 2019 in Lisbon, Portugal, and the abstract was published in *Clinical Oral Implant Research* (94). Ms. Valentina L. Kohnen presented this study as a digital poster at the 33rd. Congress of the DGI, November 28 to 30, 2019, in Hamburg, Germany. The study received a grant from Progress in Science and Education with Ceramics (PROSEC) (grant number: 125280).

The following text corresponds to the abstract of the article:

Pieralli, S., Spies, B. C., Kohnen, L. V., Beuer, F., & Wesemann, C. (2020). *Digitization of One-Piece Oral Implants: A Feasibility Study. Materials (Basel, Switzerland), 13(8), 1990.* <https://doi.org/10.3390/ma13081990>

Digitization of One-Piece Oral Implants: A Feasibility Study.

Objective

For digital impression-making of two-piece oral implants, scan bodies are used to transfer the exact intraoral implant position to the dental laboratory. In this *in vitro* investigation, the accuracy of digitizing a one-piece ceramic oral implant without a scan body (OC) was compared to that of a standard two-piece titanium implant with a scan body (TT) and a preparation of a natural single tooth (ST). Furthermore, incomplete scans of OC simulating clinical compromising situations (OC1-4) were redesigned using a virtual reconstruction tool (RT) and superimposed to OC.

Methods

OC and TT oral implants and one ST were inserted into a mandible typodont model and digitized (N = 13) using two different intraoral scanners. The resulting virtual datasets were superimposed onto a three-dimensional (3D) laser scanner-based reference. Test and reference groups were aligned using an inspection software according to a best-fit algorithm, and circumferential as well as marginal discrepancies were measured. For the statistical evaluation, multivariate analyses of variance with post-hoc Tukey tests and students t-tests to compare both scanners were performed.

Results

A total of 182 datasets were analyzed. For circumferential deviations, no significant differences were found between ST, TT, and OC ($p > 0.964$), but increased deviations



for OC1-4 ($p < 0.001$) were observed. The measurements of the marginal deviations revealed that ST had the smallest deviations, and that there were no significant differences between TT, OC, and OC1-4 ($p > 0.979$). Except for marginal deviation of OC ($p < 0.001$), the outcome was not affected by the scanner.

Conclusion

Within the limitations of this study, digitization of OC is as accurate as that of TT, but less than that of ST. In the case of known geometries, post-processing of compromised scans with a virtual reconstruction tool results in accurate data.

Article

Digitization of One-Piece Oral Implants: A Feasibility Study

Stefano Pieralli ^{1,2} , Benedikt Christopher Spies ^{1,2,*}, Luisa Valentina Kohnen ¹, Florian Beuer ¹
and Christian Wesemann ¹ 

- ¹ Department of Prosthodontics, Geriatric Dentistry and Craniomandibular Disorders, Charité—Universitätsmedizin Berlin, corporate member of Freie Universität Berlin, Humboldt-Universität zu Berlin, and Berlin Institute of Health, Aßmannshäuser Str. 4-6, 14197 Berlin, Germany; stefano.pieralli@uniklinik-freiburg.de (S.P.); luisa-valentina.kohnen@charite.de (L.V.K.); florian.beuer@charite.de (F.B.); christian.wesemann@charite.de (C.W.)
- ² Department of Prosthetic Dentistry, Faculty of Medicine, Center for Dental Medicine, Medical Center—University of Freiburg, Hugstetter Str. 55, 79106 Freiburg, Germany
- * Correspondence: benedikt.spies@uniklinik-freiburg.de; Tel.: +49-761-27049060

Received: 31 March 2020; Accepted: 23 April 2020; Published: 24 April 2020



Abstract: For digital impression-making of two-piece oral implants, scan bodies are used to transfer the exact intraoral implant position to the dental laboratory. In this in vitro investigation, the accuracy of digitizing a one-piece ceramic oral implant without a scan body (OC) was compared to that of a standard two-piece titanium implant with a scan body (TT) and a preparation of a natural single tooth (ST). Furthermore, incomplete scans of OC simulating clinical compromising situations (OC₁₋₄) were redesigned using a virtual reconstruction tool (RT) and superimposed to OC. OC and TT oral implants and one ST were inserted into a mandible typodont model and digitized ($N = 13$) using two different intraoral scanners. The resulting virtual datasets were superimposed onto a three-dimensional (3D) laser scanner-based reference. Test and reference groups were aligned using an inspection software according to a best-fit algorithm, and circumferential as well as marginal discrepancies were measured. For the statistical evaluation, multivariate analyses of variance with post-hoc Tukey tests and students *t*-tests to compare both scanners were performed. A total of 182 datasets were analyzed. For circumferential deviations, no significant differences were found between ST, TT, and OC ($p > 0.964$), but increased deviations for OC₁₋₄ ($p < 0.001$) were observed. The measurements of the marginal deviations revealed that ST had the smallest deviations, and that there were no significant differences between TT, OC, and OC₁₋₄ ($p > 0.979$). Except for marginal deviation of OC ($p < 0.001$), the outcome was not affected by the scanner. Within the limitations of this study, digitization of OC is as accurate as that of TT, but less than that of ST. In the case of known geometries, post-processing of compromised scans with a virtual reconstruction results in accurate data.

Keywords: accuracy; ceramics; dental implants; digital impression; intraoral scanner; one-piece dental implant; trueness

1. Introduction

For the manufacturing of a tooth- or implant-borne prosthesis, the shape and position of teeth and oral implants need to be transferred to the dental laboratory in a highly accurate and reliable procedure. In terms of conventional impression-making techniques, there are significant differences between teeth and oral implants [1,2]. Natural teeth present an individual shape, margin preparation line, and emergence profile. To obtain an accurate impression of subgingival areas, methods to displace the gingiva, such as retraction cords, are needed [3]. These procedures are both time-consuming for

the clinicians and uncomfortable for the patients [4,5]. In contrast, the implant-abutment connection (IAC) of an oral implant has a standardized geometry, and in-lab implant replicas with identical IACs are used for subsequent manufacturing of the restorations [6]. To transfer the precise intraoral position of an implant in a conventional workflow, an impression coping of identical IAC is screwed into the implant. For the “transfer method” impression technique a transfer cap attached to the impression coping remains in the impression material after setting and removal from the oral cavity of the closed tray [7]. This allows repositioning of the impression coping with an attached lab-replica of the implant prior to pouring. For the “pick up method,” the abutment screw of the impression coping needs to be unscrewed from the fixture after setting of the impression material, allowing the coping to remain “fixed” within it [8]. In contrast to the “transfer method,” no transfer cap, but instead an open impression tray is necessary. Furthermore, a screwless approach using impression components to snap onto the transgingival part of the implant is available, but scarcely reported in the literature [9,10]. As passive fit of implant-borne superstructures seems mandatory for long-term clinical success [11–13], it is recommended to splint impression copings in the case of multiple adjacent implants to minimize the risk of discrepancies caused by deformation of the impression material [11]. The majority of in vitro investigations have confirmed the benefit of splinted copings in edentulous and partially edentulous patients in the case of ≥ 4 implants [12].

Digitization of oral implants is based on the acquisition of images to transfer the implant position to a virtual model [13], thereby avoiding the production and storage of stone casts [14]. During impression-making, this procedure allows for simultaneous visualization of the area of interest [14], and delivers a more convenient treatment for patients compared to conventional impressions [15]. According to a recent Delphi study, the intraoral digitization of implants, followed by computer-aided design and manufacturing (computer-aided design (CAD)/computer-aided manufacturing (CAM)) of the implant-supported restorations in a fully digital workflow, is expected to replace conventional techniques within the next decade [16]. To digitize standard two-piece implants, a scan body used as reference geometry is screwed into the implant (“virtual impression coping”) and its position is recorded by means of an intraoral scanner (IOS) [17]. A recent in vitro investigation demonstrated the influence of both the scan strategy and the geometry of the scan bodies on the accuracy of the digitization process [18]. Irrespective of the system, the fit of the final restoration depends on the accuracy of the previous intraoral scan.

Besides two-piece implants, one-piece fixtures are likewise available on the market and, among other materials, are made from zirconium dioxide (zirconia, ZrO_2) [19]. These implants present a monobloc design, including the endosseous part and the abutment in one piece. In this case, prosthetic-oriented implant positioning is mandatory to prevent subsequent intraoral adjustments of the abutment portion due to prosthetic reasons (e.g., path of insertion), which are liable to weaken the entire implant–restoration complex [20]. Nevertheless, anatomical limitations such as a scarce vertical dimension of the alveolar bone may require a reduction of the abutment in both the vertical and horizontal directions, especially in the esthetic zone due to diverging angulation of the bone and anterior reconstructions [21]. Comparable to natural teeth, retraction cords might be needed to expose the implant shoulder for impression taking [22], whereas the presence of blood or saliva, as well as deeply inserted implants, can complicate the process.

When digitizing a one-piece implant, the implant abutment itself might serve as a reference geometry for reconstruction, thus avoiding the need for additional scan bodies. Furthermore, in the case of incomplete scans, a virtual reconstruction of missing parts based on the known geometry of the standardized abutment might still be possible. Therefore, this in vitro study focused on two aspects: (1) the accuracy of digital impression-making with unrestricted exposure of the abutment of a one-piece ceramic (OC) implant made from ZrO_2 , and (2) the feasibility to virtually reconstruct missing parts of a partial digitized abutment in case of a clinically compromised situation. A single-tooth (ST) preparation and a two-piece titanium (TT) implant with a scan body served as references for comparison. The

null hypothesis assumed no difference in terms of trueness between digital impressions of ST, TT, OC, and virtually reconstructed scans of OC.

2. Materials and Methods

2.1. Reference Model

A reference typodont model (ANA-4, Frasco, Tettang, Germany) of the mandible was used. An OC revealing an endosseous length of 10 mm and width of 4 mm, a transgingival part 2 mm in height, and a 4° conical abutment 4.5 mm in height (ceramic implant, vitaclinical, VITA Zahnfabrik, Bad Säckingen, Germany) was positioned in the fourth quadrant in the region of the second premolar. A TT (3.8 × 9 mm) (CAMLOG SCREW-LINE, Camlog, Basel, Switzerland) was installed on the contralateral side. A human first molar was prepared and placed in the fourth quadrant. The ST presented a rounded shoulder-shaped preparation margin with 1 mm circumferential and 1.5 mm occlusal substance removal. To obtain a virtual reference dataset, the model was digitized using a blue light three-dimensional (3D) LED scanner (D2000, 3shape, Copenhagen, Denmark), which shows a precision of 5 µm/8 µm (ISO 12836/implant).

2.2. Acquisition of the Test Datasets

Two different intraoral scanners were used to perform digital impressions: TRIOS 3, software version 1.4.7.3 (3shape) and Omnicam, software version 5.0.x (Dentsply-Sirona, York, Pennsylvania, USA). A standardized scan pattern was followed for all the scanning procedures and included both the examination area and the adjacent teeth. It started with a 45° angle from the vestibular aspect of the mesial adjacent tooth, switched to the lingual aspect until the distal end of the opposite adjacent tooth, switched to the buccal aspect, and returned to the starting point. All scans were performed solely by one trained operator (L.V.K.) under ceiling lighting.

For each of the examined samples (OC, TT, ST), 13 digital impressions with both scanners were taken, resulting in 78 datasets. The 26 scan files related to OC were subsequently duplicated and virtually modified (Figure 1). First (OC₁), the scan of OC was superimposed with the original dataset of the implant abutment provided by the manufacturer and compared to the reference dataset. Second (OC₂), a subgingival positioning of the implant shoulder was simulated. In this case, the lower third of the scanned implant head, which corresponds to 1.5 mm, was removed from all datasets. Third (OC₃), an occlusal modification of the abutment geometry by grinding was simulated. In this case, the marginal reduction was followed by an occlusal reduction of the abutment of 1 mm, and the resulting datasets were stored. Fourth (OC₄), a further lateral individualization of the implant abutment, corresponding to a lateral reduction of 45° to the vertical, followed the modifications adopted for OC₃.

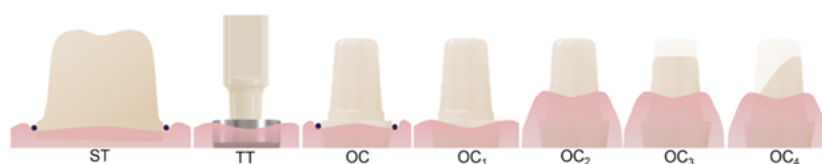


Figure 1. Schematic illustration of the investigation groups. ST, single-tooth preparation; TT, one-piece titanium implant with a scan body; OC, one-piece ZrO₂ implant; OC₁, OC for matching with reconstruction support; OC₂, simulated subgingival insertion of 1.5 mm; OC₃, additional occlusal reduction of 1 mm; OC₄, additional lateral reduction of 45°.

The original implant geometry of OC, provided by the manufacturer in the form of a digital dataset (CAD File, ceramic implant), was used to develop a virtual reconstruction tool (RT) (Figure 2).

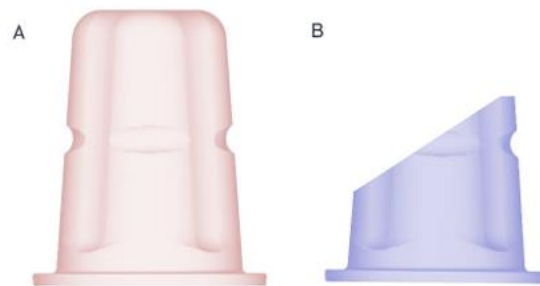


Figure 2. (A) Reconstruction tool for unmodified implants ($OC_{1,2}$); (B) reconstruction tool for intraorally adjusted ($OC_{3,4}$) implants.

The developed RT was matched with the OC_{1-4} scans to reconstruct the missing areas of the digitized abutment. For this purpose, both datasets were aligned using an inspection software (Geomagic Control X, 3-D-Systems, Rock Hill, South Carolina, USA) via a 3-point alignment, and then matched following a best-fit superimposition algorithm, according to Gauss. Both datasets were merged using Boolean operators, with the final surface of the implant head consisting of the RT. In the second subgroup (OC_2), the RT was merged into the marginal reduced scan files. In the third subgroup (OC_3), the RT was matched to the marginal and occlusal reduced datasets based on the remaining implant areas. In the fourth subgroup (OC_4), the remaining 30% of the implant surface after marginal, occlusal, and lateral reduction was used to match the RT and thus to recreate the missing data (Figure 3). The resulting subgroups from OC consisted of a further 104 modified and reconstructed datasets.



Figure 3. Reconstruction procedure: (A) OC_2 with 1.5 mm missing data marginally; (B) OC_2 matched with RT; (C) both datasets combined.

2.3. Data Analysis

To calculate the deviations of the test datasets, these were superimposed with the reference dataset using the Geomagic Control X software and a local best-fit algorithm. The superimposition was performed over the two respective adjacent teeth. Subsequently, 3D surface comparisons were performed, separately, for the circumferential and marginal areas of the datasets. Marginal areas were defined as the horizontal areas of the implant shoulder for OC, OC_{1-4} , and TT, as well as the rounded shoulder preparation margin to the transition from round to conical areas for ST. The absolute values of the surface deviation were used for further evaluation of the deviations. Therefore, the definition of marginal deviation adopted in this article must be referred to a surface not a line.

2.4. Statistical Analysis

Surface deviations of the study groups were separately analyzed for both scanners using multivariate analyses of variance (MANOVA) with post-hoc Tukey pairwise comparisons for the two dependent variables—circumferential and marginal deviations. In addition, both scanners were compared with students *t*-tests for the respective correlating groups. The analysis was performed with

SPSS 22.0. The level of significance was set as $p < 0.05$. A priori sample size calculation based on five pilot scans of ST and OC revealed a required sample size of $n = 13$ to show differences with an $\alpha = 0.05$ and a given Power of $\beta = 0.80$ as significant (Effect size $d = 1.16$)

3. Results

For each of the seven groups (OC, OC₁₋₄, ST, and TT), 13 digital impressions with two scanners each (TRIOS 3 and Omnicam) were performed, resulting in 182 datasets in total. The descriptive statistics of the absolute circumferential and marginal deviations are presented in Table 1. Figures 4 and 5 present the results for the lateral and marginal deviations visualized as box and whisker plots. MANOVA revealed significant differences between the study groups for both circumferential ($p < 0.001$) and marginal deviations ($p < 0.001$).

Table 1. Mean, standard deviation (SD), and confidence intervals (CIs) of the circumferential and marginal surface deviations. For each group $n = 13$.

IOS	Group	Circumferential Surface Deviations (μm)		Marginal Surface Deviations (μm)	
		Mean \pm SD	95% CI	Mean \pm SD	95% CI
TRIOS 3	ST	33 \pm 10 ^a	[28, 37]	24 \pm 10 ^a	[20, 28]
	TT	37 \pm 17 ^a	[30, 44]	40 \pm 20 ^b	[32, 49]
	OC	35 \pm 13 ^a	[30, 40]	45 \pm 6 ^b	[43, 48]
	OC ₁	55 \pm 20 ^b	[47, 63]	36 \pm 11 ^b	[31, 40]
	OC ₂	56 \pm 20 ^b	[48, 64]	36 \pm 11 ^b	[31, 40]
	OC ₃	55 \pm 19 ^b	[48, 63]	35 \pm 10 ^b	[31, 39]
	OC ₄	55 \pm 19 ^b	[47, 63]	38 \pm 15 ^b	[32, 44]
	Significance *	$F(6,175) = 10.66, p < 0.001$		$F(6,175) = 6.7, p < 0.001$	
Omnicam	ST	32 \pm 11 ^a	[28, 36]	26 \pm 12 ^a	[21, 30]
	TT	35 \pm 23 ^a	[23, 44]	41 \pm 24 ^b	[31, 50]
	OC	35 \pm 16 ^a	[16, 42]	38 \pm 6 ^b	[35, 41]
	OC ₁	56 \pm 21 ^b	[21, 64]	36 \pm 10 ^b	[32, 40]
	OC ₂	56 \pm 20 ^b	[20, 64]	36 \pm 11 ^b	[32, 40]
	OC ₃	55 \pm 19 ^b	[19, 63]	36 \pm 12 ^b	[31, 40]
	OC ₄	56 \pm 20 ^b	[20, 64]	37 \pm 12 ^b	[32, 42]
	Significance *	$F(6,175) = 10.62, p < 0.001$		$F(6,175) = 3.76, p < 0.001$	

Results labeled with the same superscript letter within a column were not significantly different (* one-way ANOVA with post-hoc Tukey test). IOS, intraoral scanner.

3.1. Circumferential Deviation

The digital impressions obtained with TRIOS 3 showed a minor mean surface deviation when digitizing ST (33 \pm 10 μm) (Figure 4). This outcome did not significantly differ from the digitization of TT (37 \pm 17 μm ; $p = 0.964$) or OC (35 \pm 13 μm ; $p = 0.999$) when using the same scanning system. The virtually reconstructed implants (OC₁₋₄) showed significantly higher deviations than OC ($p < 0.001$), but no significant differences between the reconstructed groups were found ($p > 0.999$). Digitization with Omnicam likewise demonstrated no significant differences between ST, TT, and OC ($p < 0.975$). The lowest mean deviation value was recorded for ST (32 \pm 11 μm), followed by OC (35 \pm 16 μm) and then TT (35 \pm 23 μm). The reconstructed implant scans showed higher mean deviation values than the aforementioned groups and ranged from OC₃ (55 \pm 19 μm) to OC₁ (56 \pm 21 μm). Finally, significant differences were found between OC and OC₁₋₄ ($p < 0.001$), with no significant differences between the reconstructed groups ($p > 0.999$). The t -tests between the corresponding groups scanned with TRIOS 3 and Omnicam showed no significant differences ($p > 0.459$).

3.2. Marginal Deviation

The digital impressions using TRIOS 3 showed that, of the tested groups, ST had the smallest deviation from the reference, with $24 \pm 10 \mu\text{m}$ (Figure 5). These scans were significantly more accurate than for TT ($40 \pm 20 \mu\text{m}$; $p < 0.001$) and OC ($45 \pm 6 \mu\text{m}$; $p < 0.001$). Furthermore, compared to OC, all of the reconstructed groups (OC_{1-4}) showed decreased mean marginal deviation values, between $35 \pm 10 \mu\text{m}$ (OC_3) and $38 \pm 15 \mu\text{m}$ (OC_4), and no significant differences between the groups were found, independent of the extent of the reconstruction ($p > 0.979$). The digitized data obtained with Omnicam showed similar results compared to TRIOS 3. In fact, significantly lower deviations were found for ST ($26 \pm 12 \mu\text{m}$) compared to TT ($41 \pm 24 \mu\text{m}$; $p < 0.001$) and OC ($38 \pm 6 \mu\text{m}$; $P < 0.007$). In addition, the reconstructed implants (OC_{1-4}) showed mean marginal deviations ranging between a minimum of $36 \pm 10 \mu\text{m}$ (OC_1) and a maximum of $37 \pm 12 \mu\text{m}$ (OC_4). No statistically significant differences between OC_{1-4} were found ($p < 0.999$). Finally, scan accuracy was not affected by the IOS used, except for OC ($p < 0.001$) which showed a lower deviation with Omnicam.

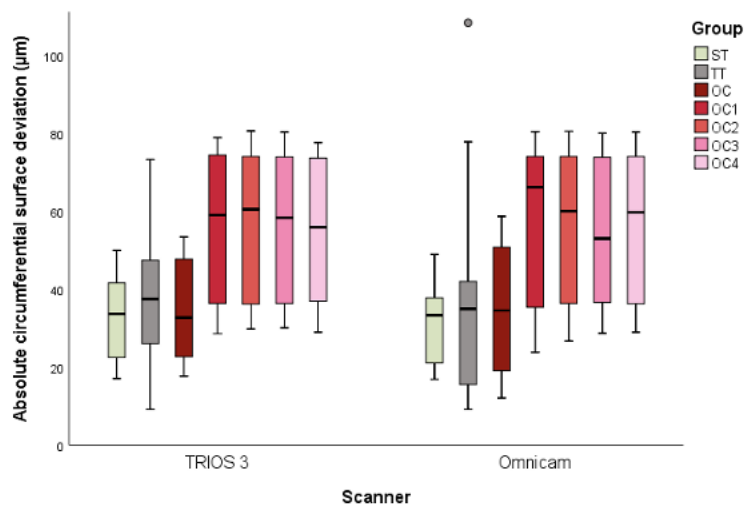


Figure 4. Box and whisker plots of the minimum, maximum, interquartile range, median, and outliers for the absolute circumferential surface deviations.

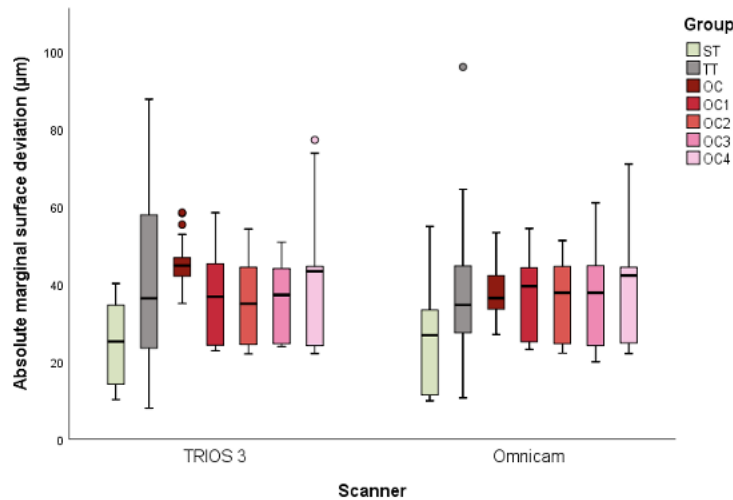


Figure 5. Box and whisker plots of the minimum, maximum, interquartile range, median, and outliers for the absolute marginal surface deviations.

4. Discussion

The term accuracy is defined as a “closeness of agreement between a measured quantity value and a true quantity value of a measurand” [23] and refers to both the trueness and the precision of a system [24]. Trueness is related to the closest representation of the measurement and precision to the repeatability and consistency of the measurement itself. In this investigation, to the authors knowledge the first one evaluating digitization of OC, accuracy was assessed by measuring the deviation between the test groups (OC, ST, TT) and their superimposed reference using a surface matching software [25]. In particular, trueness was considered the mean deviation between the positive and negative values, and precision depended on the corresponding standard deviations, according to comparable studies [26,27]. Two different IOS systems were used for the digitization of OC, ST, and TT. A 3D laser scanner, to date considered a sophisticated instrument in terms of accuracy, delivered a reliable reference dataset. As reported by Flügge et al., the assessment of a true reference model represents a major issue, especially in vivo, when evaluating spatial deviations [8]. The in vitro design of this study allowed further favorable conditions: a simplified scanning procedure avoiding limitations in space and the absence of intraoral fluids. This might have led to more precise results compared to a clinical routine [28].

The primary aim of this investigation was to evaluate the feasibility of scan body-free digital impressions of OC compared to scans of TT with a scan body and ST. Statistical analysis showed that circumferential trueness of the test group (OC) was not significantly different from the control groups (TT and ST). In contrast, the marginal trueness of OC showed no statistically significant deviations compared to TT, but significant differences compared to ST. Therefore, the null hypothesis must be partially rejected, as ST was more accurate than OC analysis.

A secondary objective of this investigation was to evaluate the feasibility and accuracy of the virtual reconstruction of the abutment of OC based on simulated clinically compromised situations. For this purpose, a virtual RT was created based on the original virtual dataset of the abutment. The absence of significant differences between the reconstructed implants (OC₁₋₄), irrespective of the extent of the reconstruction, indicates the feasibility of the virtual RT used in the present study and makes it recommendable for clinical application. However, when comparing the trueness of OC₁₋₄ to OC, disparities between the two methods were found: circumferential deviations with

reconstruction increased in OC_{1-4} compared to OC , while marginal deviations decreased. The highest mean deviation for OC_{1-4} for the circumferential aspect was $56 \pm 21 \mu\text{m}$ (OC_1 -Omnica) compared to $38 \pm 15 \mu\text{m}$ (OC_4 -TRIOS 3) for the marginal aspect. To date, a clear definition of passive fit in implant prosthodontics is still not available in the literature [29], and marginal discrepancies in a range of 30–150 μm between implant and prosthetic components are considered acceptable [30]. Therefore, the results of this study are in accordance with the current literature.

Virtual reconstruction of partial/compromised scans by means of digital post-processing with a given dataset simplified the simulated intraoral digitization process, showing that even one third of a captured abutment seems to be sufficient for reconstructive purposes. Another advantage in terms of standardization and automatization of the workflow is represented by the conversion of surface data from a polygonal free form into a standard geometry. This allows the automatized determination of the implant shoulder margin (Figure 6) and the possibility to predefine individualized spacer settings for subsequent cementation of the suprastructure.

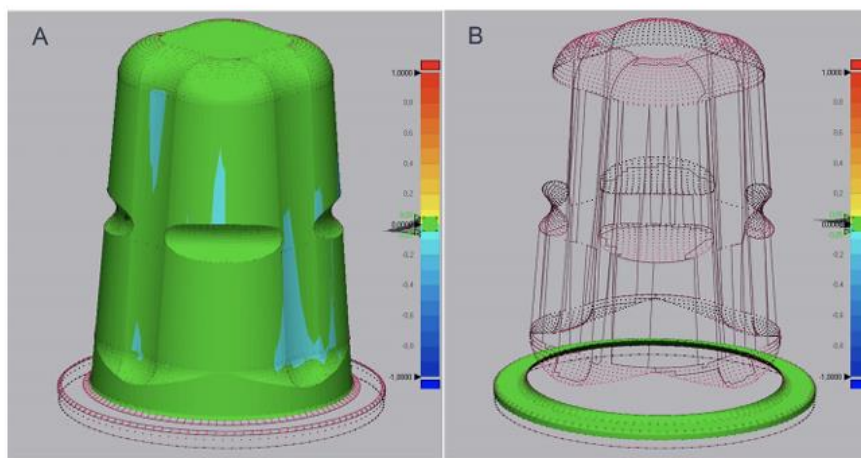


Figure 6. Representative measurements of OC_2 with a tolerance of $\pm 50 \mu\text{m}$ (green regions) for (A) circumferential deviations and (B) marginal deviations.

The digital workflow, which is “expected to replace the traditional indirect methods used in traditional dentistry” [16], can be divided into three parts: computer-aided impression (CAI) of oral structures, and CAD and manufacturing (CAM) of the restoration [31]. Every step is associated with potential discrepancies that are propagated to the next stage. The evaluated spatial deviations of the digitized OC , ST , and TT assessed the accuracy of the first part of the digital workflow. In addition, reconstructed OC_{1-4} showed that a partial scan can be accurately reconstructed virtually during the second part of the process. The possibility to virtually reconstruct OC might be useful for the clinician, in particular in compromising clinical circumstances, and may permit a more patient-friendly impression-making procedure. Furthermore, CAD based on standard geometries instead of free-form surfaces would facilitate the subsequent workflow in the lab. To allow these procedures, the geometries of one-piece implants should be included in the databases of CAD programs. Therefore, the prosthetic disadvantage of one-piece implants would be partially compensated by avoiding the need for scan bodies; however, more investigations are necessary to confirm these findings in vivo. Comparative clinical studies might assess the reliability of the presented workflow also for similar implant systems.

5. Conclusions

Taking the limitations of the present in vitro setup into account, digitization of one-piece zirconia implants without a scan body results in an accurate virtual model and presents a potential alternative to conventional impression-making methods. Incomplete scans can be digitally reconstructed based on a known abutment geometry.

Author Contributions: All authors read and agreed to the published version of the manuscript. Conceptualization, S.P., C.W., and F.B.; methodology, B.C.S. and L.V.K.; validation, F.B., S.P., C.W., and B.C.S.; formal analysis, L.V.K.; data curation, L.V.K.; writing—original draft preparation, S.P.; writing—review and editing, C.W. and B.C.S.; visualization, C.W.; supervision, F.B. and B.C.S.

Funding: This research was funded by PROSEC, grant number 125280.

Acknowledgments: The article processing charge was funded by the Baden-Wuerttemberg Ministry of Science, Research and Art and the University of Freiburg in the funding program Open Access Publishing.

Conflicts of Interest: The authors declare no conflicts of interest. The funders had no role in the design of the study; in the collection, analyses, or interpretation of data; in the writing of the manuscript; or in the decision to publish the results.

References

- Punj, A.; Bompolaki, D.; Garaicoa, J. Dental Impression Materials and Techniques. *Dent. Clin. N. Am.* **2017**, *61*, 779–796. [[CrossRef](#)] [[PubMed](#)]
- Moreira, A.H.J.; Rodrigues, N.F.; Pinho, A.C.M.; Fonseca, J.C.; Vilaca, J.L. Accuracy Comparison of Implant Impression Techniques: A Systematic Review. *Clin. Implant. Dent. R* **2015**, *17*, E751–E764. [[CrossRef](#)] [[PubMed](#)]
- Kuhr, F.; Schmidt, A.; Rehmman, P.; Wostmann, B. A new method for assessing the accuracy of full arch impressions in patients. *J. Dent.* **2016**, *55*, 68–74. [[CrossRef](#)] [[PubMed](#)]
- Huang, C.; Somar, M.; Li, K.; Mohadeb, J.V.N. Efficiency of Cordless Versus Cord Techniques of Gingival Retraction: A Systematic Review. *J. Prosthodont.* **2017**, *26*, 177–185. [[CrossRef](#)]
- Su, T.S.; Sun, J. Intraoral Digital Impression Technique: A Review. *J. Prosthodont.* **2015**, *24*, 313–321.
- Alsharbaty, M.H.M.; Alikhasi, M.; Zarrati, S.; Shamshiri, A.R. A Clinical Comparative Study of 3-Dimensional Accuracy between Digital and Conventional Implant Impression Techniques. *J. Prosthodont.* **2019**, *28*, E902–E908. [[CrossRef](#)] [[PubMed](#)]
- Abdel-Azim, T.; Zandinejad, A.; Elathamna, E.; Lin, W.; Morton, D. The influence of digital fabrication options on the accuracy of dental implant-based single units and complete-arch frameworks. *Int. J. Oral Maxillofac. Implant.* **2014**, *29*, 1281–1288. [[CrossRef](#)]
- Flugge, T.; van der Meer, W.J.; Gonzalez, B.G.; Vach, K.; Wismeijer, D.; Wang, P. The accuracy of different dental impression techniques for implant-supported dental prostheses: A systematic review and meta-analysis. *Clin. Oral Implan. Res.* **2018**, *29*, 374–392. [[CrossRef](#)]
- Fernandez, M.A.; Paez de Mendoza, C.Y.; Platt, J.A.; Levon, J.A.; Hovijitra, S.T.; Nimmo, A. A Comparative Study of the Accuracy between Plastic and Metal Impression Transfer Copings for Implant Restorations. *J. Prosthodont.* **2013**, *22*, 367–376. [[CrossRef](#)]
- Balamurugan, T.; Manimaran, P. Evaluation of accuracy of direct transfer snapon impression coping closed tray impression technique and direct transfer open tray impression technique: An in vitro study. *J. Indian Prosthodont. Soc.* **2013**, *13*, 226–232. [[CrossRef](#)]
- Papaspyridakos, P.; Chen, C.J.; Gallucci, G.O.; Doukoudakis, A.; Weber, H.P.; Chronopoulos, V. Accuracy of implant impressions for partially and completely edentulous patients: A systematic review. *Int. J. Oral Maxillofac. Implant.* **2014**, *29*, 836–845. [[CrossRef](#)] [[PubMed](#)]
- Lee, H.; So, J.S.; Hochstedler, J.L.; Ercoli, C. The accuracy of implant impressions: A systematic review. *J. Prosthet Dent.* **2008**, *100*, 285–291. [[CrossRef](#)]
- Muhlemann, S.; Kraus, R.D.; Hammerle, C.H.F.; Thoma, D.S. Is the use of digital technologies for the fabrication of implant-supported reconstructions more efficient and/or more effective than conventional techniques: A systematic review. *Clin. Oral Implan. Res.* **2018**, *29*, 184–195. [[CrossRef](#)] [[PubMed](#)]

14. Grunheid, T.; McCarthy, S.D.; Larson, B.E. Clinical use of a direct chairside oral scanner: An assessment of accuracy, time, and patient acceptance. *Am. J. Orthod. Dentofac.* **2014**, *146*, 673–682. [[CrossRef](#)] [[PubMed](#)]
15. Mangano, A.; Beretta, M.; Luongo, G.; Mangano, C.; Mangano, F. Conventional Vs Digital Impressions: Acceptability, Treatment Comfort and Stress Among Young Orthodontic Patients. *Open Dent. J.* **2018**, *12*, 118–124. [[CrossRef](#)]
16. Sanz, M.; Noguerol, B.; Sanz-Sanchez, I.; Hammerle, C.H.F.; Schliephake, H.; Renouard, F.; Sicilia, A.; Cordaro, L.; Jung, R.; Klinge, B.; et al. European Association for Osseointegration Delphi study on the trends in Implant Dentistry in Europe for the year 2030. *Clin. Oral Implan. Res.* **2019**, *30*, 476–486. [[CrossRef](#)]
17. Fluegge, T.; Att, W.; Metzger, M.; Nelson, K. A Novel Method to Evaluate Precision of Optical Implant Impressions with Commercial Scan Bodies An Experimental Approach. *J. Prosthodont.* **2017**, *26*, 34–41. [[CrossRef](#)]
18. Motel, C.; Kirchner, E.; Adler, W.; Wichmann, M.; Matta, R.E. Impact of Different Scan Bodies and Scan Strategies on the Accuracy of Digital Implant Impressions Assessed with an Intraoral Scanner: An In Vitro Study. *J. Prosthodont.* **2019**. [[CrossRef](#)]
19. Pieralli, S.; Kohal, R.J.; Jung, R.E.; Vach, K.; Spies, B.C. Clinical Outcomes of Zirconia Dental Implants: A Systematic Review. *J. Dent. Res.* **2017**, *96*, 38–46. [[CrossRef](#)]
20. Bethke, A.; Pieralli, S.; Kohal, R.-J.; Burkhardt, F.; von Stein-Lausnitz, M.; Vach, K.; Spies, B.C. Fracture Resistance of Zirconia Oral Implants In Vitro: A Systematic Review and Meta-Analysis. *Materials* **2020**, *13*, 562. [[CrossRef](#)]
21. Spies, B.C.; Pieralli, S.; Vach, K.; Kohal, R.J. CAD/CAM-fabricated ceramic implant-supported single crowns made from lithium disilicate: Final results of a 5-year prospective cohort study. *Clin. Implant. Dent. R* **2017**, *19*, 876–883. [[CrossRef](#)] [[PubMed](#)]
22. Spies, B.C.; Kohal, R.J.; Balmer, M.; Vach, K.; Jung, R.E. Evaluation of zirconia-based posterior single crowns supported by zirconia implants: Preliminary results of a prospective multicenter study. *Clin. Oral Implan. Res.* **2017**, *28*, 613–619. [[CrossRef](#)]
23. Knapp, W. Accuracy. In *CIRP Encyclopedia of Production Engineering*; Laperrière, L., Reinhart, G., Eds.; Springer: Berlin/Heidelberg, Germany, 2014; pp. 6–9. [[CrossRef](#)]
24. Arakida, T.; Kanazawa, M.; Iwaki, M.; Suzuki, T.; Minakuchi, S. Evaluating the influence of ambient light on scanning trueness, precision, and time of intra oral scanner. *J. Prosthodont. Res.* **2018**, *62*, 324–329. [[CrossRef](#)] [[PubMed](#)]
25. Malik, J.; Rodriguez, J.; Weisbloom, M.; Petridis, H. Comparison of Accuracy between a Conventional and Two Digital Intraoral Impression Techniques. *Int. J. Prosthodont.* **2018**, *31*, 107–113. [[CrossRef](#)] [[PubMed](#)]
26. Medina-Sotomayor, P.; Pascual-Moscardo, A.; Camps, I. Accuracy of 4 digital scanning systems on prepared teeth digitally isolated from a complete dental arch. *J. Prosthet. Dent.* **2019**, *121*, 811–820. [[CrossRef](#)]
27. Wesemann, C.; Muallah, J.; Mah, J.; Bumann, A. Accuracy and efficiency of full-arch digitalization and 3D printing: A comparison between desktop model scanners, an intraoral scanner, a CBCT model scan, and stereolithographic 3D printing. *Quintessence Int.* **2017**, *48*, 41–50.
28. Flugge, T.V.; Att, W.; Metzger, M.C.; Nelson, K. Precision of Dental Implant Digitization Using Intraoral Scanners. *Int. J. Prosthodont.* **2016**, *29*, 277–283. [[CrossRef](#)]
29. Moore, A.J.; Stubbings, A.; Swallow, E.B.; Dusmet, M.; Goldstraw, P.; Porcher, R.; Moxham, J.; Polkey, M.I.; Ferenczi, M.A. Passive properties of the diaphragm in COPD. *J. Appl. Physiol.* **2006**, *101*, 1400–1405. [[CrossRef](#)]
30. Klineberg, I.J.; Murray, G.M. Design of superstructures for osseointegrated fixtures. *Swed Dent. J. Suppl.* **1985**, *28*, 63–69. [[PubMed](#)]
31. Patzelt, S.B.M.; Emmanouilidi, A.; Stampf, S.; Strub, J.R.; Att, W. Accuracy of full-arch scans using intraoral scanners. *Clin. Oral Invest.* **2014**, *18*, 1687–1694. [[CrossRef](#)]



3 DISCUSSION

Throughout this thesis, the six included studies clarified some crucial points for successfully implementing digital technologies designed for current implant prosthodontic rehabilitation. Furthermore, the summarized results revealed significant implications in terms of virtual implant planning, implant selection, guided implant placement, and intraoral implant digitization. The main results are reported hereafter and compared with the current literature.

3.1 Study outcomes

The authors pointed out in Manuscript 1 that a wider FOV does not necessarily lead to more accurate registration intended as true and precise when performing virtual implant planning for sCAIS. The findings are consistent with the results proposed by Hamilton et al. in a similar investigation addressing registration precision (small FOV: 0.37 ± 0.25 mm and large FOV: 0.35 ± 0.23 mm at implant entry point) (95). In the present study, mean SD intervals were limited to ≤ 0.25 mm at the implant shoulder. In the case of posterior rehabilitation on single implants and the absence of sources of artifacts, the reduction of FOV to adjacent teeth did not affect registration trueness by more than 0.1 mm compared with larger FOV extensions. However, due to the study's pilot design, further comparisons with similar studies were not possible. Clinical advantages of smaller CBCT FOV volumes include fewer radiations for the patient (96), less time to acquire and reconstruct the 3D scan, and smaller areas to examine and report for the radiologist or dentist.

In Manuscript 2, the authors demonstrated that the clinically evaluated CAD/CAM RAI system has potential advantages and limitations compared to prefabricated screw-shaped immediate implants. The investigated RAI system showed high esthetic outcomes with beneficial peri-implant soft tissue adaptation (97). This might be due to the selection of ZrO₂ as the abutment material, which leads to increased esthetic results also with screw-shaped stock implants (98). In addition, the fully anatomical design, especially in the area of the emergence profile, might increase soft tissue adaptability and help to prevent peri-implant biologic complications (99). On the other hand, no advantages to screw-shaped implants were assessed in terms of marginal bone loss (0.40 ± 0.41 mm on average after 10.8 ± 7.0 months from loading). Moreover, a moderate survival rate of 94.4% was reported for the tested RAI system after less than 24 months on average. These results are comparable to 10-year data (94.6%) of screw-shaped implants available in the literature (100) and, therefore, considered below expectations.

Manuscripts 3–5 referred to the following topic: AM by ME of sterilizable surgical guides made of PLA. In Manuscript 3, the authors pointed out that implant installation with high trueness is possible using the tested ME-based surgical guides. As a control group, market-available drilling guides created by SLA were used. Mean discrepancies between the test and control groups were limited to < 1 mm linear and $\leq 3^\circ$ angular errors. In terms of final implant position, comparable errors were reported in vitro using surgical guides created by DLP and SLA (101). Furthermore, metal sleeves do not seem to increase implant positioning trueness in partially edentulous patients. This outcome is in accordance with the results from Adams et al. (102) and Tallarico et al. (103).

In Manuscript 4, the focus was set on the potential influence of using various implant planning programs or modifications of the original surgical guide design on both the trueness and precision of implant installation. Both variables, planning software and design, significantly influenced the outcome. However, deviations at the implant entry point of ≤ 0.32 mm and $\leq 2.63^\circ$ might be considered clinically acceptable. Results are consistent with those of similar studies that used various 3D printing techniques for AM of the surgical guides (104, 105).

The potential cytotoxicity of the polymers intended for fabrication of the surgical guides of Manuscripts 3 and 4 was investigated in Manuscript 5. The ISO guidelines 10993-5:2009 (106) and 10993-12:2021 (107) were respected in conducting this study. For this purpose, HGKs were exposed to eluates of the tested biocopolyester and of a polypropylene-based material, also intended for ME (108). As a control group, a medically certified resin meant for SLA printing was used. According to the results of Manuscript 5, none of the three evaluated materials exceeded the $< 70\%$ viability in MTT, which is considered the limit for cytotoxicity, according to ISO 10993-5:2009. The cell proliferation, measured with impedance-related indices, revealed minimal differences between the biocopolyester and the polypropylene. Differently, the control group showed a significantly reduced cell proliferation after 72 hr. Moreover, when evaluating the PCR analysis of the 72-hr eluates, the resin-based specimens caused a significant up-regulation of genes encoding for apoptosis and inflammation. At the same time, the biocopolyester showed no regulation, and the polypropylene partially showed a down-regulation. Therefore, all investigated materials can be considered, *in vitro*, not cytotoxic for a short-term application in the oral environment.



Figure 10: Detail of the groups evaluated in Manuscript 6. ST = single tooth; TT = two-piece titanium implant with a scan body; OC = one-piece ZrO₂ implant; OC₁ = same as OC but used for superimposition with the reconstruction tool; OC₂ = modification simulating 1.5-mm deeper implant installation; OC₃ = modification simulating additional 1-mm occlusal reduction; OC₄ = modification simulating additional lateral reduction.

Reproduced with permission from: Pieralli, S., Spies, B. C., Kohnen, L. V., Beuer, F., & Wesemann, C. (2020). Digitization of one-piece oral implants: A feasibility study. Materials (Basel, Switzerland), 13(8), 1990. <https://doi.org/10.3390/ma13081990>

The last included manuscript described the feasibility of one-piece ZrO₂ implant digitization without a scan body. Our research group demonstrated that the integrated ZrO₂ abutment could be digitized with comparable accuracy to a scan body mounted on a two-piece, bone-level, titanium implant. No significant differences in circumferential or marginal discrepancies resulted between TT, OC, and OC₁₋₄ ($p > 0.964$). The second objective of the study was to assess the feasibility of a self-developed virtual reconstruction tool based on the known abutment geometry to complete partial scans automatically. Similar discrepancies between the four reconstructed scans were reported. Maximal mean differences in terms of marginal (OC: $45 \pm 6 \mu\text{m}$; OC₁₋₄: $< 38 \pm 15 \mu\text{m}$) and circumferential deviations (OC: $35 \pm 16 \mu\text{m}$; OC₁₋₄: $< 56 \pm 31 \mu\text{m}$) were assessed when comparing OC and OC₁₋₄. Digitizing one-third of the abutment was considered sufficient for reconstructive purposes. In addition, the conversion of surface data from a polygonal free form to a standard geometry allowed for automated determination of the implant shoulder margin. Prior

to this investigation, only conventional impression techniques were described for the presented implant system.

3.2 Outlook and future perspectives

The results of the six included studies highlighted some advantages and limitations of the current digital workflow in implant prosthodontics. The main limitations of the included studies are the in vitro setting (Manuscripts 1, 3, 4, 5, and 6) and the clinical retrospective design (2). Intraoperative limitations, such as reduced space, patient movement, and precarious visibility, were not reproduced in vitro. Furthermore, results from in vitro studies may underscore potential error risks compared with a clinical situation. Thus, the methodologies adapted, and the presented results should find confirmation in successive high-level prospective clinical investigations.

3.2.1 Virtual implant imaging with reduced field of view

Adhesion to the ALADA/ALARA principles must be pursued when virtual implant planning (109), and international guidelines for implant imaging with lower irradiation than today's routine are still needed. As reported by Bornstein et al., narrowing the FOV can considerably reduce the effective radiation dose (96). Future investigations should include novel methods for FOV reduction, different FOV sizes, and more clinical indications, including the anterior region or cases with few residual teeth.

Registration with reduced FOV and in the presence of metal-induced artifacts is challenging. Efforts to reduce radiographic artifacts are needed to increase the

registration accuracy. Registration tools, such as reference markers, positioned outside the artifact beam might be helpful, especially when using a small FOV. For this purpose, prefabricated registration trays to provide common landmarks (110) or metal artifact reduction tools, as described by Alhossaini et al. (111), are proposed. A further imaging technology applied to virtual implant planning and sCAIS and avoiding ionizing irradiation is magnetic resonance imaging (MRI) (112). As for CBCT technology, artifacts induced by certain dental restorations or dental implants are a technical complication for MRI as well (113), and methods for artifact reduction for MRI are being investigated (114).

Additional studies should assess the cost benefit of virtual implant planning with reduced FOV size in terms of the time needed for registration or planning and calculating the time needed to examine and report the radiographic dataset. Currently, full-arch radiographic scans are used for sCAIS, irrespective of the clinical scenario (96). Based on the results of this investigation, the significance of this clinical routine practice might be questioned.

3.2.2 CAD/CAM custom-made root-analogue implants for immediate placement

Implant selection is crucial for successful implant prosthodontic rehabilitation. RAI systems are available on the market as an alternative to threaded implants for immediate implant installation. However, data regarding CAD/CAM RAI systems are mostly limited to case reports (115) or moderate patient cohorts (116). Clinical data from high-level prospective studies are scarce; therefore, mid- and long-term RCTs

addressing various CAD/CAM RAI systems are needed (61). Future perspectives include the preclinical and clinical evaluation of RAI systems with a two-piece design and made of different materials (e.g., titanium, ZrO₂). The costs of a single RAI evaluated in Manuscript 2 exceed those of a standard screw-shaped implant. Therefore, novel methods for manufacturing RAIs, such as 3D printing, should also be investigated to reduce production expenses.

One major advantage of using RAIs is their fit into the post-extraction sockets. Therefore, accurate manufacturing is crucial to avoid mismatch. In an in vitro comparative study by Aldesoki et al., the accuracy of 3D-printed and milled RAIs made of titanium and ZrO₂ was evaluated. The highest precision in terms of surface anatomy was obtained by 3D-printed ZrO₂ RAIs, especially in concave areas. In addition, the milled ZrO₂ implants revealed the highest trueness compared to the virtually designed one (63). Depending on the bulk material used and the manufacturing technology applied, volumetric changes of the CAD/CAM RAI can occur and must be further evaluated. The investigated RAI system showed a limited survival rate and drawbacks in terms of marginal bone loss and restoration margin integrity. Therefore, the evaluated implant system cannot be clinically recommended. The investigated REPLICATE Immediate Tooth Replacement System was retired from the market in early 2020 when the manufacturer, Natural Dental Implants (NDI Berlin, Germany), ceased the activity.

3.2.3 Surgical guides fabricated with material extrusion technology

Accurate implant installation can be achieved using the tested economic and straightforward ME method to produce surgical guides. Before Manuscript 3 was published, articles reporting on the accuracy of implant positioning with ME-based surgical guides in a preclinical setting were scarce (117). Almost 3 years later, an increasing number of in vitro and clinical studies include surgical guides created by ME in the analysis (118, 119). The mechanical properties of the object printed by ME are a function of the raw material used but are also strictly dependent on other parameters, such as printing speed and nozzle temperature (120). Therefore, future investigations should include new protocols for ME of surgical guides depending on the 3D printing system and the material used.

According to the results of Manuscript 4, the planning software has a significant but clinically questionable impact on the accuracy of implant installation with ME-based surgical guides. Considering the fees charged annually or per unit for exporting the STL file of the surgical guide, alternative high-level software, such as 3D slicer (Slicer; <https://www.slicer.org/>) (121), might be considered for lower-budget options. Talmazov et al. applied a nondental software, namely 3D modeling Blender (Blender Foundation, Amsterdam, Netherlands), to produce surgical guides by SLA with promising results (average horizontal deviation at implant apex level: 0.76 ± 0.3 mm) (122). Considering the low production costs per unit (approximately 0.40€) with the presented AM technology, also reducing the planning software–related fees would represent a chance to increase the number of sCAIS users worldwide. Furthermore, a modification of the original closed-frame design of the surgical guide did not increase

the accuracy of implant installation. This implies that complex shapes, such as the occlusal plane, can be reliably reproduced with the presented ME protocol.

Future studies should include various designs of surgical guides and supports (e.g., teeth, mucosa), including multifunctional stackable templates, as described for other 3D printing techniques (123). A steam-sterilization protocol in an autoclave was applied to the surgical guides of Manuscripts 3 and 4. Regardless of the 3D printing technique applied, sterilizing the surgical guides can decrease the risk of contaminating the surgical field (124). Future studies are needed to assess the ideal disinfection/sterilization procedures, including plasma sterilization, for surgical guides created by ME.

The experimental biocopolyester used in Manuscripts 3 and 4 can be considered, *in vitro*, biocompatible for short-term intraoral use (Manuscript 5). For this investigation, HGKs were used as the target cell population. Future studies should include further cell types, such as fibroblasts (125) and osteoblasts (126), which can also be exposed during sCAIS. In this study, gene expression analysis was performed for ANXA5, CASP, CASP9, IL1B, IL6, and TNF. Subsequent studies should include a supplementary evaluation of genes related to cytotoxic cellular events. In addition, interactive cell systems can create a more reliable *in vivo* environment (108). Considering the availability of numerous raw materials for ME and the lack of data on their potential intraoral cytotoxicity, additional studies assessing the biological risk on human tissue-specific cells are urgently needed.

3.2.4 Scan body–free implant digitization

The scan body–free digitization of the investigated one-piece ZrO₂ implant system revealed, in vitro, comparable results in terms of the accuracy to a two-piece titanium implant with a scan body (Manuscript 6). Future studies should include more implant systems with different bulk materials and modern scanning systems for digitization. In addition, validating the presented workflow for partial scan reconstruction is still necessary. Two-piece implants are more common than implants with a one-piece design (127). To digitize a two-piece implant, a scan body is needed and serves as a reference of the subgingivally positioned implant for the IOS. Nevertheless, parameters such as scan body bevel location (128) and material (79) can affect the scanning accuracy. As modern IOS systems claim accurate intra-radicular digitization (e.g., of the prepared post space) (129), the feasibility of the scan body–free digitization of two-piece implants should be further evaluated. For reconstructive purposes, the implant shoulder or internal geometry might be used as a reference by the CAD software instead of the scan body geometry. Both tissue- and bone-level two-piece implants, gradually positioned at the subgingival level, should be included in future analyses regarding scan body-free digitization. The average price of a single scan body is approximately 30€; thus, avoiding the use of scan bodies could also reduce the costs and the time needed for implant digitization.

4 CONCLUSION

Based on the results of the six included manuscripts of this thesis, the following conclusions can be drawn:

- Reducing the FOV of CBCT scans does not affect the registration accuracy for single tooth gaps in the posterior area. Caution is required when reducing the FOV for multiple-tooth gaps, especially in the presence of metal-induced artifacts (Manuscript 1).
- The CAD/CAM RAI system shows high esthetic results and peri-implant soft-tissue affinity but also a moderate survival rate after less than 2 years. Therefore, it cannot be recommended as an alternative to stock implants. Furthermore, the implant system was retired from the market on January 31, 2020 (Manuscript 2).
- The presented ME-based surgical guides show comparable trueness in terms of implant installation to market-available surgical guides created by SLA. Moreover, metal sleeves do not increase the accuracy of implant installation (Manuscript 3).
- Variables such as planning software and surgical guide design can affect the trueness and precision of implant installation using the presented ME-based surgical guides. However, mean errors at the entry point and main axis level are within clinical acceptability (Manuscript 4).
- The biocopolyester used to create the surgical guides by ME in Manuscripts 3 and 4 can be considered, *in vitro*, biocompatible for short-term intraoral usage. It shows, after a longer period of time (72 hr), less cytotoxic effects of apoptosis

and inflammation compared to a resin approved for VAT photopolymerization of medical devices (Class 1) (Manuscript 5).

- Scan body–free digitization of the investigated one-piece ZrO₂ implant is possible and comparable, in terms of accuracy, to scanning a two-piece titanium implant with a scan body. In addition, partial scans can be completed with a self-developed virtual reconstruction tool (Manuscript 6).

5 SUMMARY

Implant prosthodontics refers to rehabilitating partially or edentulous patients with removable or fixed prostheses anchored to one (or more) dental implant(s). The workflow, intended through data collection to transfer the implants' intraoral position to the dental lab in order to create a prosthesis, was once completely analog. To this day, various digital technologies have been applied to the reconstructive process, both in the clinic and the lab. However, many aspects still require investigation.

To date, to install a single implant in the posterior area, full-arch CBCT scans are used and display anatomical structures outside of the region of interest. According to the results of Manuscript 1, the radiographic FOV reduction does not affect the accuracy of registration for single tooth gaps in the posterior area and in the absence of sources of artifacts. Improvements are needed to further decrease patients' radiation dose for virtual implant planning purposes.

After registration of the radiographic and surface scans, the ideal implant must be selected. Prefabricated titanium thread-shaped implants are founded on long-term data from the literature. An alternative option for immediate implant installation is offered by RAIs. CAD/CAM custom-made RAIs reproduce the shape of the dental root(s) based on the digitally segmented 3D radiographic dataset and are fabricated before surgery. In the included retrospective investigation (Manuscript 2), clinical outcomes and PROMs from a patient cohort rehabilitated with FDPs supported by custom-made RAIs were collected and analyzed. An optimal esthetic outcome and favorable results in terms of peri-implant soft tissues were reported after a mean follow-up of 19 months. Data regarding marginal bone loss (1.20 ± 0.73 mm after 12.1 ± 6.9 months) and survival rate (94.4% after 18.9 ± 2.4 months), however, were

comparable or inferior to data on threaded stock implants. It also appears that the implementation of RAls bears, at this moment, no relation to the necessary expenses and production efforts. In addition, Natural Dental Implants (NDI Berlin), the company marketing the evaluated implant system, ceased operations at the end of January 2020.

For accurate implant installation, a surgical guide can be used. In Manuscripts 3 and 4, a protocol to create economic and sterilizable surgical guides by ME was described. Comparable results in terms of the trueness of the final implant position to market-available surgical guides created by SLA were assessed (Manuscript 3). In the second manuscript, the impact of variables (e.g., implant planning software and surgical guide designs) on the accuracy, intended as trueness and precision, of implant positioning was evaluated (Manuscript 4). Both evaluated variables revealed a significant influence on the outcome, but low mean deviations of ≤ 0.32 mm and $\leq 2.63^\circ$ were assessed. Moreover, the cytotoxicity of the biopolymer used to create the surgical guides was tested in vitro in Manuscript 5 and confirmed the biocompatibility for short-term intraoral use.

The last study in the present thesis (Manuscript 6) investigated the feasibility of scanning a one-piece ZrO₂ implant without a scan body, revealing comparable accuracy to a two-piece titanium implant with a scan body. Furthermore, a digital reconstruction tool was applied to complete incomplete scans. The use of one-piece implants is limited due to surgical and prosthetic limitations. Nevertheless, scan body-free digitization might also be applicable to two-piece implants at some point. For reconstructive purposes, CAD systems might rely on the implant shoulder and internal conformation rather than the scan body geometry in the future.

6 REFERENCES

1. Pjetursson BE, Sailer I, Latyshev A, Rabel K, Kohal RJ, Karasan D. A systematic review and meta-analysis evaluating the survival, the failure, and the complication rates of veneered and monolithic all-ceramic implant-supported single crowns. *Clin Oral Implants Res.* 2021;32 Suppl 21(Suppl 21):254-88.
2. Sailer I, Strasding M, Valente NA, Zwahlen M, Liu S, Pjetursson BE. A systematic review of the survival and complication rates of zirconia-ceramic and metal-ceramic multiple-unit fixed dental prostheses. *Clin Oral Implants Res.* 2018;29 Suppl 16:184-98.
3. Feine J, Abou-Ayash S, Al Mardini M, de Santana RB, Bjelke-Holtermann T, Bornstein MM, et al. Group 3 ITI Consensus Report: Patient-reported outcome measures associated with implant dentistry. *Clin Oral Implants Res.* 2018;29 Suppl 16:270-5.
4. The Glossary of Prosthodontic Terms: Ninth Edition. *J Prosthet Dent.* 2017;117(5s):e1-e105.
5. Brånemark P-I. Osseointegration and its experimental background. *J Prosthet Dent.* 1983;50(3):399-410.
6. Garcia-Sanchez R, Dopico J, Kalemaj Z, Buti J, Pardo Zamora G, Mardas N. Comparison of clinical outcomes of immediate versus delayed placement of dental implants: A systematic review and meta-analysis. *Clin Oral Implants Res.* 2022;33(3):231-77.
7. Pitta J, Zarauz C, Pjetursson B, Sailer I, Liu X, Pradies G. A Systematic Review and Meta-Analysis of the Influence of Abutment Material on Peri-implant Soft Tissue Color Measured Using Spectrophotometry. *Int J Prosthodont.* 2020;33(1):39-47.
8. Pieralli S, Kohal RJ, Jung RE, Vach K, Spies BC. Clinical Outcomes of Zirconia Dental Implants: A Systematic Review. *J Dent Res.* 2017;96(1):38-46.
9. Sanz M, Noguerol B, Sanz-Sanchez I, Hammerle CHF, Schliephake H, Renouard F, et al. European Association for Osseointegration Delphi study on the trends in Implant Dentistry in Europe for the year 2030. *Clin Oral Implants Res.* 2019;30(5):476-86.
10. Pjetursson BE, Zarauz C, Strasding M, Sailer I, Zwahlen M, Zembic A. A systematic review of the influence of the implant-abutment connection on the clinical outcomes of ceramic and metal implant abutments supporting fixed implant reconstructions. *Clin Oral Implants Res.* 2018;29 Suppl 18:160-83.
11. Jung RE, Zembic A, Pjetursson BE, Zwahlen M, Thoma DS. Systematic review of the survival rate and the incidence of biological, technical, and aesthetic complications of single crowns on implants reported in longitudinal studies with a mean follow-up of 5 years. *Clin Oral Implants Res.* 2012;23 Suppl 6:2-21.

12. Brandeburski SBN, Della Bona A. Quantitative and qualitative analyses of ceramic chipping. *J. Mech. Behav. Biomed. Mater.* 2020;110:103928.
13. Pieralli S, Kohal RJ, Rabel K, von Stein-Lausnitz M, Vach K, Spies BC. Clinical outcomes of partial and full-arch all-ceramic implant-supported fixed dental prostheses. A systematic review and meta-analysis. *Clin Oral Implants Res.* 2018;29 Suppl 18:224-36.
14. Wittneben JG, Joda T, Weber HP, Brägger U. Screw retained vs. cement retained implant-supported fixed dental prosthesis. *Periodontol 2000.* 2017;73(1):141-51.
15. Quaranta A, Lim ZW, Tang J, Perrotti V, Leichter J. The Impact of Residual Subgingival Cement on Biological Complications Around Dental Implants: A Systematic Review. *Implant Dent.* 2017;26(3):465-74.
16. Linkevicius T, Vindasiute E, Puisys A, Linkeviciene L, Maslova N, Puriene A. The influence of the cementation margin position on the amount of undetected cement. A prospective clinical study. *Clin Oral Implants Res.* 2013;24(1):71-6.
17. Linkevicius T, Puisys A, Vindasiute E, Linkeviciene L, Apse P. Does residual cement around implant-supported restorations cause peri-implant disease? A retrospective case analysis. *Clin Oral Implants Res.* 2013;24(11):1179-84.
18. Bidra AS, Tischler M, Patch C. Survival of 2039 complete arch fixed implant-supported zirconia prostheses: A retrospective study. *T J. Prosthet. Dent.* 2018;119(2):220-4.
19. Papaspyridakos P, Bordin TB, Natto ZS, El-Rafie K, Pagni SE, Chochlidakis K, et al. Complications and survival rates of 55 metal-ceramic implant-supported fixed complete-arch prostheses: A cohort study with mean 5-year follow-up. *J. Prosthet. Dent.* 2019;122(5):441-9.
20. Barootchi S, Askar H, Ravidà A, Gargallo-Albiol J, Travan S, Wang HL. Long-term Clinical Outcomes and Cost-Effectiveness of Full-Arch Implant-Supported Zirconia-Based and Metal-Acrylic Fixed Dental Prostheses: A Retrospective Analysis. *Int J Oral Maxillofac Implants.* 2020;35(2):395-405.
21. Maló P, de Araújo Nobre M, Lopes A, Ferro A, Nunes M. The All-on-4 concept for full-arch rehabilitation of the edentulous maxillae: A longitudinal study with 5-13 years of follow-up. *Clin Implant Dent Relat Res.* 2019;21(4):538-49.
22. Kern JS, Kern T, Wolfart S, Heussen N. A systematic review and meta-analysis of removable and fixed implant-supported prostheses in edentulous jaws: post-loading implant loss. *Clin Oral Implants Res.* 2016;27(2):174-95.
23. Hauck KE, Trentin MS, Skiba THI, Shibli JA, De Carli JP. Clinical and satisfaction outcomes of using one or two dental implants for mandibular overdentures: preliminary short-term follow-up of a randomized clinical trial. *Int J Implant Dent.* 2021;7(1):10.

24. Wakam R, Benoit A, Mawussi KB, Gorin C. Evaluation of Retention, Wear, and Maintenance of Attachment Systems for Single- or Two-Implant-Retained Mandibular Overdentures: A Systematic Review. *Materials (Basel)*. 2022;15(5).
25. Mitchell M, Kan L. Digital Technology and the Future of Health Systems. *Health Syst Reform*. 2019;5(2):113-20.
26. Spagnuolo G, Sorrentino R. The Role of Digital Devices in Dentistry: Clinical Trends and Scientific Evidences. *J Clin Med*. 2020;9(6).
27. Jacobs R, Salmon B, Codari M, Hassan B, Bornstein MM. Cone beam computed tomography in implant dentistry: recommendations for clinical use. *BMC Oral Health*. 2018;18(1):88.
28. Jacobs R. Dental cone beam CT and its justified use in oral health care. *JBR-BTR*. 2011;94(5):254-65.
29. Bornstein MM, Scarfe WC, Vaughn VM, Jacobs R. Cone beam computed tomography in implant dentistry: a systematic review focusing on guidelines, indications, and radiation dose risks. *Int J Oral Maxillofac Implants*. 2014;29 Suppl:55-77.
30. Memon A, Rogers I, Paudyal P, Sundin J. Dental X-Rays and the Risk of Thyroid Cancer and Meningioma: A Systematic Review and Meta-Analysis of Current Epidemiological Evidence. *Thyroid*. 2019;29(11):1572-93.
31. Aiello M, Esposito G, Pagliari G, Borrelli P, Brancato V, Salvatore M. How does DICOM support big data management? Investigating its use in medical imaging community. *Insights Imaging*. 2021;12(1):164.
32. Kernen F, Kramer J, Wanner L, Wismeijer D, Nelson K, Flugge T. A review of virtual planning software for guided implant surgery - data import and visualization, drill guide design and manufacturing. *BMC Oral Health*. 2020;20(1):251.
33. Harris D, Horner K, Gröndahl K, Jacobs R, Helmrot E, Benic GI, et al. E.A.O. guidelines for the use of diagnostic imaging in implant dentistry 2011. A consensus workshop organized by the European Association for Osseointegration at the Medical University of Warsaw. *Clin Oral Implants Res*. 2012;23(11):1243-53.
34. de Castro HS, Kehrwald R, Matheus RA, Gomes AF, Queiroz PM. Influence of Low-Dose Protocols of CBCT on Dental Implant Planning. *Int J Oral Maxillofac Implants*. 2021;36(2):307-12.
35. Yeung AWK, Jacobs R, Bornstein MM. Novel low-dose protocols using cone beam computed tomography in dental medicine: a review focusing on indications, limitations, and future possibilities. *Clin Oral Investig*. 2019;23(6):2573-81.
36. Schmidt A, Wöstmann B, Schlenz MA. Accuracy of digital implant impressions in clinical studies: A systematic review. *Clin Oral Implants Res*. 2022;33(6):573-85.

37. Siqueira R, Galli M, Chen Z, Mendonça G, Meirelles L, Wang H-L, et al. Intraoral scanning reduces procedure time and improves patient comfort in fixed prosthodontics and implant dentistry: a systematic review. *Clin. Oral Investig.* 2021;1-15.
38. Bishti S, Tuna T, Rittich A, Wolfart S. Patient-reported outcome measures (PROMs) of implant-supported reconstructions using digital workflows: A systematic review and meta-analysis. *Clin Oral Implants Res.* 2021;32 Suppl 21:318-35.
39. Wesemann C, Kienbaum H, Thun M, Spies BC, Beuer F, Bumann A. Does ambient light affect the accuracy and scanning time of intraoral scans? *J. Prosthet. Dent.* 2021;125(6):924-31.
40. Revilla-León M, Gohil A, Barmak AB, Gómez-Polo M, Pérez-Barquero JA, Att W, et al. Influence of ambient temperature changes on intraoral scanning accuracy. *J Prosthet Dent.* 2022.
41. Majeed-Saidan A, Dutra V, Levon JA, Chu TG, Morton D, Alfaraj A, et al. The trueness of scans using one intraoral scanner in different partially edentulous conditions. *J Prosthodont.* 2022.
42. Abad-Coronel C, Atria PJ, Romero Muñoz C, Conejo J, Mena Córdova N, Pendola M, et al. Analysis of the mesh resolution of an .STL exported from an intraoral scanner file. *J Esthet Restor Dent.* 2022;34(5):816-25.
43. Al-Haj Husain N, Molinero-Mourelle P, Janner SFM, Brägger U, Özcan M, Schimmel M, et al. Digital workflow for implant-supported fixed complete dentures based on backwards planning in an edentulous patient. *Int J Comput Dent.* 2021;24(1):89-101.
44. Flugge T, Kramer J, Nelson K, Nahles S, Kernen F. Digital implantology-a review of virtual planning software for guided implant surgery. Part II: Prosthetic set-up and virtual implant planning. *BMC Oral Health.* 2022;22(1):23.
45. Flugge T, Derksen W, Te Poel J, Hassan B, Nelson K, Wismeijer D. Registration of cone beam computed tomography data and intraoral surface scans - A prerequisite for guided implant surgery with CAD/CAM drilling guides. *Clin Oral Implants Res.* 2017;28(9):1113-8.
46. Taheri Otaghsara SS, Joda T, Thieringer FM. Accuracy of dental implant placement using static versus dynamic computer-assisted implant surgery: An in vitro study. *J Dent.* 2023;132:104487.
47. Guentsch A, Bjork J, Saxe R, Han S, Dentino AR. An in-vitro analysis of the accuracy of different guided surgery systems - They are not all the same. *Clin Oral Implants Res.* 2023.
48. Wei SM, Zhu Y, Wei JX, Zhang CN, Shi JY, Lai HC. Accuracy of dynamic navigation in implant surgery: A systematic review and meta-analysis. *Clin Oral Implants Res.* 2021;32(4):383-93.
49. Oliveira TT, Reis AC. Fabrication of dental implants by the additive manufacturing method: A systematic review. *J Prosthet Dent.* 2019;122(3):270-4.

50. Thome G, Sandgren R, Bernardes S, Trojan L, Warfving N, Bellon B, et al. Osseointegration of a novel injection molded 2-piece ceramic dental implant: a study in minipigs. *Clin Oral Investig*. 2021;25(2):603-15.
51. Shalabi MM, Gortemaker A, Van't Hof MA, Jansen JA, Creugers NH. Implant surface roughness and bone healing: a systematic review. *J Dent Res*. 2006;85(6):496-500.
52. Kligman S, Ren Z, Chung CH, Perillo MA, Chang YC, Koo H, et al. The Impact of Dental Implant Surface Modifications on Osseointegration and Biofilm Formation. *J Clin Med*. 2021;10(8).
53. Iglhaut G, Schwarz F, Winter RR, Mihatovic I, Stimmelmayer M, Schliephake H. Epithelial Attachment and Downgrowth on Dental Implant Abutments—A Comprehensive Review. *J Esthet Restor Dent*. 2014;26(5):324-31.
54. Menini M, Dellepiane E, Deiana T, Fulcheri E, Pera P, Pesce P. Comparison of Bone-Level and Tissue-Level Implants: A Pilot Study with a Histologic Analysis and a 4-Year Follow-up. *Int J Periodontics Restorative Dent*. 2022;42(4):535-43.
55. Slotte C, Gronningsaeter A, Halmoy AM, Ohrnell LO, Stroh G, Isaksson S, et al. Four-millimeter implants supporting fixed partial dental prostheses in the severely resorbed posterior mandible: two-year results. *Clin Implant Dent Relat Res*. 2012;14 Suppl 1:e46-58.
56. Nielsen HB, Schou S, Bruun NH, Starch-Jensen T. Single-crown restorations supported by short implants (6 mm) compared with standard-length implants (13 mm) in conjunction with maxillary sinus floor augmentation: a randomized, controlled clinical trial. *Int J Implant Dent*. 2021;7(1):66.
57. Schiegnitz E, Al-Nawas B. Narrow-diameter implants: A systematic review and meta-analysis. *Clin Oral Implants Res*. 2018;29 Suppl 16:21-40.
58. Lee H, Jo M, Sailer I, Noh G. Effects of implant diameter, implant-abutment connection type, and bone density on the biomechanical stability of implant components and bone: A finite element analysis study. *J Prosthet Dent*. 2022;128(4):716-28.
59. Messias A, Karasan D, Nicolau P, Pjetursson BE, Guerra F. Rehabilitation of full-arch edentulism with fixed or removable dentures retained by root-form dental implants: A systematic review of outcomes and outcome measures used in clinical research in the last 10 years. *J Clin Periodontol*. 2022.
60. Hodosh M, Shklar G, Povar M. The porous vitreous carbon/polymethacrylate tooth implant: preliminary studies. *J Prosthet Dent*. 1974;32(3):326-34.
61. Dantas T, Madeira S, Gasik M, Vaz P, Silva F. Customized Root-Analogue Implants: A Review on Outcomes from Clinical Trials and Case Reports. *Materials (Basel)*. 2021;14(9).
62. Nimmawitt P, Aliyu AAA, Lohwongwatana B, Arunjaroenusuk S, Puncreobutr C, Mattheos N, et al. Understanding the Stress Distribution on Anatomic Customized

Root-Analog Dental Implant at Bone-Implant Interface for Different Bone Densities. *Materials (Basel)*. 2022;15(18).

63. Aldesoki M, Keilig L, Dörsam I, Evers-Dietze B, Elshazly TM, Bourauel C. Trueness and precision of milled and 3D printed root-analogue implants: A comparative in vitro study. *J Dent*. 2023;130:104425.

64. Smitkarn P, Subbalekha K, Mattheos N, Pimkhaokham A. The accuracy of single-tooth implants placed using fully digital-guided surgery and freehand implant surgery. *J Clin Periodontol*. 2019;46.

65. Tan PLB, Layton DM, Wise SL. In vitro comparison of guided versus freehand implant placement: use of a new combined TRIOS surface scanning, Implant Studio, CBCT, and stereolithographic virtually planned and guided technique. *Int J Comput Dent*. 2018;21(2):87-95.

66. Henprasert P, Dawson DV, El-Kerdani T, Song X, Couso-Queiruga E, Holloway JA. Comparison of the Accuracy of Implant Position Using Surgical Guides Fabricated by Additive and Subtractive Techniques. *J Prosthodont*. 2020;29(6):534-41.

67. Schweiger J, Edelhoff D, Guth JF. 3D Printing in Digital Prosthetic Dentistry: An Overview of Recent Developments in Additive Manufacturing. *J Clin Med*. 2021;10(9).

68. Unkovskiy A, Schmidt F, Beuer F, Li P, Spintzyk S, Kraemer Fernandez P. Stereolithography vs. Direct Light Processing for Rapid Manufacturing of Complete Denture Bases: An In Vitro Accuracy Analysis. *J Clin Med*. 2021;10(5).

69. Unkovskiy A, Bui PH, Schille C, Geis-Gerstorfer J, Huettig F, Spintzyk S. Objects build orientation, positioning, and curing influence dimensional accuracy and flexural properties of stereolithographically printed resin. *Dent Mater*. 2018;34(12):e324-e33.

70. Mostafavi D, Methani MM, Piedra-Cascon W, Zandinejad A, Att W, Revilla-Leon M. Influence of the polymerization post-processing procedures on the accuracy of additively manufactured dental model material. *Int J Prosthodont*. 2021.

71. Sun Y, Ding Q, Tang L, Zhang L, Sun Y, Xie Q. Accuracy of a chairside fused deposition modeling 3D-printed single-tooth surgical template for implant placement: An in vitro comparison with a light cured template. *J Craniomaxillofac Surg*. 2019;47(8):1216-21.

72. Lüchtenborg J, Burkhardt F, Nold J, Rothlauf S, Wesemann C, Pieralli S, et al. Implementation of Fused Filament Fabrication in Dentistry. *Appl. Sci*. 2021;11(14):6444.

73. Fico D, Rizzo D, Casciaro R, Esposito Corcione C. A Review of Polymer-Based Materials for Fused Filament Fabrication (FFF): Focus on Sustainability and Recycled Materials. *Polymers (Basel)*. 2022;14(3).

74. Singh S, Singh G, Prakash C, Ramakrishna S. Current status and future directions of fused filament fabrication. *J Manuf Process*. 2020;55:288-306.

75. Noriega A, Blanco D, Alvarez BJ, Garcia A. Dimensional accuracy improvement of FDM square cross-section parts using artificial neural networks and an optimization algorithm. *Int. J. Adv. Manuf. Technol.* 2013;69(9):2301-13.
76. Revilla-Leon M, Subramanian SG, Att W, Krishnamurthy VR. Analysis of Different Illuminance of the Room Lighting Condition on the Accuracy (Trueness and Precision) of An Intraoral Scanner. *J Prosthodont.* 2021;30(2):157-62.
77. Cakmak G, Yilmaz H, Trevino A, Kokat AM, Yilmaz B. The effect of scanner type and scan body position on the accuracy of complete-arch digital implant scans. *Clin Implant Dent Relat Res.* 2020;22(4):533-41.
78. Revilla-León M, Smith Z, Methani MM, Zandinejad A, Özcan M. Influence of scan body design on accuracy of the implant position as transferred to a virtual definitive implant cast. *J Prosthet Dent.* 2021;125(6):918-23.
79. Arcuri L, Pozzi A, Lio F, Rompen E, Zechner W, Nardi A. Influence of implant scanbody material, position and operator on the accuracy of digital impression for complete-arch: A randomized in vitro trial. *J Prosthodont Res.* 2020;64(2):128-36.
80. Motel C, Kirchner E, Adler W, Wichmann M, Matta RE. Impact of Different Scan Bodies and Scan Strategies on the Accuracy of Digital Implant Impressions Assessed with an Intraoral Scanner: An In Vitro Study. *J Prosthodont.* 2020;29(4):309-14.
81. Boulanger M, Johnson ME, Luko SN. Reviews of Standards and Related Material: Statistical Standards and ISO, Part 1. *Qual Eng.* 2012;24(1):94-101.
82. Yilmaz B, Gouveia D, Marques VR, Diker E, Schimmel M, Abou-Ayash S. The accuracy of single implant scans with a healing abutment-scanpeg system compared with the scans of a scanbody and conventional impressions: An in vitro study. *J Dent.* 2021;110:103684.
83. Abou-Ayash S, Mathey A, Gäumann F, Mathey A, Donmez MB, Yilmaz B. In vitro scan accuracy and time efficiency in various implant-supported fixed partial denture situations. *J. Dent.* 2022;127:104358.
84. Papaspyridakos P, Vazouras K, Chen YW, Kotina E, Natto Z, Kang K, et al. Digital vs Conventional Implant Impressions: A Systematic Review and Meta-Analysis. *J Prosthodont.* 2020;29(8):660-78.
85. Kernen F, Schlager S, Seidel Alvarez V, Mehrhof J, Vach K, Kohal R, et al. Accuracy of intraoral scans: An in vivo study of different scanning devices. *J Prosthet Dent.* 2022;128(6):1303-9.
86. Kernen FR, Recca M, Vach K, Nahles S, Nelson K, Flugge TV. In vitro scanning accuracy using different aids for multiple implants in the edentulous arch. *Clin Oral Implants Res.* 2022;33(10):1010-20.
87. Wu TH, Lin WC, Chen WK, Chang YC, Hwang JJ. Predicting cancer risks from dental computed tomography. *J Dent Res.* 2015;94(1):27-35.

88. EAO-407 / OC-BR-005 | Impact of the radiographic field of view on the accuracy of virtual implant planning. *Clin Oral Implants Res.* 2021;32(S22):8-.
89. W. H. Böse M, Hildebrand D, Beuer F, Wesemann C, Schwerdtner P, Pieralli S, et al. Root-analogue implants for immediate implant placement: A retrospective case series. *Clin Oral Implants Res.* 2020;31(S20):275-.
90. Yogui FC, Verri FR, de Luna Gomes JM, Lemos CAA, Cruz RS, Pellizzer EP. Comparison between computer-guided and freehand dental implant placement surgery: A systematic review and meta-analysis. *Int J Oral Maxillofac Surg.* 2021;50(2):242-50.
91. Hromadnik V, Pieralli S, Spies B, Beuer F, Wesemann C. Accuracy of a workflow using sleeveless 3D printed surgical guides made from a cost-effective and biodegradable material: An in vitro study. *Clin Oral Implants Res.* 2019;30(S19):519-.
92. EAO-822/OC-07 | Accuracy of implant installation using cost-effective extrusion-based sterilizable surgical guides. *Clin Oral Implants Res.* 2022;33(S24):3-55.
93. EAO-202/PO-BR-001 | Biocompatibility of sterilizable and recyclable polymers for extrusion-based printing. *Clin Oral Implants Res.* 2021;32(S22):61.
94. Pieralli S, Spies B, Hromadnik V, Beuer F, Wesemann C. How accurate is digitization of one-piece zirconia oral implants without scan bodies? A feasibility study. *Clin Oral Implants Res.* 2019;30(S19):366-.
95. Hamilton A, Singh A, Friedland B, Jamjoom FZ, Griseto N, Gallucci GO. The impact of cone beam computer tomography field of view on the precision of digital intra-oral scan registration for static computer-assisted implant surgery: A CBCT analysis. *Clin Oral Implants Res.* 2022;33(12):1273-81.
96. Bornstein MM, Horner K, Jacobs R. Use of cone beam computed tomography in implant dentistry: current concepts, indications and limitations for clinical practice and research. *Periodontol 2000.* 2017;73(1):51-72.
97. Belser UC, Grütter L, Vailati F, Bornstein MM, Weber HP, Buser D. Outcome evaluation of early placed maxillary anterior single-tooth implants using objective esthetic criteria: a cross-sectional, retrospective study in 45 patients with a 2- to 4-year follow-up using pink and white esthetic scores. *J Periodontol.* 2009;80(1):140-51.
98. Naveau A, Rignon-Bret C, Wulfman C. Zirconia abutments in the anterior region: A systematic review of mechanical and esthetic outcomes. *J Prosthet Dent.* 2019;121(5):775-81.e1.
99. Hashim D, Cionca N, Combescure C, Mombelli A. The diagnosis of peri-implantitis: A systematic review on the predictive value of bleeding on probing. *Clin Oral Implants Res.* 2018;29 Suppl 16:276-93.
100. Moraschini V, Poubel LA, Ferreira VF, Barboza Edos S. Evaluation of survival and success rates of dental implants reported in longitudinal studies with a follow-up

period of at least 10 years: a systematic review. *Int J Oral Maxillofac Surg.* 2015;44(3):377-88.

101. Gjelvold B, Mahmood DJH, Wennerberg A. Accuracy of surgical guides from 2 different desktop 3D printers for computed tomography-guided surgery. *J Prosthet Dent.* 2019;121(3):498-503.

102. Adams CR, Ammoun R, Deeb GR, Bencharit S. Influence of Metal Guide Sleeves on the Accuracy and Precision of Dental Implant Placement Using Guided Implant Surgery: An In Vitro Study. *J Prosthodont.* 2023;32(1):62-70.

103. Tallarico M, Czajkowska M, Cicciù M, Giardina F, Minciarelli A, Zadrożny Ł, et al. Accuracy of surgical templates with and without metallic sleeves in case of partial arch restorations: A systematic review. *J. Dent.* 2021;115:103852.

104. Herstell H, Berndt S, Kühne C, Reich S. Accuracy of guided implant surgery obtained using 3D-printed surgical guides - An in vitro comparison of four evaluation methods. *Int J Comput Dent.* 2022;25(2):161-72.

105. Schneider D, Sax C, Sancho-Puchades M, Hämmerle CHF, Jung RE. Accuracy of computer-assisted, template-guided implant placement compared with conventional implant placement by hand—An in vitro study. *Clin. Oral Implants Res.* 2021;32(9):1052-60.

106. 10993-5:2009 I. Biological evaluation of medical devices: Part 5: Tests for in vitro cytotoxicity. 2009.

107. 10993-12:2021 I. Biological evaluation of medical devices: Part 12: Sample preparation and reference materials. 2021.

108. Roesch-Ely M, Steinberg T, Bosch FX, Müssig E, Whitaker N, Wiest T, et al. Organotypic co-cultures allow for immortalized human gingival keratinocytes to reconstitute a gingival epithelial phenotype in vitro. *Differentiation.* 2006;74(9-10):622-37.

109. Jaju PP, Jaju SP. Cone-beam computed tomography: Time to move from ALARA to ALADA. *Imaging Sci Dent.* 2015;45(4):263-5.

110. Yuan C, Wei L, Li X, Wang P. A technique for registering digital dental casts onto cone beam computed tomography scans with excessive metallic artifacts. *J Prosthet Dent.* 2021;125(1):29-33.

111. Alhossaini SJ, Neena AF, Issa NO, Abouelkheir HM, Gaweesh YY. Accuracy of markerless registration methods of DICOM and STL files used for computerized surgical guides in mandibles with metal restorations: An in vitro study. *J Prosthet Dent.* 2022.

112. Flügge T, Ludwig U, Winter G, Amrein P, Kernen F, Nelson K. Fully guided implant surgery using Magnetic Resonance Imaging - An in vitro study on accuracy in human mandibles. *Clin Oral Implants Res.* 2020;31(8):737-46.

113. Bohner L, Hanisch M, Sesma N, Blanck-Lubarsch M, Kleinheinz J. Artifacts in magnetic resonance imaging caused by dental materials: a systematic review. *Dentomaxillofac. Radiol.* 2022;51.
114. Bohner L, Hanisch M, Parize H, Sesma N, Kleinheinz J, Meier N. SEMAC + VAT for Suppression of Artifacts Induced by Dental-Implant-Supported Restorations in Magnetic Resonance Imaging. *J. Clin. Med.* 2023;12(3):1117.
115. Pirker W, Wiedemann D, Lidauer A, Kocher AA. Immediate, single stage, truly anatomic zirconia implant in lower molar replacement: a case report with 2.5 years follow-up. *Int J Oral Maxillofac Surg.* 2011;40(2):212-6.
116. Mangano FG, De Franco M, Caprioglio A, Macchi A, Piattelli A, Mangano C. Immediate, non-submerged, root-analogue direct laser metal sintering (DLMS) implants: a 1-year prospective study on 15 patients. *Lasers Med Sci.* 2014;29(4):1321-8.
117. Sommacal B, Savic M, Filippi A, Kühn S, Thieringer FM. Evaluation of Two 3D Printers for Guided Implant Surgery. *Int J Oral Maxillofac Implants.* 2018;33(4):743–6.
118. Sun Y, Ding Q, Yuan F, Zhang L, Sun Y, Xie Q. Accuracy of a chairside, fused deposition modeling three-dimensional-printed, single tooth surgical guide for implant placement: A randomized controlled clinical trial. *Clin. Oral Implants Res.* 2022;33(10):1000-9.
119. Yang H, Liu Y. Accuracy of Models Fabricated by a Chair-side Fused Deposition Modeling (FDM) Printer in Stomatology. *Oper Dent.* 2022;47(5):E233-e40.
120. He F, Ning H, Khan M. Effect of 3D Printing Process Parameters on Damping Characteristic of Cantilever Beams Fabricated Using Material Extrusion. *Polymers.* 2023;15(2):257.
121. Fedorov A, Beichel R, Kalpathy-Cramer J, Finet J, Fillion-Robin JC, Pujol S, et al. 3D Slicer as an image computing platform for the Quantitative Imaging Network. *Magn Reson Imaging.* 2012;30(9):1323-41.
122. Talmazov G, Bencharit S, Waldrop TC, Ammoun R. Accuracy of Implant Placement Position Using Nondental Open-Source Software: An In Vitro Study. *J Prosthodont.* 2020;29(7):604-10.
123. García-Sala Bonmati F, Pérez-Barquero JA, Ilzarbe Ripoll LM, Labaig Rueda C, Fernandez-Estevan L, Revilla-León M. An additively manufactured, magnetically retained, and stackable implant surgical guide: A dental technique. *J Prosthet Dent.* 2022.
124. Török G, Gombocz P, Bognár E, Nagy P, Dinya E, Kispélyi B, et al. Effects of disinfection and sterilization on the dimensional changes and mechanical properties of 3D printed surgical guides for implant therapy - pilot study. *BMC Oral Health.* 2020;20(1):19.

125. Beltrami R, Colombo M, Rizzo K, Di Cristofaro A, Poggio C, Pietrocola G. Cytotoxicity of Different Composite Resins on Human Gingival Fibroblast Cell Lines. *Biomimetics* (Basel). 2021;6(2).
126. Osman MA, Alamoush RA, Kushnerev E, Seymour KG, Shawcross S, Yates JM. Human osteoblasts response to different dental implant abutment materials: An in-vitro study. *Dent. Mater.* 2022;38(9):1547-57.
127. de Oliveira Limírio JPJ, Lemos CAA, de Luna Gomes JM, Minatel L, Alves Rezende MCR, Pellizzer EP. A clinical comparison of 1-piece versus 2-piece implants: A systematic review and meta-analysis. *J. Prosthet. Dent.* 2020;124(4):439-45.
128. Gómez-Polo M, Álvarez F, Ortega R, Gómez-Polo C, Barmak AB, Kois JC, et al. Influence of the implant scan body bevel location, implant angulation and position on intraoral scanning accuracy: An in vitro study. *J Dent.* 2022;121:104122.
129. Elter B, Diker B, Tak Ö. The trueness of an intraoral scanner in scanning different post space depths. *J. Dent.* 2022;127:104352.

7 ACKNOWLEDGMENT

My gratitude goes first and foremost to Univ.-Prof. Dr. Florian Beuer MME for his trust in me and for the opportunity to complete my scientific projects in his department and under his supervision.

I would like to thank Univ.-Prof. Dr. Benedikt Spies for his support during my years at the Department of Prosthetic Dentistry of the University of Freiburg and at the Department of Prosthodontics, Geriatric Dentistry and Craniomandibular Disorders of the Charité—Universitätsmedizin Berlin.

I would like to express my gratitude to PD Dr. Christian Wesemann for sharing part of this scientific research journey with me.

My sincere gratitude goes to all the coauthors who participated in the included studies, especially, Mr. Christoph Beyer, Dr. Mats Böse, Dr. Felix Burkhardt, Dr. Valentin Hromadnik, Ms. Valentina Kohlen, MDT Robert Nicic, Mr. Severin Rothlauf, and PD Dr. Manja von Stein-Lausnitz.

I would like to thank the entire team from the Department of Prosthodontics, Geriatric Dentistry and Craniomandibular Disorders of the Charité—Universitätsmedizin Berlin. My special gratitude here goes to Dr. Ufuk Adali, Dr. Maria Bruhnke, Dr. Simon Peroz and Ms. Betül Özün.

My gratitude goes to my former colleagues at the Department of Prosthetic Dentistry and Oral and Maxillofacial Surgery of the University of Freiburg, in particular Prof. Dr. Samir Abou-Ayash, Dr. Manrique Fonseca, Dr. Irene Garcia Martin, Dr. Mireia Haro Adanez and Dr. Emilia Lopez Hernandez.

I would like to express my gratitude to my colleagues from Brazil, in particular Prof. Dr. Pedro Tortamano, Dr. Diego Diaz Gamba, and Dr. Kelly Vaz Moreira.

I thank my parents, Luise and Daniele, and my sister, Patrizia, for always motivating me to continue my education path even if it meant being away from home.

To conclude, I would like to express my deepest gratitude to Carolina for her unconditional support from the beginning to the end of this project.

EIDESSTATTLICHE ERKLÄRUNG

gem. § 4 Abs. 3 (k) der HabOMed der Charité

Hiermit erkläre ich, dass

- weder früher noch gleichzeitig ein Habilitationsverfahren durchgeführt oder angemeldet wurde,
- die vorgelegte Habilitationsschrift ohne fremde Hilfe verfasst, die beschriebenen Ergebnisse selbst gewonnen sowie die verwendeten Hilfsmittel, die Zusammenarbeit mit anderen Wissenschaftlern/Wissenschaftlerinnen und mit technischen Hilfskräften sowie die verwendete Literatur vollständig in der Habilitationsschrift angegeben wurden,
- mir die geltende Habilitationsordnung bekannt ist.

Ich erkläre ferner, dass mir die Satzung der Charité-Universitätsmedizin Berlin zur Sicherung Guter Wissenschaftlicher Praxis bekannt ist und ich mich zur Einhaltung dieser Satzung verpflichte.

Ort, Datum Unterschrift